การระบุเมแทบอไลต์และยีนที่แสดงออกเปลี่ยนไปในข้าว *Oryza sativa* L. พันธุ์ขาวดอกมะลิ 105 ที่มีการแสดงออกเกินปกติของยีน *OsCaM1-1*

นายสุรชาติ ตั้งประณมกร

วิทยานิพนธ์นี้เป็นส่วนหนึ่งของการศึกษาตามหลักสูตรปริญญาวิทยาศาสตรมหาบัณฑิต
สาขาวิชาชีวเคมีและชีววิทยาโมเลกุล ภาควิชาชีวเคมี
คณะวิทยาศาสตร์ จุฬาลงกรณ์มหาวิทยาลัย
ปีการศึกษา 2557

IDENTIFICATION OF METABOLITES AND DIFFERENTIALLY EXPRESSED GENES IN RICE *Oryza sativa* L. 'KDML105' OVEREXPRESSING *OsCaM1-1*

Mr. Surachat Tangpranomkorn

A Thesis Submitted in Partial Fulfillment of the Requirements
for the Degree of Master of Science Program in Biochemistry and Molecular Biology
Department of Biochemistry
Faculty of Science
Chulalongkorn University
Academic Year 2014

Thesis Title	IDENTIFICATION OF METABOLITES AND DIFFERENTIALLY EXPRESSED GENES IN RICE *Oryza sativa* L. 'KDML105' OVEREXPRESSING *OsCaM1-1*
By	Mr. Surachat Tangpranomkorn
Field of Study	Biochemistry and Molecular Biology
Thesis Advisor	Assistant ProfessorSupaart Sirikantaramas, Ph.D.

Accepted by the Faculty of Science, Chulalongkorn University in Partial Fulfillment of the Requirements for the Master's Degree

.....Dean of the Faculty of Science
(ProfessorSupot Hannongbua, Ph.D.)

THESIS COMMITTEE

.....Chairman
(ProfessorAnchalee Tassanakajon, Ph.D.)

.....Thesis Advisor
(Assistant ProfessorSupaart Sirikantaramas, Ph.D.)

.....Examiner
(Associate ProfessorTeerapong Buaboocha, Ph.D.)

.....Examiner
(Assistant ProfessorKunlaya Somboonwiwat, Ph.D.)

.....External Examiner
(Associate ProfessorJarunya Narangajavana, Ph.D.)

สุรชาติ ตั้งประณมกร : การระบุเมแทบอไลต์และยีนที่แสดงออกเปลี่ยนไปในข้าว *Oryza sativa* L. พันธุ์ขาวดอกมะลิ 105 ที่มีการแสดงออกเกินปกติของยีน *OsCaM1-1* (IDENTIFICATION OF METABOLITES AND DIFFERENTIALLY EXPRESSED GENES IN RICE *Oryza sativa* L. 'KDML105' OVEREXPRESSING *OsCaM1-1*) อ.ที่ปรึกษาวิทยานิพนธ์หลัก: ผศ. ดร.ศุภอรรจ ศิริกันทรมาศ, 139 หน้า.

ข้าว (*Oryza sativa* L.) ที่มีการแสดงออกเกินปกติของยีน *OsCaM1-1* แสดงความสามารถในการทนความเครียดจากความเค็มได้มากขึ้น การศึกษานี้จึงใช้ cDNA-AFLP GC-TOF/MS และ LC-MS/MS เพื่อระบุการเปลี่ยนแปลงในระดับทรานสคริปและเมแทบอไลต์ในข้าวดัดแปลงพันธุกรรมดังกล่าว เทคนิค cDNA-AFLP สามารถระบุยีนที่เปลี่ยนแปลงระดับการแสดงออกในข้าวดัดแปลงพันธุกรรมได้ 31 ยีน อย่างไรก็ตาม การวิเคราะห์ qRT-PCR ของตัวแทนทั้งหมด 10 ยีน พบว่าระดับการแสดงออกของยีนเหล่านี้ไม่แตกต่างอย่างมีนัยสำคัญระหว่างข้าวปกติและข้าวดัดแปลงพันธุกรรม PLS-DA score plot และ Hierarchical clustering analysis จากข้อมูลเมแทโบโลมิกส์ของข้าวดัดแปลงพันธุกรรมและข้าวกลุ่มควบคุมระบุว่า *Os*CaM1-1 ทำให้เกิดการเปลี่ยนแปลงในระดับเมแทบอไลท์ในข้าวดัดแปลงพันธุกรรม การสะสมที่เพิ่มขึ้นของสารตัวกลางหลายชนิดในวิถีเมแทบอลิซึมสร้างพลังงาน รวมไปถึงกรดอะมิโนหลายชนิด และ ไทรซินกลูโคไซด์ แสดงว่าอาจมีการเหนี่ยวนำข้าวดัดแปลงพันธุกรรมที่มีการแสดงออกเกินปกติของยีน *OsCaM1-1* ให้อยู่ในสภาวะโปรแอคทีฟ เพื่อศึกษาความสัมพันธ์ระหว่างเมแทบอไลท์และยีน ได้เลือกยีนตัวแทน คือ อาร์จิเนส กลูต้าไทโอนซินทีเทส และอินโนซิทอล-1-โมโนฟอสฟาเทส โดยพิจารณาจากข้อมูลเมแทโบโลม อย่างไรก็ตาม ไม่พบการเปลี่ยนแปลงของระดับการแสดงออกของยีนเหล่านี้ ซึ่งอาจบอกได้ว่ามีการควบคุมในระดับหลังการแปลรหัส จึงทำการวิเคราะห์เพิ่มเติมโดยทำนายหาบริเวณในโปรตีนเหล่านี้ที่อาจเกิดปฏิสัมพันธ์กับคัลมอดูลิน ควบคู่กับการทำนายโครงสร้างสามมิติของโปรตีน ซึ่งผลการวิเคราะห์ระบุว่า กลูต้าไทโอนซินทีเทส และอินโนซิทอล-1-โมโนฟอสฟาเทส อาจเป็นคู่ปฏิสัมพันธ์กับคัลมอดูลิน การศึกษานี้ให้ข้อมูลใหม่เกี่ยวกับหน้าที่ที่เป็นไปได้ของโปรตีน *Os*CaM1-1

ภาควิชา ชีวเคมี ลายมือชื่อนิสิต .....

สาขาวิชา ชีวเคมีและชีววิทยาโมเลกุล ลายมือชื่อ อ.ที่ปรึกษาหลัก .....

ปีการศึกษา 2557

5572159923 : MAJOR BIOCHEMISTRY AND MOLECULAR BIOLOGY
KEYWORDS: ORYZA SATIVA L. / CALMODULIN / CDNA-AFLP / METABOLOMICS / SALT STRESS

SURACHAT TANGPRANOMKORN: IDENTIFICATION OF METABOLITES AND DIFFERENTIALLY EXPRESSED GENES IN RICE *Oryza sativa* L. 'KDML105' OVEREXPRESSING *OsCaM1-1*. ADVISOR: ASST. PROF.SUPAART SIRIKANTARAMAS, Ph.D., 139 pp.

OsCaM1-1-overexpressing rice (Oryza sativa L.) has been shown to gain salt stress-tolerant capability. In this study, cDNA-AFLP, GC-TOF/MS, and LC-MS/MS were performed to identify transcriptomic and metabolomic changes in the transgenic rice overexpressing OsCaM1-1. A total of 31 candidate genes being differentially expressed in the transgenic rice were identified by cDNA-AFLP. However, qRT-PCR analysis of 10 selected candidate genes did not show any significant different expression between the transgenic rice lines and wild type rice. From metabolomic data of transgenic rice and control transgenic rice, PLS-DA score plot and hierarchical clustering analysis indicated that OsCaM1-1 caused an alteration in transgenic rice metabolomes. Up-accumulation of many intermediates in energy metabolisms together with amino acids and tricin glucoside suggested that OsCaM1-1-overexpressing rice was induced to a proactive state. To investigate a metabolite-to-gene correlation, several candidate genes, e.g. arginase, glutathione synthetase, and inositol-1-monophosphatase, were selected based on the metabolome data. However, no differentially expressed genes were found, implying a possible post-translational regulation in those steps. Subsequent analyses of CaM binding site prediction and homology modeling suggested that one isoform of glutathione synthetase, and inositol-1-monophosphatase are potential CaM interacting partners. This study provides novel information about possible roles of OsCaM1-1.

Department:	Biochemistry	Student's Signature .....
Field of Study:	Biochemistry and Molecular Biology	Advisor's Signature .....
Academic Year:	2014	

ACKNOWLEDGEMENTS

I would like to express my sincere appreciation to my advisor, Assistant Professor Supaart Sirikantaramas, Ph.D. for his guidance, continuous support, and encouragement throughout my Master's course. He taught me not only in scientific knowledge but also self-discipline, research skill, and written and spoken scientific communications. My work would not be successful without him.

I would like to thank Associate Professor Teerapong Buaboocha, Ph.D., Department of Biochemistry, Chulalongkorn University for providing transgenic and wild type 'KDML 105' rice seeds and also his kind supports. My special thanks also go to Associate Professor Suchada Sukrong, Ph.D., Department of Pharmacognosy and Pharmaceutical Botany, Chulalongkorn University, for her guidance and facilities for cDNA-AFLP experiment. I am especially indebted to Dr. Miyako Kusano and Dr. Ryo Nakabayashi, RIKEN Center for Sustainable Resource Science, Japan, for performing GC-TOF/MS and LC-MS/MS analyses and metabolite annotation. I also thank Mr. Worawat Yuenyong for sharing his rice for my gene expression analysis.

I am thankful to Prof. Dr. Anchalee Tassanakajon, Assoc. Prof. Dr. Teerapong Buaboocha, Assoc. Prof. Dr. Jarunya Narangajavana, and Asst. Prof. Dr. Kunlaya Somboonwiwat for being my thesis committees. Their comments and suggestions were really valuable to me.

I also thank my colleagues, both graduated and present friends, including Supaluk Tantong, Channarong Boonrueng, Kwankao Karnpakdee, Krisana Boonpa, and all members in Plant Biochemistry laboratory 708 for their friendships and supports.

I would like to acknowledge the following financial supports: Special Task Force for Activating Research: Biochemical and Molecular Mechanisms of Rice in Changing Environments, The 90th Anniversary of Chulalongkorn University Fund (Ratchadaphiseksomphot Endowment Fund), and Chulalongkorn University Graduate Scholarship to Commemorate the 72th Anniversary of His Majesty the King Bhumibol Adulyadej.

Finally I am grateful for my family, especially my parents for their love, encouragement and support for my whole life.

CONTENTS

Page

Page

Page

Page

LIST OF TABLES

LIST OF FIGURES

CHAPTER I
INTRODUCTION

Saline soil has long been one of the threats to rice cultivation in many countries. Many areas of Thailand especially in the northeast region are affected by this problem. As a result, the grain yields have been decreased in both quantity and quality including drops in grain weight and in the numbers of tiller, spikelet, and panicle per plant (Zeng and Shannon 2000; Sahi et al. 2006).

From the previous study, it has been shown that the expression of rice calmodulin 1-1 (*OsCaM1-1*) was induced during salt stress (Phean-o-pas et al. 2005). Despite having many rice calmodulin isoforms, only *OsCaM1-1* is strikingly up-regulated in response to salt stress. This suggested that *OsCaM1-1* is an important signaling protein for rice acclimation to salt stress. In addition to being regulated under salt stress, *Os*CaM1-1 was reported to be up-regulated against wounding, osmotic, and heat stresses (Phean-o-pas et al. 2005; Saeng-ngam et al. 2012; Wu et al. 2012). Also, Arabidopsis and rice overexpressing *OsCaM1-1* have been shown to become more tolerant to heat and salt stress, respectively (Wu et al. 2012; Saeng-ngam et al. 2012). However, the mechanisms underlying these processes remain obscure. In this study, cDNA-Amplified Fragment Length Polymorphism (cDNA-AFLP) was used to study transcriptome, and gas chromatography time-of-flight/mass spectrometry (GC-TOF/MS) and liquid chromatography tandem mass spectrometry (LC-MS/MS) were used to study metabolome in transgenic rice *Oryza sativa* 'Khao Dawk Mali 105' (KDML 105) overexpressing *OsCaM1-1*. By comparing these transgenic rice plants with non-overexpressing line, alterations in gene expressions and metabolite accumulations affected by the *OsCaM1-1* overexpression could be revealed. This would help in understanding the biological roles of *Os*CaM1-1 which lead to the improvement of transgenic plant acclimation to the stresses. More information on related topics is reviewed in this chapter.

1.1 Rice

Rice, *Oryza sativa* L., is an important food crop feeding billions of life every day. It is also economically valuable for many countries including Thailand. Rice is believed to be a crop that has been continuously grown for the longest in the history. The first rice crop cultivation in Thailand was found around 4500 B.C. (Gnanamanickam 2009). It belongs to the grass family and is easily grown in the tropics. Rice grain is rich in carbohydrate and contributes greatly to caloric intake for most Asians. It also provides various vitamins, protein, and minerals (Table 1) (Gnanamanickam 2009).

Moldenhauer et al. (2013) provide thorough knowledge of rice growth and development. In short, life cycle of rice plant ranges from 105-145 days varying between cultivars and environmental factors. Rice growth can be divided into three main developmental stages, e.g. vegetative, reproductive, and grain filling & maturation stage (Figure 1). During vegetative stage, rice plants gradually increase in height with active tillering and leaves emerge at regular intervals. This is the main phase determining the growth duration of each cultivar. Rice generally produces 10 to 30 tillers per plant when space is available. Tiller number can be declined due to competitive effect. Next, rice plants enter reproductive phase by culm elongation, booting, emergence of flag leaf, heading and flowering. This phase usually lasts 30 days in most cultivars. Finally, ripening & maturation stage involves grain growth after ovary fertilization. Light intensity is an important factor in this stage in which 60% or more of carbohydrates used in grain filling are synthesized through photosynthesis. At maturity, grains change color from green to gold and hardened. Rice grains are ready for harvest when grain moisture reaches approximately 20-22 percents.

O. sativa L. 'KDML105' is a Thai jasmine rice used in this experiment. It is popularly grown in Thailand since it has good aroma and favorable texture when cooked. It is also high in price and market demand. The major cultivation area of KDML 105 in Thailand is in Tungkularonghai mainly located in Roi-Et province (Kong-nrern et al. 2011).

Table 1. Nutritional value of white long-grain rice per 100 g according to USDA nutrient database (taken from Gnanamanickam (2009))

Nutrient	Amount/Percent relative to recommendations for adults, U.S.)
Carbohydrates	79.95 g
Sugars	0.12 g
Dietary fiber	1.3 g
Fat	0.66 g
Protein	7.13 g
Thiamin	0.07 mg (5%)
Riboflavin	0.05 mg (3%)
Niacin	1.6 mg (11%)
Pentothenic acid	1.01 mg (20%)
Vitamin B6	0.16 mg (13%)
Calcium	28 mg (3%)
Iron	0.8 mg (6%)
Magnesium	25 mg (7%)
Phosphorus	115 mg (16%)
Potassium	115 mg (2%)
Zinc	1.09 mg (11%)
Manganese	1.09 mg

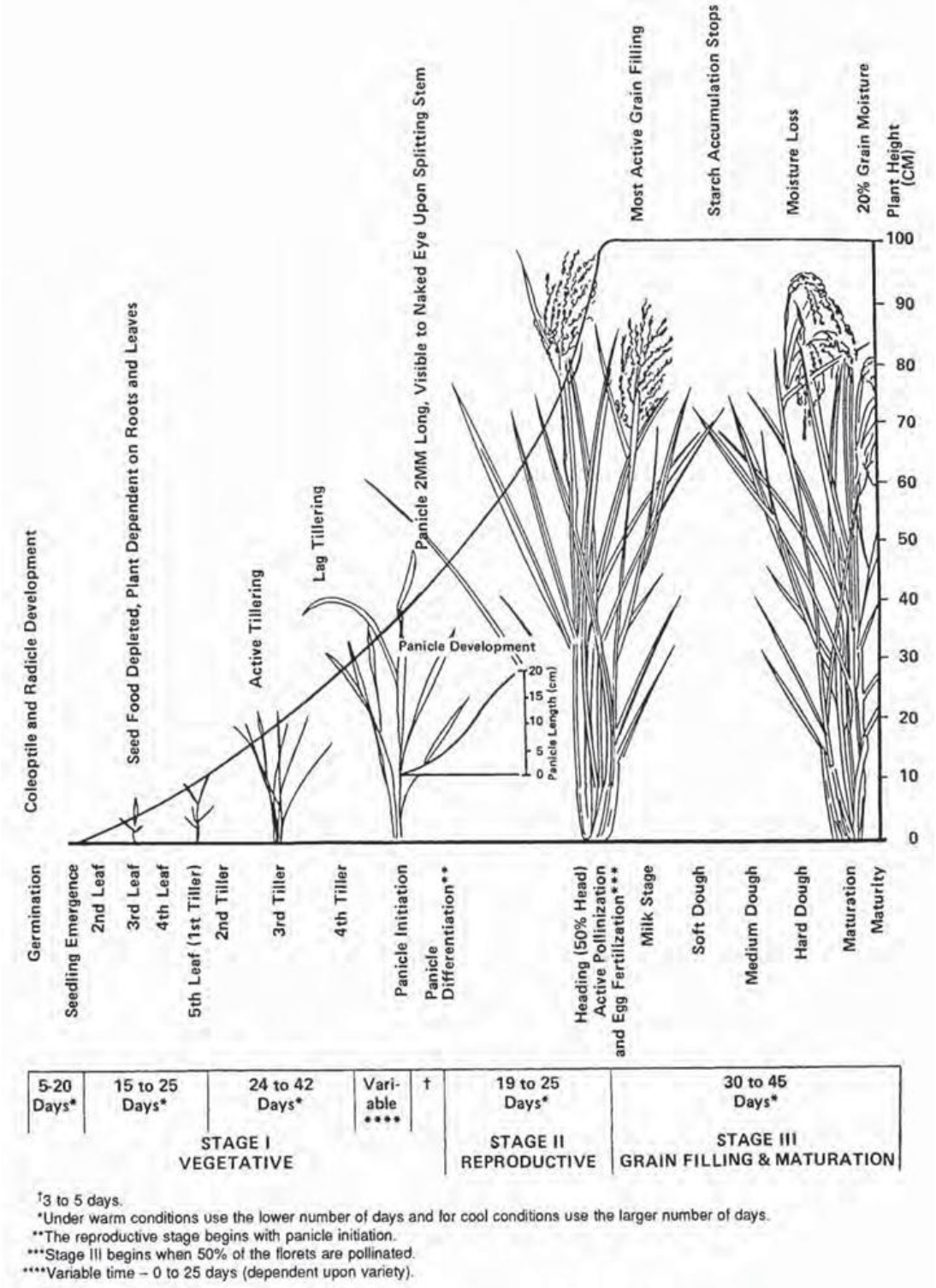

Figure 1. Three agronomic phases of rice plant development: vegetative stage, reproductive stage, and grain filling & maturation stage. (Taken from Moldenhauer et al. (2013))

1.2 Salt stress and plant adaptation

Saline soil is enriched in mineral salts and composed of cation and anion electrolytes. In nature, major cations in saline soil are Na^{+}, Ca^{2+}, Mg^{2+}, and K^{+}; and anions are, Cl^{-}, SO_4^{2-}, HCO_3^{-}, CO_3^{2-}, and NO_3^{-}. It was estimated that around 20% of cultivated lands and up to 50% of irrigated lands may be salt-affected (Zhu 2001; Pitman and Lauchli 2002). This is crucial for low yielding problem in crop cultivation since most crops are non-halophytic (Rathinasabapathi et al. 1993; Hoshida et al. 2000). High salinity soil or salt stress could induce three stress conditions to the plant: (1) water stress due to a decrease in water potential of the environment; (2) ionic stress by an accumulation of ions above physiological level; and (3) secondary stress from the generation of reactive oxygen species. These stresses lead to many adverse effects such as plant growth discontinuance, inhibition of enzymes activities, and molecular damage (Hernandez et al. 1995; Lee et al. 2001; Zhu 2001). For plant to tolerate salt stress, Zhu (2001) suggested that three events should be occurred: (1) damages relieved or prevented; (2) re-establishment of plant cellular homeostasis; and (3) growth resumed. To overcome the stress, plants have evolved stress response mechanisms involving complex array of signaling pathways. One important pathway is the signal transduction through the transient change of cytoplasmic Ca^{2+} concentration. Ca^{2+}, a second messenger, signals the growth, development, and stress response resulting in regulated cellular processes (Reddy 2001). When plant detects the stress signal, cytoplasmic Ca^{2+} is elevated and the change is then sensed by calcium-binding proteins which carry on the signal for stress-specific adaptation. The fluxes of Ca^{2+} are well maintained and the increase of Ca^{2+} could be provided by various sources. Figure 2 illustrates possible Ca^{2+} transportation among organelles and Ca^{2+} concentration at resting state of the cell.

Plant responses toward salt stress have been extensively studied and reviewed (Hasegawa and Bressan 2000; Zhu 2001; Vinocur and Altman 2005; Ji et al. 2013). As mentioned above, salinity stress could induce three different kinds of stresses and plants cope with these abiotic stress conditions differently. For water stress, depending on species, plants induce the biosynthesis of many osmolytes,

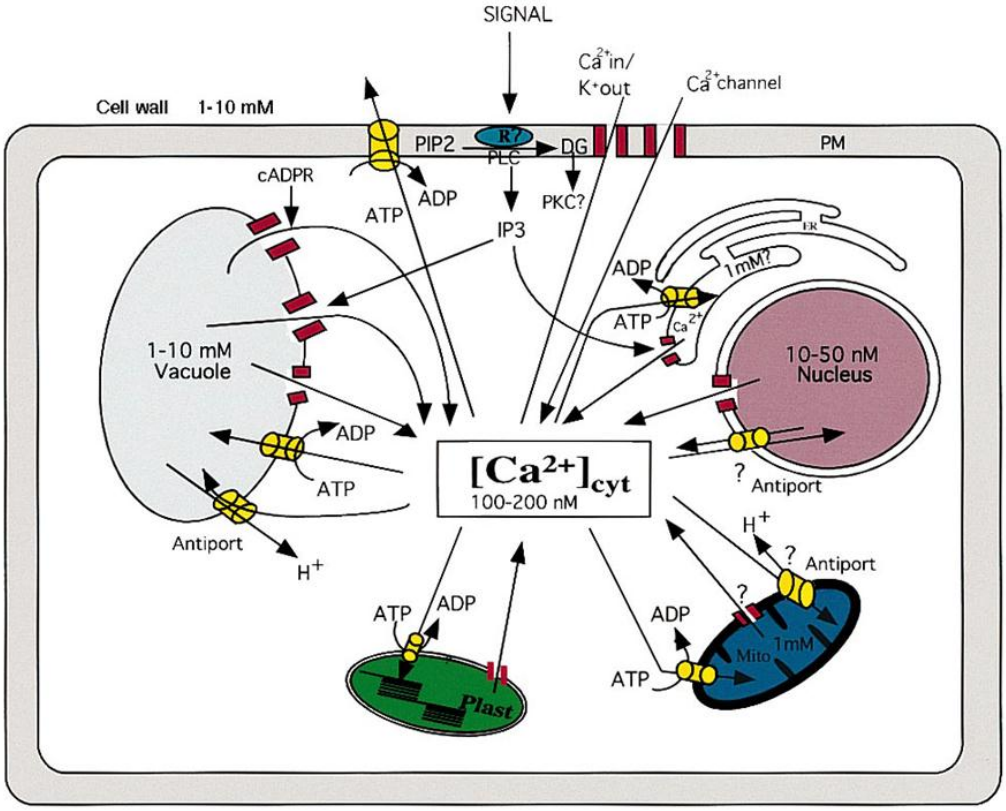

Figure 2. Calcium ion concentrations in plant cellular organelles at resting state. The arrows indicate the directions of Ca^{2+} flows across ion channels (red) and Ca^{2+} ATPase and antiporters (yellow) which connect to cytoplasmic Ca^{2+} concentration. (taken from Reddy (2001))

such as proline, glycine betaine, and sugar polyols. The accumulations of these molecules help in cell osmotic adjustment. For ionic stress, plants maintain ion homeostasis by decreasing Na^+ transportation into cell, compartmentation of Na^+ ions, and increasing Na^+ efflux out of the cell. The well-known example of such acclimation is SOS pathway studied in Arabidopsis which involves in Na^+ transportation (Sanders 2000; Mahajan et al. 2008; Ji et al. 2013). In short, a Ca^{2+} sensor, SOS3, activates SOS2 protein kinase by forming a complex. SOS3-SOS2 complex is then activates SOS1, a Na^+/H^+ antiporter, and leads to reestablishment of ion homeostasis. For oxidative stress, plants possess detoxification system involving antioxidative enzymes and metabolites. Many rice antioxidant enzymes activities were found to be increased during salt stress to neutralize reactive oxygen species, preventing cellular damages (Lee et al. 2001).

1.3 Calmodulin (CaM)

CaM, a small protein (around 150 amino acid-long), is highly conserved among eukaryotic species (Figure 3A, 3B). Plant CaMs are ~16.7 kDa in size and have many isoforms in a single plant species. They have four calcium-binding domains presented as the form of helix-loop-helix EF-hand motif (Zielinski 1998; Tuteja and Mahajan 2007). During different developmental stages or engagement of environmental stimuli, plant generates "Ca^{2+} spike" signals, a transient increase in Ca^{2+} concentration. EF-hand containing proteins or so-called calcium sensors then decode and transduce these signals. As for CaM, the conformational change upon binding to Ca^{2+} lead to an expose of hydrophobic cavity and polar rim of calcium-CaM which contributes to the subsequent binding with corresponding target proteins (Figure 3C) (Ikura 1996; Perochon et al. 2011; Bender and Snedden 2013; Das et al. 2014). Alterations of modulated-protein activities provide further signals and contribute to plant acclimation towards stimuli-responsive mechanisms. CaM-mediated cellular responses can be categorized into two types, direct response and indirect response (Figure 4).

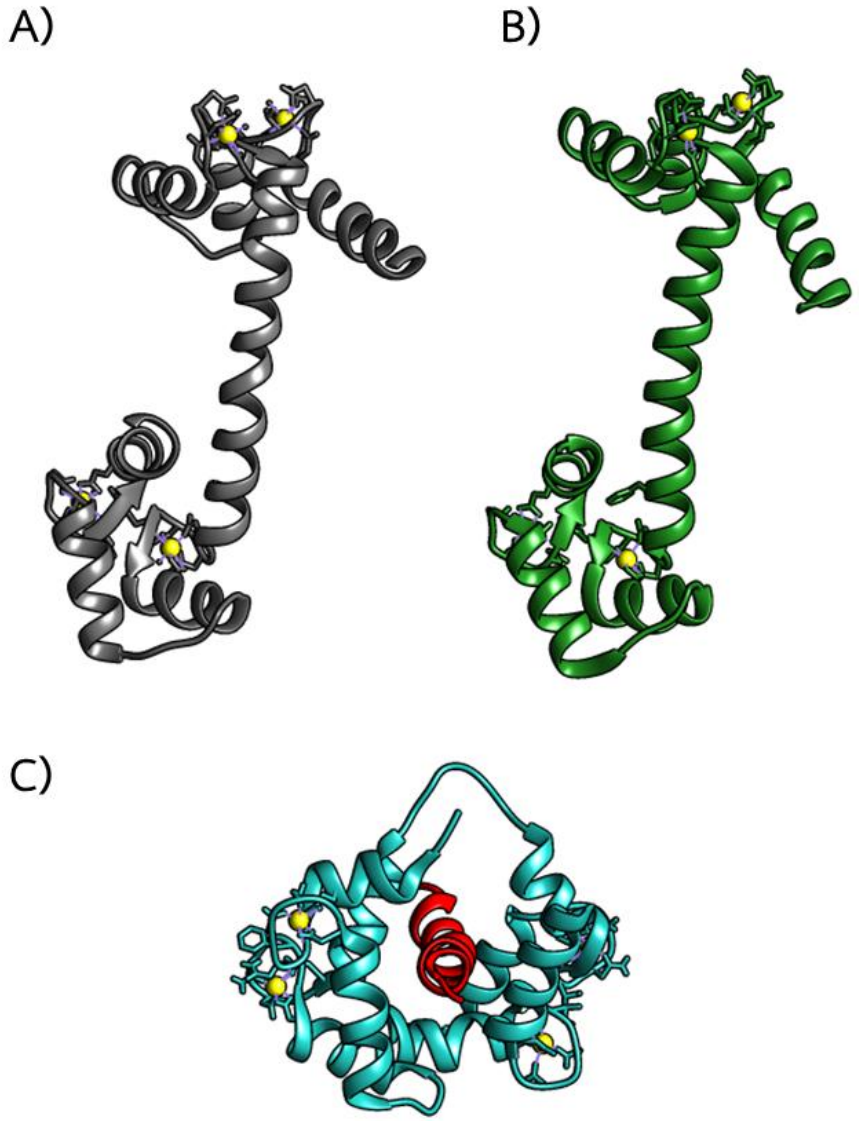

Figure 3. Three-dimensional structure of CaMs visualized by UCSF Chimera software: http://www.cgl.ucsf.edu/chimera. A) crystal structure of Ca^{2+}-bound mammalian CaM (retrieved from Protein Data Bank; accession 1CLN, based on Babu et al. (1988)), **B)** crystal structure of Ca^{2+}-bound plant CaM (retrieved from Protein Data Bank; accession 1RFJ, based on Yun et al. (2004)), and **C)** solution structure of a CaM-target peptide complex (retrieved from Protein Data Bank; accession 2BBM, based on Ikura et al. (1992)). Ca^{2+}-bound CaM is a dumbbell shape protein with two globular domains at N- and C- termini linked by a long central helix providing flexibility to the protein.

Direct response involves in the interaction between CaMs and their target proteins. Modulation of protein activities results in a rapid change (within seconds to minutes) of cellular processes. Many CaM-binding proteins in plant covering various kinds of cellular functions have been identified, for example, proteins involved in metabolism, ion transport, and DNA-binding (Table 2). Mechanisms of target protein activation/inactivation by CaM were also studied (Figure 5). The first model is the alleviation of auto-inhibition by CaM binding as demonstrated in plant glutamate decarboxylase (GAD) (Snedden et al. 1996). Active-site remodeling is another mechanism observed in anthrax adenylyl cyclase. Binding of CaM leads to reconstruction of the binding site of the enzyme (Drum et al. 2002). The activation by CaM in a 2:2 ratio of CaM:target was also observed in SK2 K^+ channel activation (Schumacher et al. 2001). Yap et al. (2003) found that one molecule of CaM could bind to two C-terminal peptides of *Petunia hybrida* GAD simultaneously, thus stabilizing the multimeric complex. The last model involve in the occupying of ligand binding domain by CaM. It has been reported that tobacco plasma-membrane channel protein contains cyclic nucleotide-binding domain coincided with CaM binding domain (Arazi et al. 2000). Additionally, the competitive binding of CaM and a protein competitor with an overlapped binding site on target protein was also found. CaM can insert itself between the motor, kinesin-like CaM binding protein, and the microtubule causing negative regulation of intracellular transport by CaM (Vinogradova et al. 2008).

Indirect response refers to an altered cellular process affected by calmodulin-modulated gene expressions. These relatively slow (minutes to days) response takes place after transcription and translation processes (Snedden and Fromm 1998). There are many transcription factors and DNA-binding proteins reported to have interaction with CaM, such as Cauliflower nuclear protein TGA3, Arabidopsis CAMTAs family, and Arabidopsis WRKY7 transcription factor (Szymanski et al. 1996; Bouche et al. 2002; Yang and Poovaiah 2003; Park et al. 2005). So, through the actions of CaM-regulated transcription factors, wider range of cell activities could be affected since a single transcription factor could regulate a set of gene expressions.

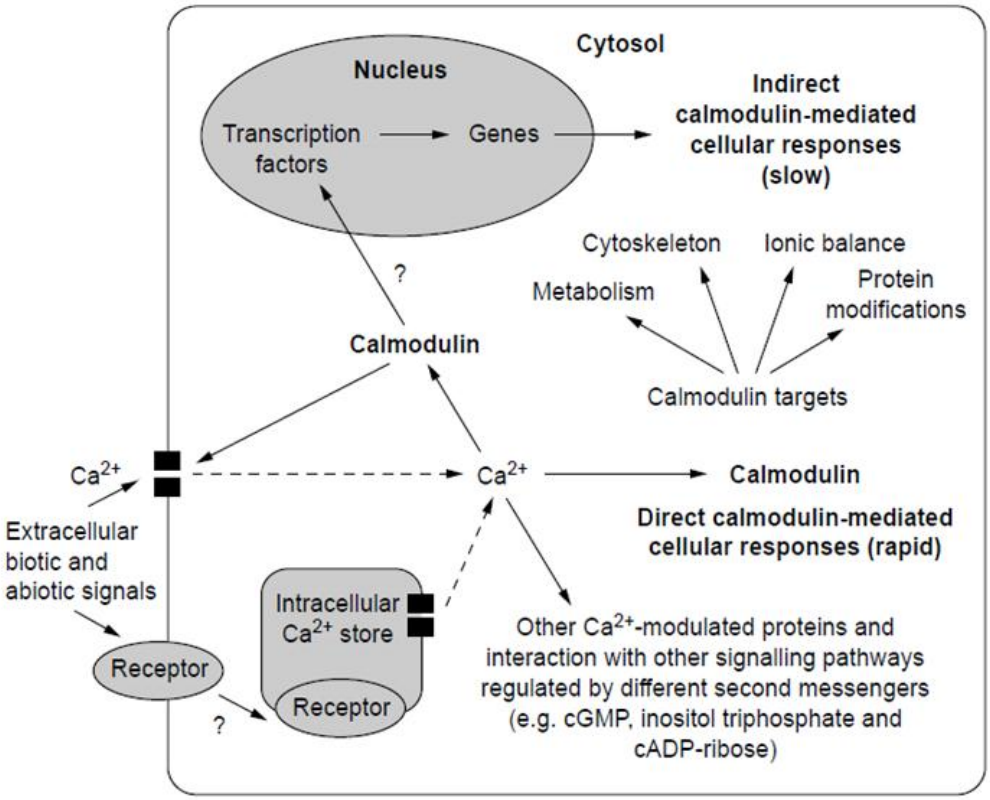

Figure 4. Calmodulin-mediated cellular responses. Detection of stress signals leads to an increase in Ca^{2+} concentration in the cytoplasm. Calcium-bound calmodulin could bind to its targets regulating metabolisms involving cytoskeleton, ionic balance, and protein modification for direct calmodulin-mediated cellular response. Moreover, calmodulin affects gene expression probably through the interaction with transcription factors for indirect calmodulin-mediated cellular response (taken from Snedden and Fromm (1998)).

Table 2. Calmodulin-binding proteins in plant (modified from Snedden and Fromm (1998))

Category	Protein	Function	Reference
Metabolism	Glutamate decarboxylase	catalyze conversion of L-glutamate to Ɣ-aminobutyric acid	Baum et al., 1996; Snedden et al., 1996; Bown and Shelp, 1997
	NAD kinase	catalyze conversion of NAD to NADP	Harding et al., 1997
	Apyrase	catalyze hydrolysis of ATP to AMP and Pi	Hsieh et al., 1996
Phosphorylation	Ca^{2+} binding, Ca^{2+}-CaM-dependent protein kinase (CCaMK)	catalyze phosphorylation reaction	Ramachandiran et al., 1997
	Kinase homologue (MCK1)	catalyze phosphorylation reaction	Lu et al., 1996
Ion transport	Ca^{2+} ATPases (BCA1 and ACA2)	endomembrane Ca^{2+} pump	Harper et al., 1998; Malmstrom et al., 1997
	Transporter-like (HvCBT1)	probable ion transporter	Schuurink et al., 1998
Cytoskeleton function	Kinesis-like (KCBP)	motor domain protein	Oppenheimer et al., 1997; Narasimhulu et al., 1997
	Elongation factor-1α (EF-1α)	translation elongation factor	Durso and Cyr, 1994
	Myosin (MYA1)	motor protein	Kinkema and Schiefelbein, 1994
DNA binding	Basic leucine zipper protein (TGA3)	transcription factor	Szymanski et al., 1996

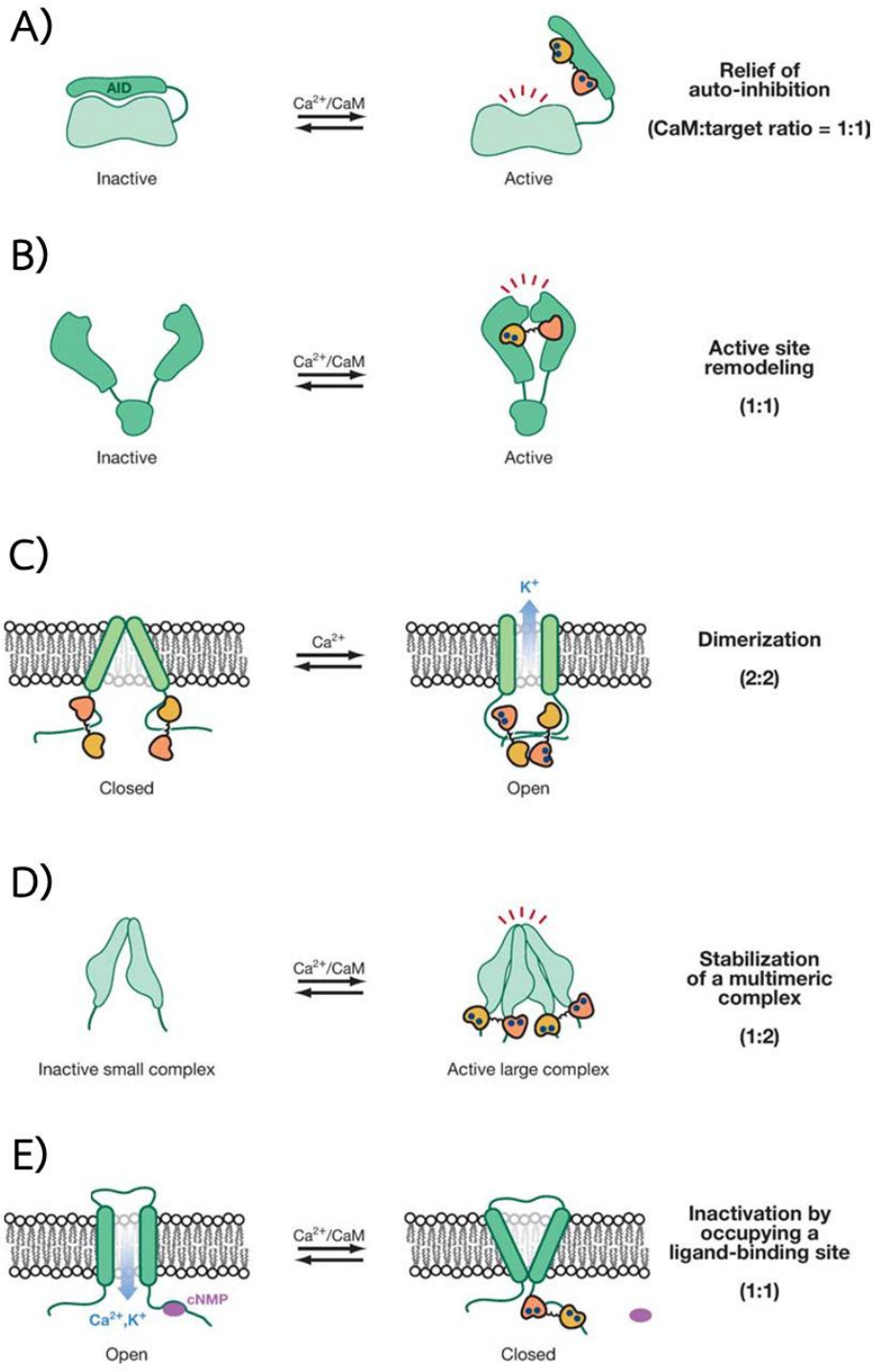

Figure 5. Mechanisms of CaM-mediated protein modulation. Five model mechanisms involve CaM binding with target proteins, **A)** relief of auto-inhibition, **B)** active site remodeling, **C)** dimerization, **D)** stabilization of multimeric complex, and **E)** inactivation by occupying a ligand-binding site (taken from Bouche et al. (2005)).

Boonburapong and Buaboocha (2007) screened rice genomic sequence and identified five rice calmodulin genes (*OsCaMs*) sharing >98.7% identity among each other. *Os*CaM1-1 (Os03g0319300), *Os*CaM1-2 (Os07g0687200), and *Os*CaM1-3 (Os01g0267900) were found to have exactly the same amino acid sequences while *Os*CaM2 (Os05g0491100) and *Os*CaM3 (Os01g0279300) have two different amino acids from that of *Os*CaM1-1. Even though many rice CaM isoforms were found in the rice genome, only *OsCaM1-1* is clearly up-regulated under salt stress condition. The up-regulation of a single CaM shows that Ca^{2+}-mediated signal transduction pathway in plant is delicately regulated and highlights the importance of *OsCaM1-1* in plant acclimation to the stress (Phean-o-pas et al. 2005). Apart from salinity stress, the stress-inducible expressions of *OsCaM1-1* were also found to be responded to heat, wounding, and osmotic stresses (Phean-o-pas et al. 2005; Wu et al. 2012). These findings lead to many studies about *OsCaM1-1*. The predicted promoter region of *OsCaM1-1* was fused with *gus* reporter gene for the expression analysis. It was found that *OsCaM1-1* promoter could drive the expression in many organs and tissues, including leaf blades, leaf sheaths, roots, lateral roots, stigmas, and panicles (Phean-o-pas et al. 2008). *Os*CaM1-1 overexpressing lines of rice and Arabidopsis were also generated to study the roles of this CaM. Analysis of transgenic Arabidopsis overexpressing *OsCaM1-1* showed that this CaM induced the expression of heat shock responsive genes at non-inducing temperature. *OsCaM1-1*-overexpressing Arabidopsis also shows higher germination rate at high temperature comparing with wild type (Wu et al. 2012). Saeng-ngam et al. (2012) demonstrated that *Os*CaM1-1 could induce abscisic acid (ABA) biosynthesis observing that the ABA content strongly correlates with *OsCaM1-1* expression. They also found that the overexpression of *OsCaM1-1* in rice up-regulates the ABA synthesizing genes and promotes the salt-tolerant capability of transgenic rice. These results substantially suggest that *Os*CaM1-1 plays an important role in plant acclimation to stresses. However, the comprehensive understanding on these stress-tolerant mechanisms in the transgenic plants overexpressing *OsCaM1-1* remains to be clarified. By assessing the effects of *OsCaM1-1* overexpression at transcriptome and metabolome levels, this information

would help reveal the role of *Os*CaM1-1 *in vivo* and clarify how the transgenic plant exhibited higher tolerant to abiotic stresses.

1.4 cDNA-AFLP

Although DNA microarray is a powerful technique for gene expression study at transcriptomics level, its major drawback is that genomic/transcript sequences of the organism of interest have to be available beforehand. cDNA-AFLP is a technique that allows genome-wide expression analysis in any organism without any prior knowledge. Some other advantages of cDNA-AFLP are relatively low cost, availability of gene discovery, and ability to distinguish highly homologous genes (Reijans et al. 2003; Vuylsteke et al. 2007). cDNA-AFLP procedure (Figure 6) includes (1) double strand cDNA (ds-cDNA) synthesis from RNA samples, (2) restriction digestion of ds-cDNA pool with two restriction enzymes creating sticky ends, (3) ligation with DNA adaptors at digested termini to create primary template, (4) production of secondary template by pre-amplification of primary template using primers complementary to the adaptor sequences, enriching transcript-derived fragments (TDFs), (5) selective-amplification by selective primers extended with a few specific bases which would subsequently bind TDF sequence connecting with the adaptor region, amplifying specific sets of TDFs, and (6) separation of TDFs by size using denaturing polyacrylamide gel electrophoresis (denaturing-PAGE) creating cDNA-AFLP transcript profiles (Bachem et al. 1998). Following the protocol, different set of TDFs will be amplified by changing specific nucleotide(s) at 3' ends of the selective primers (creating new primer combination, PC) generating new transcript profiles. Eventually, the use of many PCs would lead to genome-wide expression analysis. TDFs with interesting expression pattern could be retrieved from the gel by normal diffusion in nuclease-free water before the amplification by corresponding selective primers.

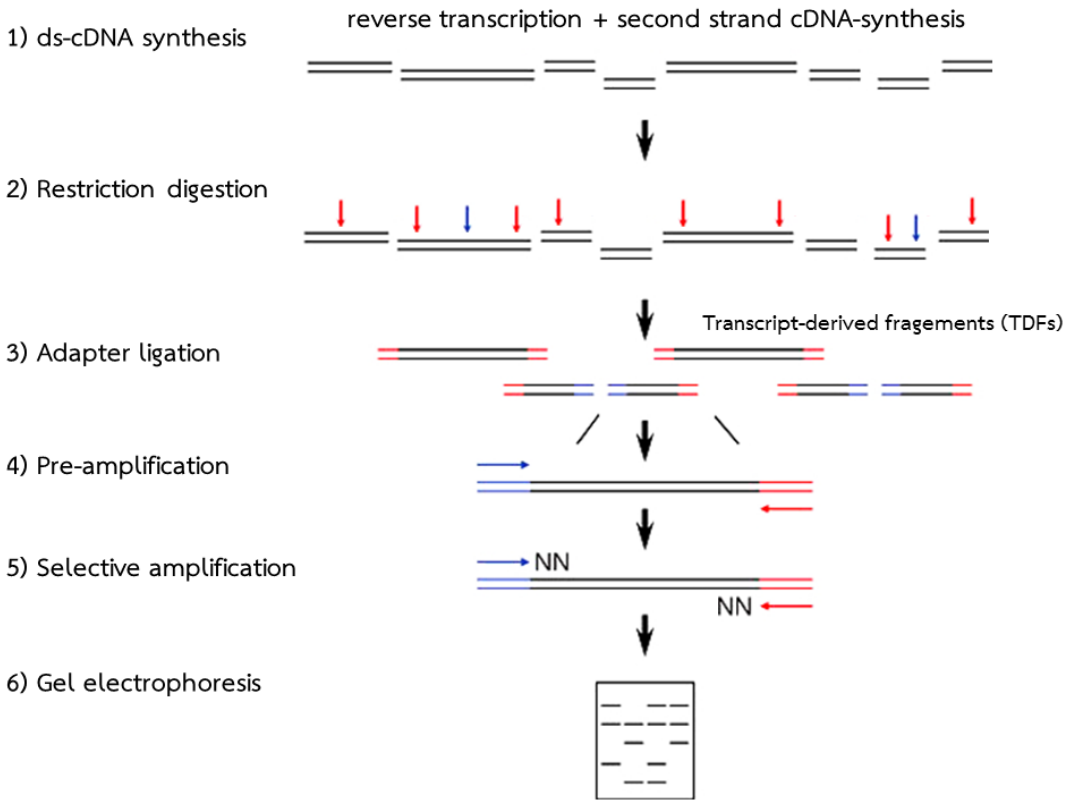

Figure 6. Steps in cDNA-AFLP. (1) double strand cDNA synthesis from mRNA sample; (2) restriction digestion by two different restriction enzymes indicated by arrows with different colors; (3) adapter ligation at digested termini with DNA adapters possessing complementary sticky ends to sites created by each restriction enzyme; (4) pre-amplification of adapter-ligated TDFs by oligonucleotide primers specific to DNA adapter sequences; (5) selective-amplification using selective primers with extended nucleotides (N denotes four possible nucleotides A, T, C, or G which generates PC diversity) to increase specificity with specific set of TDFs; and (6) separation of TDFs by denaturing-PAGE produces cDNA-AFLP transcript profiles (modified from Chial (2008)).

Many studies have been conducted to optimize and develop cDNA-AFLP technique. Silver staining protocols have successfully been used instead of radioisotope labeling for cDNA-AFLP fingerprinting (Xiao et al. 2009). Bachem et al. (1998) studied the effect of many parameters such as PCR cycle number, template dilution, and $MgCl_2$ concentration during amplification. Vuylsteke et al. (2007) provided very good considerations on the choice of restriction enzymes. Two restriction enzymes with short recognition sites, e.g. 4-base cutter often maximize the coverage of the transcriptome, however produces short less-informative TDFs. For the sample with no extensive sequence data available, informative tag could facilitate in the functional annotation of the TDFs. Short restriction site also generates redundant TDFs, i.e. many TDFs representing the same transcript, hence, the identification of interested TDFs might lead to the same transcript. A one-gene-one-tag cDNA-AFLP was developed to decrease the number of TDFs to be analyzed while maintaining the cDNA coverage. The detailed protocol was described in Vuylsteke et al. (2007). The use of *in silico* analysis for choosing appropriate restriction enzyme combination was also demonstrated, for example, in yeast (Reijans et al. 2003) and Arabidopsis (Breyne et al. 2003). With prior knowledge in genomic sequence or expressed sequence tag library, computational analysis can be conducted to predict percentage of the coverage, mean fragment length, or average redundancy of a specific restriction enzyme combination.

cDNA-AFLP was successfully used to identify genes involving in many biological processes of many plant species. Sojikul et al. (2010) identified candidate genes for storage root initiation and development of cassava. In rice, cDNA-AFLP was used to identify Rice Yellow Mottle virus and wounding associated genes for more understanding on rice-pathogen interaction (Ventelon-Debout et al. 2008). The study of salt-responsive gene expression in *Seteria italica* L. was also achieved by cDNA-AFLP (Jayaraman et al. 2008). Although the rice genome is available, in this study, cDNA-AFLP was used to identify differentially expressed gene in transgenic rice overexpressing *OsCaM1-1* because of its relatively low cost compared to other techniques, such as microarray and RNA sequencing.

1.5 Metabolomics and plant stress response

Metabolomics is a powerful tool which can reflect a metabolic status of a biological system at specific time points. It involves the comprehensive and quantitative analyses of all small molecules in the system. As a result, metabolomics is extensively used to understand metabolic networks and adaptations in many plants and other organisms during the past decade. The nature of metabolomics and its use for the studies of plant stress response were well reviewed (Shulaev et al. 2008; Obata and Fernie 2012). Generally, metabolomics could be achieved by several techniques, e.g. gas chromatography-mass spectrometry (GC-MS), liquid chromatography (LC)-MS, capillary electrophoresis (CE)-MS, and nuclear magnetic resonance (NMR) spectroscopy. Each technique has its own advantages to meet broad requirement of each particular study.

At present, GC-MS is a popular platform for plant metabolite profiling. Long history of GC-MS utilization has resulted in the development of stable protocols. It made available the sharing of retention time and mass spectral libraries of standard compounds between laboratories. However, like GC, GC-MS can only analyze thermally stable volatile compounds. This limitation restricts the analysis of high molecular weight compounds by this technique. According to these properties, GC-MS can cover a few hundreds of metabolites from plant samples including sugars, sugar alcohols, organic acids, amino acids, and polyamines which pretty much cover the primary metabolism of the plant. LC-MS separates compounds in liquid phase, thus, wide range of metabolites could be analyzed by this technique. Moreover, many kinds of column are available, making LC-MS a potent technique in analyzing a wide range of metabolites. Normally, LC-MS is used to analyze plant secondary metabolites and phytohormones to complement GC-MS analysis. Nonetheless, the main disadvantage of LC-MS is the difficulty in metabolite annotation. Due to highly flexible protocols and many instrument types, mass spectral and retention time can be varied among laboratories. In-house reference mass library is usually needed for the metabolite identification. CE-MS separates compounds by their charge-to-mass ratio. It needs only nanolitres of sample for each analysis and provides very high

separation efficiency. However, CE-MS has low reproducibility regarding migration time of each compound and enrichment of metabolites may be needed for the analysis of low abundant metabolites (Monton and Soga 2007). At present, the use of CE-MS in plant metabolomics studies is relatively low. The properties of metabolites which could be analyzed by each technique are shown in Figure 7. NMR is a non-MS-based technique which relies on the re-emission of electromagnetic radiation of certain molecules under strong magnetic field. The structural information of compound annotated by this technique could be better than MS-based techniques. NMR also allows non-destructive and subcellular measurement (Ratcliffe and Shachar-Hill 2005; Terskikh et al. 2005; Eisenreich and Bacher 2007). However, the sensitivity of this technique and number of detected compounds in a single analysis is much lower than the others.

Metabolomics is an approved platform used by many researchers in the field of plant study. It was used to study plant metabolic responses against many kinds of biotic and abiotic stresses such as, water stress (Urano et al. 2009; van Dongen et al. 2009), temperature stress (Kaplan et al. 2004), light stress (Kusano et al. 2011), ion stress (Gong et al. 2005; Kim et al. 2007), oxidative stress (Baxter et al. 2007; Lehmann et al. 2009; Lehmann et al. 2012), insect infestation (Kant et al. 2004), pathogen challenge (Allwood et al. 2010; Lopez-Gresa et al. 2010) and even combination of stresses (Rizhsky et al. 2004; Wulff-Zottele et al. 2010). It was also used to determine the effect of transgene insertion. Due to its non-target nature, it could be used to identify unintended or hidden adverse effects of transgene expression in the transgenic plants (Zhou et al. 2009; Kogel et al. 2010).

In the case of abiotic stress, normal growth is restrained by unfavourable growth conditions. It involves in the perturbation of homeostasis which leads to metabolic reprogramming. Plant acclimation usually associates with accumulation of anti-stress metabolite such as antioxidants and compatible solutes. Such adaptations could be observed by metabolomics. It enables us to track down the metabolite levels and changes in metabolic flux of each pathway of stressed plant. For example, many studies had used metabolomics to study extremophiles or compare stress-tolerant and stress-sensitive plant acclimations to the stress (Widodo et al. 2009; Liu

et al. 2011; Sanchez et al. 2011; Wu et al. 2012). The understanding of successful adaptation existing in nature would be beneficial for crop development.

These extensive studies supported that metabolomics is a powerful tool for the study of metabolic response in plant and could undoubtedly reveal the metabolic changes in the salt-tolerant transgenic rice used in this thesis. The metabolic reconfiguration caused by the overexpression of stress-counteracting *Os*CaM1-1 would shed the light on how the transgenic rice could become more tolerant to salt stress. Together with gene expression analysis, gene-to-metabolite correlations could explain the link between the point of perturbation and response endpoints for better understanding of the biological roles of *Os*CaM1-1.

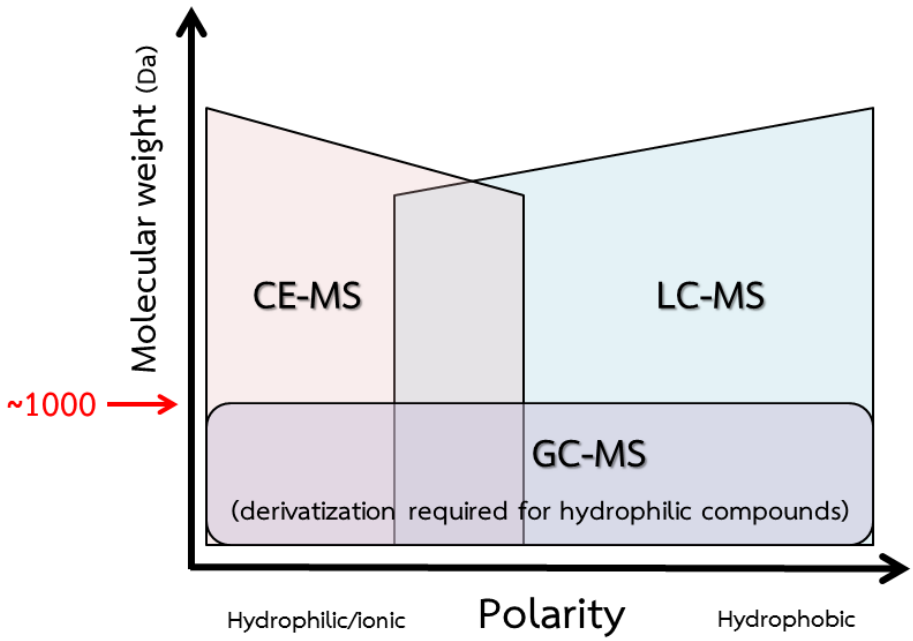

Figure 7. Analysis range of each technique used in metabolomics. GC-MS analyzes low-molecular weight compounds while LC and CE –MS could analyze wider ranges of metabolites, however, with lower reproducibility than GC-MS (modified from Agilent poster presentation, Metabolomics 2014 conference, June 23th-26th, 2014).

CHAPTER II

MATERIALS AND METHODS

2.1 Materials

2.1.1 Antibiotics

Ampicillin (Sigma Chemical Co., USA)

2.1.2 Chemicals and reagents

40% acrylamide/bis solution, 19:1 (BIO-RAD, USA)

40% formaldehyde (Carlo Erba Reagenti, Italy)

Absolute ethanol (AnalaR NORMAPUR, Ireland)

Adenosine 5'-triphosphate (ATP) disodium salt (Fluka, Germany)

Agar powder (Himedia®, India)

Agarose (Bioline, UK)

Ammonium persulfate: $(NH_4)_2S_2O_8$ (Sigma Chemical Co., USA)

Bind silane (Sigma Chemical Co., USA)

Boric acid (Ajax Finechem Pty Ltd, New Zealand)

Bromophenol blue (Carlo Erba Reagenti, Italy)

Calcium chloride (Carlo Erba Reagenti, Italy)

Ethylenediaminetetraacetic acid (Bio Basic Canada Inc., Canada)

GelRed nucleic acid gel stain (Biotium, USA)

Glacial acetic acid (Merck, Germany)

Glycerol (Ajax Finechem Pty Ltd, New Zealand)

Hydrochloric acid (Merck, Germany)

Peptone (Merck, Germany)

Potassium chloride (Carlo Erba Reagenti, Italy)

Repel silane (Karshine, Thailand)

RiboLock RNase Inhibitor (Thermo Scientific, USA)

Silver nitrate (Fisher Scienctific, USA)

Sodium carbonate (Carlo Erba Reagenti, Italy)

Sodium chloride (Ajax Finechem Pty Ltd, New Zealand)

Sodium thiosulfate (AnalaR NORMAPUR, Ireland)

Sucrose (Mitr Phol, Thailand)

TEMED: $(CH_3)_2NCH_2CH_2N(CH_3)_2$ (Invitrogen, USA)

TRI Reagent® (Molecular Research Center, USA)

Tris (SAFC, Switzerland)

Urea (AnalaR NORMAPUR, Ireland)

Yeast extract (Merck, Germany)

2.1.3 Enzymes

Restriction endonucleases: *Eco*RI and *Mse*I (New England Biolabs, UK)

RevertAid H Minus Reverse Transcriptase (Thermo Scientific, USA)

RNase-Free DNase set (Qiagen, Germany)

Taq DNA polymerase (New England Biolabs, UK)

2.1.4 Instruments

Autoclave: Labo Autoclave MLS-3020 (Sanyo Electric Co., Ltd., Japan)

Balance: PB303-L (Mettler Toledo, USA)

Gel documentation apparatus: Gel Doc™ (Syngene, England)

Gel electrophoresis apparatus: Mupid®-exU (Advance Co., LTD, Japan)

Gel electrophoresis apparatus: Sequi-Gen GT System (BIO-RAD, USA)

Gel scanner: Image Scanner III (GE Healthcare, UK)

Hot plate stirrer: C-MAG HS 7 (IKA, Malaysia)

Incubator shaker: Innova™ 4000 (New Brunswick Scientific, UK)

Incubator shaker: Kuhner shaker (Kuhner, Switzerland)

Larminar flow: Bio Clean Bench (SANYO, Japan)

Lyophilizer: Freezone 2.5 (Labconco, USA)

Magnetic stirrer: Fisherbrand (Fisher Scienctific, USA)

Microwave oven: R-362 (SHARP, Thailand)

Mixer mill: MM400 (Retsch®, Germany)

PCR: T100™ Thermal Cycle (BIO-RAD, USA)

pH meter: S220 Seven compact™ pH/ion (Mettler Toledo, USA)

Power supply: PowerPac™ HV high-voltage power supply (BIO-RAD, USA)

Refrigerator: Ultra low temperature freezer (New Brunswick Scientific, UK)

Refrigerated centrifuge: Legend XTR (Thermo Scientific, USA)

Refrigerated centrifuge: Universal 320R (Hettich, Switzerland)

Spectrophotometer: DU® 530 (Beckman Coulter™, USA)

2.1.5 Glasswares and plasticwares

1.5-ml microcentrifuge tube (Axygen Hayward, USA)

0.2 ml PCR thin wall microcentrifuge tube (Axygen Hayward, USA)

10-, 100-, 1000-µl pipette tips (Axygen Hayward, USA)

45 cm diameter polyethylene pots

Glass bottles

NIPRO disposable syringe (Nissho, Japan)

Quartz cuvette: Hellma 105.201-QS (sigma-aldrich, USA)

2.1.6 Kits

CloneJET PCR cloning kit (Thermo Scientific, USA)

Gel/PCR DNA Fragments Extraction Kit (Geneaid, Taiwan)

iScript™ cDNA Synthesis Kit (BIO-RAD, USA)

iScript™ reverse transcription supermix for RT-qPCR (BIO-RAD, USA)

Magnetic mRNA Isolation Kit (New England Biolabs, UK)

NEBNext® mRNA Second Strand Synthesis Module (New England Biolabs, UK)

Presto™ Mini Plasmid Kit (Geneaid, Taiwan)

RNeasy® Plant Mini kit (Qiagen, Germany)

SsoFast™ Evagreen® Supermix (BIO-RAD, USA)

2.1.7 Microorganisms

Escherichai coli strain DH5α

2.1.8 Oligonucleotide primers

All oligonucleotide primers used were synthesized by BIO BASIC Int, Canada

2.1.9 Plant materials

Rice seeds were kindly provided by Assoc. Prof. Teerapong Buaboocha, Ph.D.

- Rice seeds (*Oryza sativa* L. ssp. Indica cv. KDML105): wild type
- Transgenic rice seed of homozygous lines (*Oryza sativa* L. ssp. indica cv. KDML105): 2 lines of transgenic rice overexpressing *OsCaM1-1* (35S::*OsCaM1-1*::Nos), The fifth generation of transgenic line 1 and the fourth generation of transgenic line 7

- Transgenic rice seeds (*Oryza sativa* L. ssp. indica cv. KDML105): control transgenic rice (transformed by empty vector, pCAMBIA1301)

2.1.10 Software and database

Calmodulin Target Database (http://calcium.uhnres.utoronto.ca/ctdb)

CFX manager software (BIO-RAD, USA)

ClustalW (http://www.ebi.ac.uk/Tools/clustalw2/index.html)

JMP® software (SAS Institute Inc., USA)

NCBI (http://www.ncbi.nlm.nih.gov/)

Phytozome (http://www.phytozome.net/)

SIMCA software (Umetrics, Sweden)

2.2 Growth medium

Luria-Bertani broth (LB medium) (Maniatis and Fritsch 1982)

LB medium consist of 1% peptone, 1% NaCl, and 0.5% yeast extract. Reagents were dissolved in deionized water (DI water) and pH was adjusted to 7.0 by NaOH. For LB agar, agar powder was added into LB medium to make final concentration of 1.5%. The medium were autoclaved at 121°C, 15 psi for 15 min. Antibiotics of choice can be added after the medium cooled down.

Modified Yoshida's nutrient solution (modified from Yoshida et al. (1976))

Stock solutions (800x) of Yoshida's nutrient solution containing major and trace elements for plant growth was prepared with components in Table 3. Stock solutions were autoclaved for long term storage. Yoshida's nutrient solution was prepared by mixing 1.25 ml of each stock solution and brought up to 800 ml by DI water. The volume was then adjusted to 1 L after pH was adjusted to 5.8 by NaOH.

Table 3. Preparation of Yoshida's stock solution (modified from Yoshida et al. (1976))

Element	Reagent (AR grade)	Preparation (g/100 ml)	
N	NH_4NO_3	9.14	
P	$NaH_2PO_4 \cdot 2H_2O$	4.03	
K	K_2SO_4	7.14	
Ca	$CaCl_2$	8.86	
Mg	$MgSO_4 \cdot 7H_2O$	32.4	
Mn	$MnCl_2 \cdot 4H_2O$	150 mg	Dissolve separately; then combine with 5 ml of concentrated H_2SO_4. Make up to 100 ml with distilled water.
Mo	$(NH_4)_6 \cdot Mo_7O_{24} \cdot 4H_4O$	7.4 mg	
B	H_3BO_3	93.4 mg	
Zn	$ZnSO_4 \cdot 7H_2O$	3.5 mg	
Cu	$CuSO_4 \cdot 5H_2O$	3.1 mg	
Fe	$FeCl_3 \cdot 6H_2O$	770 mg	
	Citric acid (monohydrate)	1190 mg	

2.3 Methods

2.3.1 Rice cultivation

Four lines of rice seeds, namely, wild type (WT), transgenic line1 (T1), transgenic line7 (T7), and control transgenic line (BV) were surface sterilized before germination. Seeds were immersed in 70% ethanol for two min, soaked in 35% Heiter (Kao, Thailand) for 15 min with shaking, and rinsed for four times by DI water. Sterilized seeds were germinated in DI water at room temperature without light. DI water was replaced daily until white rice shoot grows 1-2 cm in length. Germinated seeds were then transferred onto 2x2 cm^2 plastic net placing on floating plastic raft supplemented with 0.5x Yoshida's nutrient solution. At least seven germinated seeds were placed on each net, were put in a growth chamber with controlled condition, 16h light/8h dark photoperiod at 25°C; 6000 lux light intensity; and 80% relative humidity, and were started counting as day 1. Half strength Yoshida's solution was added to maintain the solution level. After one week, each plastic net with rice plants was moved into separate glass bottle supplemented with Yoshida's solution. The cultivation continues in the growth chamber and rice samples were collected at 2-week-old. Rice leaves and roots were collected separately. Samples were wrapped in aluminium foil and frozen by liquid nitrogen. Rice samples were stored at -80°C until use. Each rice line was grown in six replicates for metabolomics. For cDNA-AFLP, one plant from each replicate was pooled into one sample.

Rice samples for gene expression analysis by real-time quantitative reverse transcription PCR (real-time qRT-PCR) were prepared by Mr. Worawat Yuenyong. In short, rice seeds were sterilized by similar method (75% ethanol for 3 min, 35% Heiter for 15 min) and germinated in DI water for 3 days. Rice was grown in 0.5x Yoshida's solution in growth chamber during the first week, then, moved to grow hydroponically in Yoshida's solution in transgenic green house for 2 weeks. Rice plants were grown in a completely randomized design. After 3 weeks, non-treated plants were collected, frozen immediately in liquid nitrogen, and stored at -80°C. NaCl stress treatment was applied to rice plants by transferring the plants into

Yoshida's solution containing 150 mM NaCl for 3 hr. Salt-treated rice samples were collected using the same procedure. Each line of rice was grown in four replicates.

2.3.2 RNA extraction and cDNA synthesis

Rice mRNAs were isolated using magnetic mRNA isolation kit (New England Biolabs, UK) for cDNA-AFLP experiment. Rice samples were retrieved from -80°C and immediately placed in liquid nitrogen. Mixer mill MM400 (Retsch, Germany) was used to powderize plant samples at 30 Hz for 30 seconds. Approximately 100 mg of ground sample was used for RNA extraction. RevertAid H minus reverse transcriptase (Thermo Scientific, USA) was used to synthesize first strand cDNA. The reaction mixtures were then used to synthesize double-stranded cDNA by NEBNext® mRNA second strand synthesis module (New England Biolabs, UK) following manufacturer instructions.

For real-time qRT-PCR experiment, rice samples were ground using pre-chilled mortars and pestles. Total RNAs were extracted using TRI reagent (Molecular Research Center, USA) following the manufacturer protocol. Total RNAs were incubated with DNase (Fermentas, USA) for 1 hr at 37°C followed by heat-inactivation at 65°C for 10 min. One microgram of DNase-treated RNAs was used for cDNAs synthesis using iScript™ reverse transcription supermix for RT-qPCR (BIO-RAD, USA).

2.3.3 Determination of DNA and RNA concentration

DNA or RNA concentrations were determined using spectrophotometry. Nucleic acid concentrations can be calculated using absorbance at 260 nm (A_{260}) of the solution. DNA solution has the concentration of 50 μg/ml when A_{260} is equal to 1 while RNA solution is 40 μg/ml.

2.3.4 Semi-quantitative RT-PCR analysis

Semi-quantitative RT-PCR was used to confirm *OsCaM1-1* overexpression in transgenic rice T1 and T7. cDNAs of rice samples were used as templates. PCRs were performed using *Taq* DNA polymerase with *OsCaM1-1* specific primers, OsCaM1-1-F:

5’-CACCATGGCGGACCAGCTCACC-3’; and OsCaM1-1-R: 5’-TCACTTGGCCATCATGACCT TG-3’, yielding a 454 bp-long PCR product. The PCR conditions for *OsCaM1-1* amplification were as follows: 3 min at 94˚C, 26 cycles of 30 sec at 94˚C; 30 sec at 58˚C; and 45 sec at 72˚C, followed by 5 min at 72˚C.

The PCR products were run in 1% agarose gel electrophoresis. *OsEF-1α* was used as an internal control for initial amount of cDNA in each PCR reaction (primers: OsEF-1α-F, 5’-AGATCAACGAGCCCAAGAG-3’ and OsEF-1α-R, 5’-GCAAAACGACCAAGAGG AG-3’; 574 bp amplicon). PCR condition for *OsEF-1α* amplification was as follows: 3 min at 94˚C, 28 cycles of 30 sec at 94˚C; 30 sec at 60˚C; and 45 sec at 72˚C, followed by 5 min at 72˚C.

2.3.5 cDNA-AFLP (modified from Vuylsteke et al. (2007))

2.3.5.1 Restriction digestion

Five hundred nanograms of double-stranded cDNAs were double digested by 10 U of *Eco*RI-HF and *Mse*I (New England Biolabs, UK) to create sticky ends for DNA adaptors ligation. Following components were prepared in a 0.2 ml tube:

component	volume
10x NEB buffer4	5 µl
100x BSA	0.5 µl
*Eco*RI-HF (20,000 U/ml)	0.5 µl
*Mse*I (10,000 U/ml)	1 µl
template (double-stranded cDNA)	500 ng
nuclease-free water	to 50 µl
total volume	50 µl

The reactions were incubated at 37˚C for 3 hr followed by heat-inactivation at 65˚C for 20 min. Reaction mixtures were allowed to cool down to room temperature before ligation.

2.3.5.2 Adaptor ligation

Digested cDNAs were ligated with respective DNA adaptors (Eco-F: 5'-CTCGTAGACTGCGTACC-3', Eco-R: 5'-AATTGGTACGCAGTCTAC-3', Mse-F: 5'-GACGATGAGTCCTGAG-3', Mse-R: 5'-TACTCAGGACTCAT-3') to produce primary template. Ligation mixture was prepared in a 0.2 ml tube:

component	volume
EcoRI adaptor (5 μM)	1 μl
MseI adaptor (50 μM)	1 μl
10x NEB buffer4	1 μl
100x BSA	0.1 μl
ATP (20 mM)	3 μl
*Eco*RI-HF (20,000 U/ml)	0.05 μl
ligase (40,000 U/ml)	0.5 μl
nuclease-free water	3.35 μl
total volume	10 μl

Ten microliters of ligation mixture were added into each tube of heat-inactivated double digestion reaction and incubate at 37˚C overnight.

2.3.5.3 Pre-amplification

Pre-amplifications were performed to amplify primary templates (digested cDNA flanked by DNA adaptors) using adaptor-specific primers (Eco: 5'-GACTGCGTACCAATTC-3', and Mse: 5'-GATGAGTCCTGAGTAA-3'). Following components were prepared in a 0.2 ml tube:

component	volume
10x *Taq* buffer	5 μl
dNTPs (10 mM)	1 μl
Eco (10 μM)	1.5 μl

component	volume
Mse (10 μM)	1.5 μl
nuclease-free water	37.75 μl
Taq DNA polymerase	0.75 μl
primary template	2.5 μl
total volume	50 μl

The amplification condition was as follows: 30 sec at 94˚C, 25 cycles of 30 sec at 94˚C; 30 sec at 56˚C; and 45 sec at 72˚C, followed by 30 sec at 72˚C. The amplification products were called as secondary templates. They were diluted 50-fold for using in selective amplification.

2.3.5.4 Selective amplification

Selective amplification consists of amplifications by many PCs to yield different transcript profiles. Selective primers specifically bind to adaptors with additional two nucleotides at 3' end which bind to specific TDF sequence accordingly (Eco-NN: 5'-GACTGCGTACCAATTCNN-3', and Mse-NN: 5'-GATGAGTCCTGAGTAANN-3'). Following components were prepared in a 0.2 ml tube for selective amplification:

component	volume
10x *Taq* buffer	2 μl
dNTPs (10 mM)	0.4 μl
Eco-NN (10 μM)	0.2 μl
Mse-NN (10 μM)	0.6 μl
nuclease-free water	11.5 μl
Taq DNA polymerase	0.3 μl
diluted secondary template	5 μl
total volume	20 μl

The amplification condition was as follows: 5 min at 94°C, a touchdown program of 13 cycles of 30 sec at 94°C; 30 sec at 65-0.7°C each cycle; and 1 min at 72°C, followed by 28 cycles of 30 sec at 94°C; 30 sec at 56°C; and 1 min at 72°C, finished with 5 min at 72°C. Selective amplification products were subjected to denaturing PAGE to separate amplified TDFs by size and create cDNA-AFLP transcript profiles.

2.3.6 Denaturing PAGE using Sequi-Gen® GT Nucleic Acid Electrophoresis Cell (BIO-RAD, USA)

Gel casting and electrophoresis were done following the manufacturer's instruction.

2.3.6.1 Gel casting

Glass plates were treated with chemicals using lint-free paper for convenient gel handling: long glass plate was wiped with 95% ethanol for 3 times, 0.5% bind silane in 10% acetic acid once, and another 95% ethanol for 3 times; short glass plate was wiped with 95% ethanol for 3 times followed by repel silane once. Spacer (0.4 mm thick) was placed in between treated glass plates. The glass plate sandwich was clamped and assembled into gel-caster base. Immediately after adding TEMED and ammonium persulfate to polymerize polyacrylamide solution (4.5% acrylamide/Bis (19:1) + 7.5 M urea in 0.5x TBE), a syringe was used to slowly transfer 50 ml of the polymerizing gel into glass plate sandwich starting at the bottom of gel-caster base. After the gel solution reached the far side of the glass plate, the flat edge of shark tooth comb was then inserted into the sandwich. More gel was injected to flood the comb. The syringe was left at the gel caster base until complete polymerization.

2.3.6.2 Electrophoresis

Glass plate sandwich with polymerized gel was assembled into electrophoresis cell. Proper amount of 1x TBE was added into the upper and lower chamber of the cell connecting to PowerPac™ HV power supply (BIO-RAD, USA). The gel was pre-run at constant 50 W allowing the temperature of the system to rise to

50˚C, observing from gel temperature indicator. Selective amplification reactions were mixed with formamide dye (1-2:1 sample/dye ratio). Mixed samples were heat-denatured at 95˚C for 5 min and immediately transferred into cold rack or ice-cold water to prevent renaturation of TDFs. After the pre-run, power supply was paused and shark tooth comb was removed creating a big well with flat gel surface. Unpolymerized gel was extruded from the gel surface by continuous pipetting of 1x TBE into the well. Shark tooth comb was flipped and inserted onto flat gel surface to create wells by slightly pick pointy edges of the comb into gel surface. Denatured samples were then loaded into the wells. AFLP products of leaves and roots of WT and T1 rice were run alongside to compare cDNA-AFLP transcript profiles. These processes should be done quickly since the temperature dropped overtime. The run was continued at constant 50 W (approximately 2000 V and 24 mA) for 1 hr or until bromophenol blue approaches the gel base. Electrophoresis cell was then disassembled and the gel would stick to the long glass plate.

2.3.7 Silver staining

Silver staining was done to visualize the cDNA-AFLP transcript profiles (modified from Bassam et al. (1991)). Long glass plate with gel sticking at one side was put in a tray and submerged in the following solutions (appendix C) in order: fix solution for 30 min, DI water for 2 min; 3 times, silver staining solution for 30 min, DI water for 5 sec, and refrigerated developer. Tray was placed on an orbital shaker shaking at 105 rpm in every step. Bands will appear as the temperature of the developer rises. Longer incubation would increase the background staining. The staining was stopped by soaked the gel in stop solution with shaking for 5 min. Gel was rinsed by DI water for 2 min for 3 times and then left air-dry for long term storage.

2.3.8 Gel documentation

Silver stained polyacrylamide slab gels together with glass plates were scanned by ImageScanner III (GE Healthcare, UK). LabScan and ImageMaster 2D platinum softwares were used for image acquisition in .tif file.

2.3.9 Identification of differentially expressed TDFs

TDF bands with considerable length (> 100 bp) showing different abundances in T1 transcript profiles compared with WT were extracted from the gel for further identification by the following steps.

2.3.9.1 TDF recovery

Gel area around TDF band of interest was rehydrated by putting filter paper over the area and dropped nuclease-free water onto the filter paper. Let the gel imbibe for 10 min and then remove the filter paper. TDF band of interest was excised by clean razor or pipette tip. Gel pieces were placed into clean microtubes and incubated with 100 μl of nuclease-free water at room temperature for 2 hr. DNA solutions can readily be used as templates for reamplification reactions.

2.3.9.2 Reamplification

PCR was used to reamplify the recovered TDF using selective primers which are the same PC used to generate the transcript profiles. Following components were prepared in 0.2 ml tubes:

component	volume
10x *Taq* buffer	2 μl
dNTPs (10 mM)	0.4 μl
Eco-NN (10 μM)	0.2 μl
Mse-NN (10 μM)	0.6 μl
nuclease-free water	11.5 μl
Taq DNA polymerase	0.3 μl
template	5 μl
total volume	20 μl

Same amplification condition as selective amplification was used. The reamplification can be repeated using the first reamplification product as a template if the DNA concentration is too low.

2.3.9.3 TDF sequencing and identification

Reamplification products were ligated with pJET 1.2 blunt cloning vectors (Thermo Scientific, USA) following manufacturer's protocol and cloned into *E. coli* strain DH5α. Plasmids were extracted from positive clones and sent for sequencing. At least three positive clones were sequenced for each TDF. If there are variations in obtained DNA sequences, more positive clones were sent for sequencing to determine the major TDF species. Adaptor sequences were manually excluded from the sequence results. Transcript-derived sequences were searched against National Center for Biotechnology Information (NCBI) nucleotide database using blastn algorithm to identify candidate differentially expressed genes represented by TDFs.

2.3.10 Metabolome analysis

Metabolomics was performed to study the metabolite changes in transgenic rice overexpressing *OsCaM1-1* using GC-TOF/MS and LC-MS/MS for the analyses of primary and secondary metabolites, respectively. GC-TOF/MS, LC-MS/MS, and metabolite annotation were performed by Dr. Miyako Kusano and Dr. Ryo Nakabayashi at RIKEN Center for Sustainable Resource Science, Japan.

2.3.10.1 Gas chromatography time-of-flight/mass spectrometry analysis (GC-TOF/MS) (modified from Kusano et al. (2007))

2.3.10.1.1 Metabolite extraction

Two milligrams of freeze-dried sample was extracted with 200 μl methanol/chloroform/water (3:1:1, v/v/v) extraction solvent containing 10 stable isotope as reference compounds. For each 1 μl injection, the concentration of each isotope compound was adjusted to 15 ng/μl (Jonsson et al. 2004; Jonsson et al. 2005; Jonsson et al. 2006). The extracts were centrifuged and 200 μl aliquots of the

supernatant were then transferred into glass insert vials. The aliquots were evaporated in an SPD2010 SpeedVac® concentrator (Thermo electron corporation, USA).

2.3.10.1.2 Derivatization

To render some metabolites to be more volatile, methyl oxime derivatives were obtained by derivatization. The dry extracts were dissolved in 30 μl of methoxyamine hydrochroride (20 mg/ml in pyridine) for 30 hr at room temperature. The sample was then trimethylsilylated for 1 hr by 30 μl of *N*-methyl-*N*-trimethylsilyltrifluoroacetamide (MSTFA) with shaking at 37°C. Next, 30 μl of *n*-heptane was added following the silylation. Every step was performed in the vacuum glove box VSC-1000 (Sanplatec, Japan) filled with 99.9995% (G3 grade) of dry nitrogen.

2.3.10.1.3 GC-TOF/MS

For metabolome analysis, 1 μl of derivatized sample was injected in the splitless mode by a CTC CombiPAL autosampler (CTC analytics, Switzerland) into an Agilent 6890N gas chromatograph (Agilent Technologies, USA). Capillary column used was a 30 m×0.25 mm inner diameter with a chemically bound 0.25-μm film Rtx-5 Sil MS stationary phase (RESTEK, USA). Helium was used as the carrier gas with a constant flow rate at 1 ml/min. The temperature program was as follows: 2 min at 80°C followed by increments of 30°C to a final temperature of 320°C then the temperature was maintained for 3.5 min. Pegasus III TOF mass spectrometer (LECO, USA) was used for data acquisition at the rate of 30 spectra/sec and the range of mass-to-charge ratio of *m/z* = 60–800. Alkane standard mixtures (Sigma–Aldrich, Japan) were used for the calculation of retention index (RI) (Wagner et al. 2003; Schauer et al. 2005). Peak area corrections were done using sample weight and the internal standard compound, $^{13}C_4$-hexadecanoic acid, to calculate normalized responses.

2.3.10.1.4 Mass spectral and data processing

The processes of baseline correction, peak deconvolution, and peak annotation were done using ChromaTOF optimized for Pegasus 4D software version 2.32 (Leco, USA). Data-pretreatment for non-processed MS data was performed using MATLAB software 6.5 (Mathworks, USA). This procedure included data normalization, baseline correction, and data treatments using custom scripts (Jonsson et al. 2005) for multivariate statistical analysis. The MS spectra resolved by custom scripts were matched against NIST/EPA/NIH mass spectral library (version 2.0) using the National Institute of Standards and Technology (NIST) mass spectral search program and mass spectral search software (http://www.metabolome.jp/). Two mass spectral libraries, e.g., PRIMe (Platform for RIKEN Metabolomics, http://prime.psc.riken.jp); and the library in the Golm Metabolome Database (GMD) at CSB.DB (Steinhauser et al. 2004; Kopka et al. 2005), were used for the annotation of obtained mass spectra. The identification of extracted MS spectra was done using retention index and the comparison with the reference mass spectra in the libraries.

2.3.10.2 Liquid chromatography tandem mass spectrometry analysis (LC-MS/MS) (Matsuda et al. 2012; Saika et al. 2012; Yang et al. 2014)

2.3.10.2.1 Metabolite extraction

Extraction was performed by adding extraction solvent, 80% MeOH containing 0.5 mg/L of lidocaine and 0.5 mg/L of 10-camphorsulphonic acid as internal standards, to the ratio of 50 μL/mg of dry sample. Extraction was performed by a mixer mill (MM300, Retsch) with zirconia beads for 10 min at 20 Hz. After centrifugation at 15,000 g, the extracts were applied to an Oasis HLB μ-elution plate (Waters) equilibrated with 80% MeOH, including 0.1% acetic acid for filtration. The eluate was dried under vacuum and then suspended in 100 μl water. Insoluble residue was removed by filtration using an Ultrafree-MC filter with 0.2 μm pore size (Millipore, Germany).

2.3.10.2.2 LC-MS/MS

The filtered samples (3 μl) were subsequently subjected to metabolome analysis by liquid chromatography coupled with electrospray quadrupole time-of-flight tandem mass spectrometry (LC-ESI-Q-TOF-MS) using an Acquity BEH ODS column (LC, Waters Acquity UPLC system; Q-TOF-MS, Waters Q-TOF Premier). Metabolome analysis and data processing were performed as described previously (Matsuda et al., 2009, 2010). Briefly, the metabolome data were obtained in both positive and negative ion mode (m/z 100–2000; dwell time 0.45 sec; inter-scan delay 0.05 sec), from which a data matrix was generated using MetAlign (De Vos et al., 2007; Lommen, 2009).

2.3.10.3 Multivariate data analysis by Partial Least Square Discriminant Analysis (PLS-DA)

Metabolomics is a high-throughput technique which generates huge amount of data. Hundreds of metabolites were quantified in each sample. Since the experiment was done in six biological replicates. Vast amount of data were generated from GC-TOF/MS and LC-MS/MS. To simplify the data processing, multivariate data analyses were done using SIMCA software (Umetrics, Sweden) utilizing PLS-DA algorithm.

Metabolite data arranged in the Microsoft Excel file, .xlsx, were imported into SIMCA. Sample name was set as Primary ID, other information; such as metabolite annotation and retention index were set as Secondary ID, normalized signal of metabolites were set as Quantitative data. In the statistic mode, model type was set to PLS-DA, classes were set according to sample groups (leaves and roots: WT, T1, T7, BV). At least five biological replicates of each sample group were used to assess multivariate analysis. The models were autofitted and PLS-DA score plots were generated. Respective loading plots were sorted and exported for lists of metabolites considered to be significant by the analysis.

2.3.10.4 Identification of differentially accumulated metabolites

Quantitative data of annotated metabolites suggested by PLS-DA loading plots were retrieved for comparison between individual transgenic rice (T1 or T7) and control transgenic rice (BV). Student's T-test was carried out using Microsoft Excel 2010. The calculated *P* value of <0.05 were considered significant. Metabolites with the same accumulation trend in transgenic rice, i.e. significant and up/down -accumulated in both T1 and T7 when compared to BV, were regarded as differentially accumulated metabolites.

Differentially accumulated metabolite names were listed in tables together with their fold changes and significant levels. Accumulation profiles of several metabolites in primary metabolism were visualized as colored metabolic maps using PathVisio 3 software (www.pathvisio.org; van Iersel et al. (2008)).

2.3.10.5 Hierarchical clustering analysis (HCA) and cluster heat map construction

HCA is a statistical analysis which could cluster metabolite profiles based on their similarities and present the relationship as dendrograms. Cluster heat maps were then generated after HCA. These clustering could help in the sample validation of which biological replicates should have similar metabolite profiles, thus being clustered together.

The signal intensities of differentially accumulated metabolite signatures were transformed to Z-score by subtracting individual signal of each sample with population mean signal of the particular metabolite then divided by standard deviation of the population. After that, the data sets were subjected to two-dimensional HCA (HCA was performed on both samples and variables) using Ward's minimum variance method. Cluster heat maps were then generated with the color key of green to black to red. Three different colors represent Z-score ranges of the individual intensity: green; Z<0, black; Z≈0, and red; Z>0. Z-score transformation was done using Microsoft Excel 2010. HCA and heat map construction were done using JMP statistical software (SAS Institute Inc., USA).

2.3.11 Selection of candidate differentially expressed genes for real-time qRT-PCR

2.3.11.1 Candidate genes from cDNA-AFLP

Since cDNA-AFLP transcript profiles showed that selected TDF abundances were different in the transgenic rice, candidate genes were arbitrarily selected from the gene list identified from the TDFs of interest. Transcript sequences were obtained from Phytozome (www.phytozome.net) and NCBI (www.ncbi.nlm.nih.gov) databases for primer design.

2.3.11.2 Candidate genes from metabolite data

To identify metabolite-to-gene correlations, candidate genes from metabolite data were selected according to metabolite accumulation level in transgenic rice. Corresponding rice genes encoding enzymes catalyzing the conversion of accumulated metabolite were acquired from KEGG metabolic pathway database (www.kegg.jp). Transcript sequences were obtained from Phytozome for primer design.

2.3.11.3 Candidate differentially expressed genes in salt-stressed rice

Candidate differentially expressed genes in salt-stressed rice were selected based on the candidate genes from cDNA-AFLP and metabolomics results. GENEVESTIGATOR online platform (www.genevestigator.com) was used to screen for salt-responsive genes using five microarray experiments, with GEO accession as follows: GSE3053, GSE6901, GSE13735, GSE14403, and GSE16108, involving in salt stress treatment in rice. Candidate genes with salt-affected expression were chosen for expression analysis by real-time qRT-PCR in salt-stressed rice.

2.3.12 Gene expression analysis by real-time qRT-PCR

The real-time PCR reactions were performed using SsoFast™ EvaGreen® Supermix (BIO-RAD, USA). The following reaction was set up in a clean environment:

component	volume
SsoFast EvaGreen Supermix	5 μl
Forward primer (10 μM)	0.5 μl
Reverse primer (10 μM)	0.5 μl
nuclease-free water	2 μl
cDNA template (5 ng RNA-equivalent/μl)	2 μl
total volume	10 μl

Real-time PCR reactions were performed in a CFX96™ Real-Time PCR Detection System (BIO-RAD, USA). Temperature profiles were set as follows: denaturation at 95˚C for 30 sec, 40 cycles of denaturation (95˚C for 5 sec); and annealing and extension (T_A˚C for 10 sec, when T_A = primer-dependent annealing temperature; see Table 4), denaturation at 95˚C for 15 sec, and melt curve construction starting from 65˚C for 15 sec (0.5˚C increment until 95˚C). Plate read was conducted every cycle at the end of annealing and extension step, and after each increment for melting curve.

To determine amplification efficiency of each primer pair, real-time PCR was performed with a series of template concentration (prepared by serial dilution of a template). C_T values of at least five cDNA concentrations were plotted on x-axis against log cDNA dilution on y-axis to create standard curve. PCR efficiency was then calculated from: $E = 10^{-1/slope}$, where E is the efficiency. Percent PCR efficiency or (E-1)*100% should be within 90-110%. All real-time PCRs were done in triplicate.

Relative gene expression levels were calculated by comparative C_T method (Schmittgen and Livak 2008) using *OsEF-1α* as a reference gene. Fold change of gene expression between two samples is equal to $2^{-\Delta\Delta CT}$ where $\Delta\Delta C_T = (C_{T\ gene\ of\ interest} - C_{T\ OsEF\text{-}1\alpha})$ sample A - $(C_{T\ gene\ of\ interest} - C_{T\ OsEF\text{-}1\alpha})$ sample B. At least three biological replicates were used in every real-time qRT-PCR experiment.

2.4 Prediction of CaM binding site

2.4.1 Prediction of CaM binding site by Calmodulin Target Database

Amino acid sequences of candidate genes were retrieved from www.phytozome.net and used as queries for putative CaM binding site search on web-based platform, http://calcium.uhnres.utoronto.ca/ctdb (Yap et al. 2000). This publicly available platform reported to have 80% accuracy in identifying CaM binding motif from preliminary test (Yap et al. 2000). By considering many factors, such as hydropathy; alpha-helical propensity; residue charge; hydrophobic residue content; and occurrence of particular residues, the score from 0 (unlikely) to 9 (very likely) will be given to each amino acid in the protein sequence calculating from 20-residue sliding window. Calcium/calmodulin-dependent protein kinase type II subunit alpha (UniProt accession: P11275) was used as a positive control that was experimentally proved to have CaM-binding motif (PDB accession: 1CM1).

2.4.2 Visualization of putative CaM binding sites by homology modeling

To screen out any unlikely putative CaM binding site (false positive), homology modeling was used to verify that predicted CaM binding sites are presented at the surface of the protein tertiary structure. Protein Homology/analogy Recognition Engine V 2.0 (Phyre^2, http://www.sbg.bio.ic.ac.uk/phyre2) (Kelley and Sternberg 2009) was used to model the 3D structure of candidate gene. The putative CaM binding site region is then visualized in the model using UCSF Chimera software (Pettersen et al. 2004).

Table 4. Oligonucleotide primers used in real-time qRT-PCR

Locus name	Gene	Primer	Sequence (5'-3')	Amplicon size (bp)	Annealing temp. (°C)
Os03g0177400	elongation factor 1-alpha	Forward	ATGGTTGTGGAGACCTTC	127	59
		Reverse	TCACCTTGGCACCGGTTG		
Os12g0176800	eukaryotic translation initiation factor 2 subunit gamma (TDF3)	Forward	GCAGCATTCTCAGAGGAG	181	52
		Reverse	GTTCCAACACCAATAAGACC		
Os11g0148700	PHD-finger family protein (TDF4)	Forward	CGAGGTAGCATGTGACAG	201	52
		Reverse	GCTCTCAGGTAACAAGTG		
Os03g0239200	potyvirus VPg interacting protein (TDF10)	Forward	TGAACCCCATTTCAGCAC	117	54
		Reverse	TCCTTCCTGGCATCATCG		
Os07g0516500	unknown (TDF18)	Forward	CGGTTCTAGCTCAAGTCC	110	53.5
		Reverse	TTGCCCCTGTCATCCTG		
Os03g0147400	citrate transporter protein (TDF23)	Forward	GTCTGGAGAAGGTGTCATAC	139	52
		Reverse	CCCTTAGCACTGTCAATTCG		
Os02g0184200	inorganic H^+ pyrophosphatase (TDF24)	Forward	TCCCAAAGGTTCCGATCC	138	54
		Reverse	AAGAAGGGGGCGAAAACG		
Os05g0105000	methionine S-methyltransfe F34)	Forward	AAACAGCAGCTCATGGACAG	111	58
		Reverse	ACCAACTCCTTGAAGCGAAC		

Locus name	Gene	Primer	Sequence (5'-3')	Amplicon size (bp)	Annealing temp. (℃)
Os03g0230300	ATP8 (TDF39)	Forward	TGGAGCACAGACATGAACAC	109	58
		Reverse	TCTTCAGCTTCGATCCCAACC		
Os10g0363300	acetyl-CoA carboxylase (TDF44)	Forward	ATGGGAGGTTTTGAGATGGC	145	58
		Reverse	AACAACATTCCGTGCCTGAC		
Os10g0537300	unknown (TDF53)	Forward	TGGGATGAAGATGGTGTTGTGG	78	58
		Reverse	ATTTTGGAACCCGTCAGCAG		
Os04g0106300	arginase	Forward	CCCAGACTCCTTTAGCTGTTAG	198	59
		Reverse	AGCATGTTGCCTGAAAGCAC		
Os11g0642800	glutathione synthetase	Forward	TGCTCCAGTCAACTTCAACC	173	58
		Reverse	ACTCTTGCTACCTTGCTTCCTC		
Os12g0263000	glutathione synthetase	Forward	ACAGCGTATTCCTGACATGAC	189	58
		Reverse	TCTCGGCTGATAGCGAAATC		
Os12g0528400	glutathione synthetase	Forward	AGGCCCTCACAATATCTGAGC	177	58
		Reverse	TCGCCTTGTCGGTTAAGTAC		
Os02g0169900	inositol-1-monophosphatase	Forward	AAGTTGAACTCCTCACCCAGAG	131	58
		Reverse	AGTCGATGGCTGAGTCAAAGG		
Os03g0587000	inositol-1-monophosph	Forward	TCTGATGGCACGAAGAATGG	196	58
		Reverse	ACTTTTCCGCAACAGGCATG		

CHAPTER III
RESULTS

3.1 *OsCaM1-1* overexpression in the transgenic rice plants

I checked *OsCaM1-1* expression levels in all rice samples used in both cDNA-AFLP and metabolomics. These samples include wild type rice (WT), two lines of transgenic rice overexpressing *OsCaM1-1* under 35S promoter (T1 and T7), and one line of transgenic rice transformed with the blank vector as a control transgenic line (BV). *OsEF-1α* was used as a house-keeping reference gene. Although Saeng-ngam et al. (2012) showed the overexpression of *OsCam1-1* in the leaves of the transgenic rice, the *OsCam1-1* expression level has not been analyzed in the roots. I reconfirmed the *OsCaM1-1* overexpression in the leaves and showed that the overexpression was also found in the roots as demonstrated by the semiquantitative RT-PCR analysis in two-week-old transgenic rice seedlings (T1 and T7) when compared to WT and BV (Figure 8A).

In addition, I confirmed the overexpression of *OsCaM1-1* in all three-week-old rice samples used in real-time qRT-PCR experiments. The result shows that the expressions of *OsCaM1-1* in both transgenic rice lines were much higher than WT and BV lines under normal and salt stress conditions (Figure 8B and 8C). Therefore, these results assured that the rice samples used in these experiments were applicable.

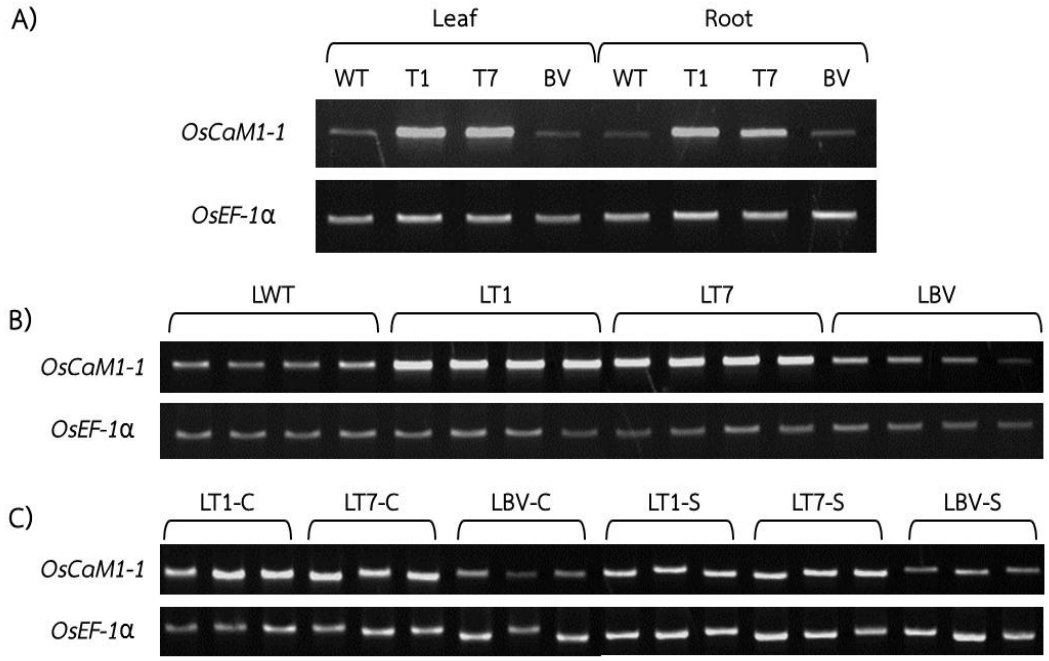

Figure 8. *OsCaM1-1* expression analysis of rice samples used in all studies. A) pooled rice leaves and roots samples used in cDNA-AFLP and metabolomics experiments, **B)** four biological replicates of rice leaves collected at normal condition, and **C)** three biological replicates of rice leaves collected at three hours normal condition (-C) and 3 hours salt-stressed condition (-S) used in real-time qRT-PCR experiments. *OsEF1α* was used as the reference house-keeping gene in RT-PCR analysis. Sample labels were as follows: WT, wild type rice; T1, transgenic rice line 1; T7, transgenic rice line 7; and BV, control transgenic line.

3.2 Identification of differentially expressed genes by cDNA-AFLP

3.2.1 cDNA-AFLP transcript profiles of wild type and transgenic rice plants and the identification of differentially expressed genes

In this study, two-week-old pooled WT and T1 rice samples were used to compare differentially expressed gene fragments. Differentially expressed candidate genes identified from cDNA-AFLP analysis would then be confirmed in all rice lines by real-time qRT-PCR.

Rice double-stranded cDNAs were digested, adapter-ligated, and selectively amplified as described in chapter II. Selective amplification products were then run on denaturing-PAGE and subjected to silver staining to create cDNA-AFLP transcript profiles of wild type and transgenic rice line1 for comparison (Figure 9). The results show that unique profile can be produced by each PC, thus allowing the untargeted high-throughput gene expression analysis by comparing band intensities of the TDFs between WT and T1 sample. Using 33 PCs, 100 differentially expressed TDFs were found. Most differentially expressed TDFs were specifically found in either leaves or roots with only a few showing the same pattern in two organs. Twenty-three up-regulated TDFs and 24 down-regulated TDFs were found in leaves only. Twenty-two up-regulated and 25 down-regulated TDFs were found in roots only. There were two up-regulated TDFs and three down-regulated TDFs exhibiting the same pattern in both leaves and roots. Only one TDF was down-regulated in leaves but up-regulated in roots. A portion of TDFs were successfully recovered from polyacrylamide gel and cloned for sequencing. Blasting against NCBI database, I identified a total of 31 candidate genes that were differentially expressed in leaves and roots of the T1 as follows: three down-regulated genes in both leaves and roots; four and six up-regulated genes in leaves and roots, respectively; seven and 11 down-regulated genes in leaves and roots, respectively. Locus numbers and functional annotations of candidate genes were listed in Table 5.

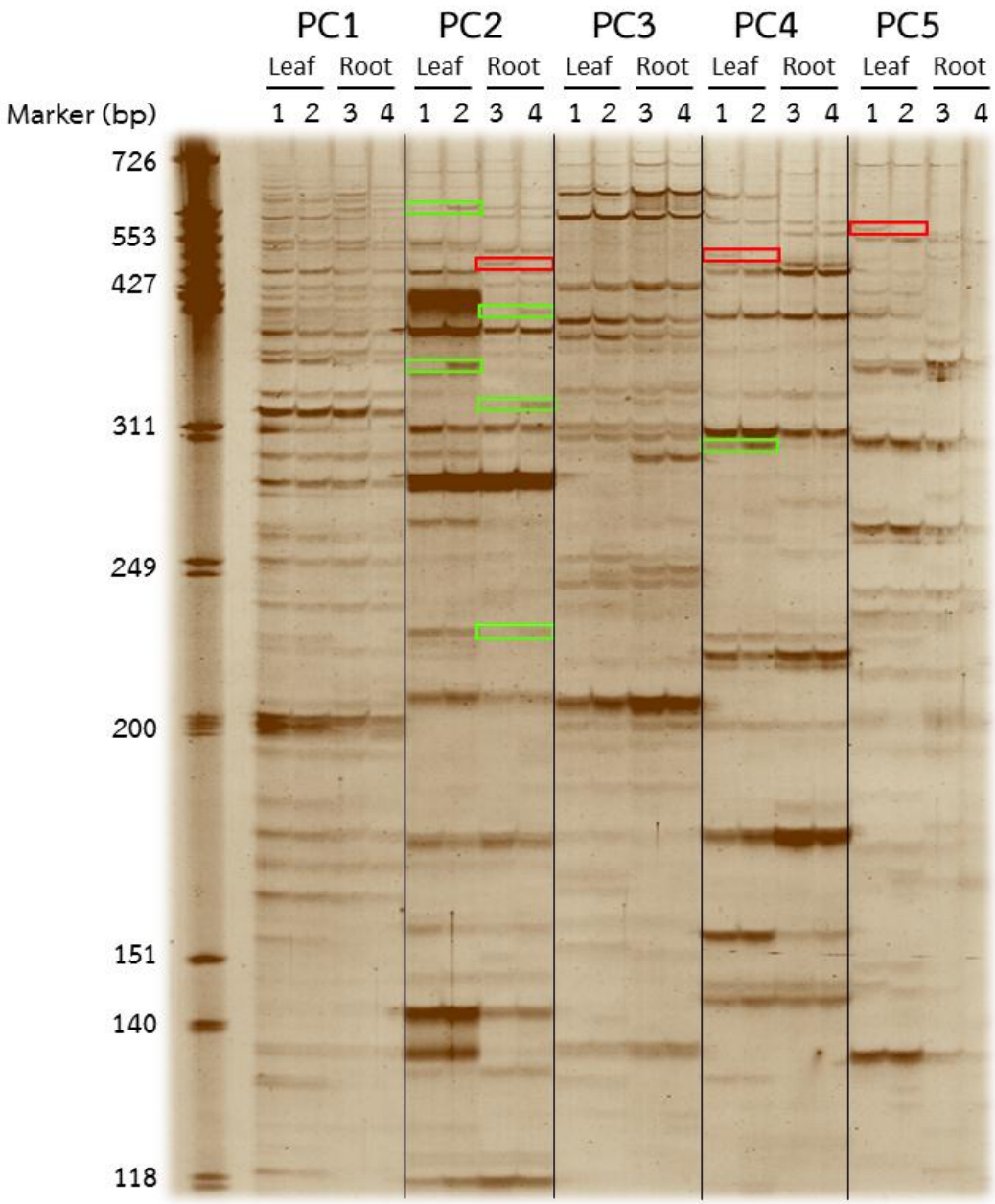

Figure 9. cDNA-AFLP transcript profiles created by five different PCs. Each lane represents leaves of wild type (1), leaves of transgenic rice (2), roots of wild type (3), and roots of transgenic rice (4). Some differentially expressed TDFs were highlighted in the box, up-regulated TDFs in green boxes and down-regulated TDFs in red boxes.

Table 5. Candidate differentially expressed genes from cDNA-AFLP transcript profiles

Organ	TDF	Feature (in transgenic)	Gene ID	Gene annotation
Leaf	3	up-regulated	Os12g0176800	eukaryotic translation initiation factor 2 subunit gamma
	4	up-regulated	Os11g0148700	PHD-finger family protein
	10	up-regulated	Os03g0239200	potyvirus VPg interacting protein, putative
	44	up-regulated	Os10g0363300	acetyl-CoA carboxylase, putative
	6	down-regulated	Os03g0197700	zinc finger, C2H2-type domain containing protein
	23	down-regulated	Os03g0147400	citrate transporter protein, putative
	24	down-regulated	Os02g0184200	inorganic H^+ pyrophosphatase, putative, expressed
	34	down-regulated	Os05g0105000	methionine S-methyltransferase, putative
	51	down-regulated	Os09g0497100	pumilio-family RNA binding repeat containing protein
	53	down-regulated	Os10g0537300	expressed protein
	96	down-regulated	Os06g0170200	conserved hypothetical protein
Root	2	up-regulated	Os04g0581000	naringenin,2-oxoglutarate 3-dioxygenase, putative
	14	up-regulated	Os07g0583300	zinc finger family protein, putative
	37	up-regulated	Os04g0566400	ZOS4-11 - C2H2 zinc finger protein
	89	up-regulated	Os03g0711400	coatomer alpha subunit, putative
	95	up-regulated	Os05g0486200	keratinocytes-associated protein 2, putative
	100	up-regulated	Os10g0559450	conserved hypothetical protein
	20	down-regulated	Os05g0102200	zinc knuckle family protein
	21	down-regulated	CT832277.1 (NCBI)	none
	27	down-regulated	Os01g0730300	trehalose synthase, putative, expressed
	29	down-regulated	Os03g0736600	ATP synthase F1, delta subunit family protein, putative
	31	down-regulated	Os01g0775100	plus-3 domain containing protein
	56	down-regulated	Os09g0451500	*Os*PDIL2-3 protein disulfide isomerase PDIL2-3
	64	down-regulated	Os03g0358100	glutathione peroxidase domain containing protein
	65	down-regulated	Os05g0105300	tubulin-specific chaperone E, putative
	66	down-regulated	Os11g0525600	lysosomal alpha-mannosidase precursor, putative
	91	down-regulated	Os12g0230100	ATP-dependent Clp protease ATP-binding subunit clpA homolog, putative
	92	down-regulated	Os05g0180400	MAR-binding filament-like protein 1, putative
Leaf and root	18	down-regulated	Os07g0516500	none
	39	down-regulated	Os03g0230300	ATP8, putative
	86	down-regulated	Os11g0632200	expressed protein

3.2.2 Validation of differentially expressed genes by real-time qRT-PCR

To validate the differential expression of candidate genes, the quantitative technique, real-time qRT-PCR, was used for all rice samples. Three-week-old rice cDNAs were synthesized using iScript™ Reverse Transcriptase Supermix for RT-qPCR (BIO-RAD). Real-time PCR data were calculated using comparative CT method (Schmittgen and Livak 2008). Figure 10 represents relative expression level in leaves of each transgenic (LT1 and LT7) and control transgenic rice (LBV) compared to the wild type rice (LWT). However, the result from ten candidate genes tested showed non-significant differences in gene expression level between the transgenic and wild type rice plants suggesting the inconsistency of cDNA-AFLP analysis in this experiment.

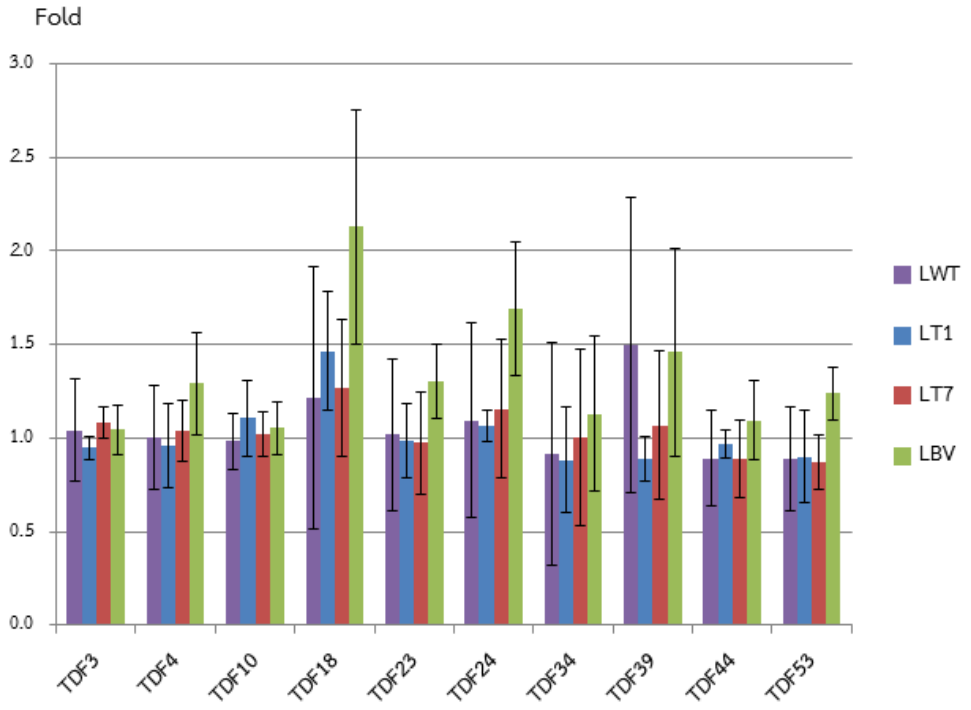

Figure 10. Relative expression levels of candidate genes in transgenic and control rice compared to wild type rice. LWT: leaves of wild type, LT1: leaves of transgenic line1, LT7: leaves of transgenic line7, and LBV: leaves of control transgenic line.

3.3 Metabolite profile of transgenic rice overexpressing *OsCaM1-1*

There were 101 metabolites identified by GC-TOF/MS and a large mass signal dataset detected by LC-MS/MS. To simplify the data processing, multivariate data analyses were performed.

3.3.1 Overall metabolic changes by PLS-DA score plots

By using PLS-DA algorithm, metabolomics data were analyzed. All metabolite data in each replicate were projected as a single dot in PLS-DA score plot (Figure 11). The score plots of GC-TOF/MS data from rice leaf and root samples showed that all metabolites in each sample group (six biological replicates of WT, T1, T7, and BV), represented as a dot in the same color, were clustered together suggesting similar metabolite profiles of each replicate in each sample group (Figure 11A). GC-TOF/MS analysis revealed that both T1 and T7 show similar metabolite profiles when compared to BV and WT in both leaves and roots. Surprisingly, metabolite profiles of WT samples were located on the score plot with a considerable distance away from both transgenic and BV group. These observations suggested that metabolites in transgenic rice plants were affected by the genetic transformation regardless of a gene inserted. Therefore, BV would serve as a better control than WT for metabolomics data analysis.

PLS-DA score plots were reconstructed from the metabolite data of three sample groups, namely T1, T7, and BV. Score plots of GC-TOF/MS data from leaves and roots showed similar pattern in which all of the three clusters were separated, however, two lines of transgenic rice overexpressing *OsCaM1-1* were plotted near to each other comparing with the distance between transgenic and blank vector control group suggesting metabolite profiles of transgenic lines were similar to each other (Figure 11B). Score plots of LC-MS/MS data in both positive and negative ion modes were shown in Figure 11C and 11D. Four score plots from LC-MS/MS also showed similar pattern to the GC-TOF/MS. However, they showed that the difference in metabolite profiles analyzed by GC-TOF/MS was much greater than that analyzed by LC-MS/MS. These results demonstrated that there

are differences in metabolite profiles caused by the overexpression of *OsCaM1-1* in the transgenic rice plants.

3.3.2 Differentially accumulated metabolites by PLS-DA loading plots

PLS-DA loading plots can prioritize the significance of metabolites accumulating at different level in each sample group. Using the list of metabolites guided by PLS-DA loading plot, I identified many metabolites which were differentially accumulated in the transgenic rice plants comparing to control transgenic line. The significant metabolites and their fold changes in both transgenic rice lines were listed in Table 6–8. Also, from the list of differentially accumulated metabolites, I used these data to visualize the effect of *OsCaM1-1* overexpression by mapping significantly changed metabolites in both leaves and roots into the primary pathway (Figure 12A and 12B). Concerning primary metabolites, a larger number of metabolites were affected in the leaves of both transgenic rice lines when compared to the roots. This suggests that there might be more *Os*CaM1-1 targets presented in the leaves more than roots. However, some similar metabolic changes can be found between the leaves and the roots. There are some up-accumulated intermediates in the glycolysis and TCA cycle of both transgenic rice lines. Sugars, polyols, and amino acids contents were also found to be affected by the *OsCaM1-1* overexpression. Stress-associated metabolites such as inositol and polyamine were up-accumulated specifically in the transgenic leaves. Major metabolic changes observed in transgenic rice plants were up-accumulations. Only down-accumulations of a few metabolites such as trehalose, lysine, and histidine were found in the transgenic roots. For secondary metabolites from the LC-MS/MS analysis, only tricin 7-*O*-glucopyranoside is a known metabolite up-accumulated in transgenic leaves with four fold higher accumulation compared to control transgenic line. Some other mass signals with accumulation level different by more than two folds were also listed in Table 8. From these results, similar changes were found between T1 and T7. They strongly

suggested that changes in metabolite accumulation are the effect of *OsCaM1-1* overexpression.

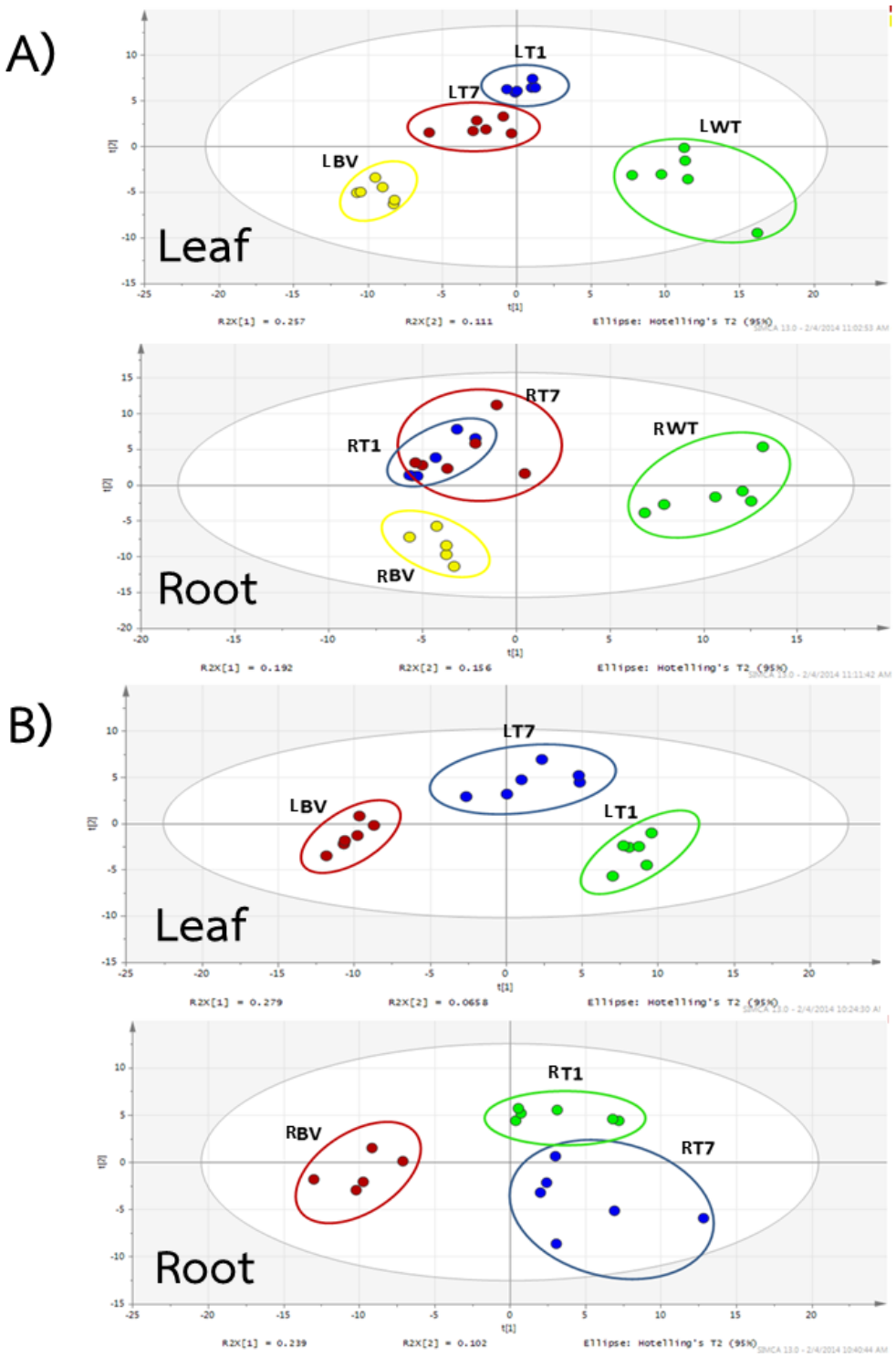

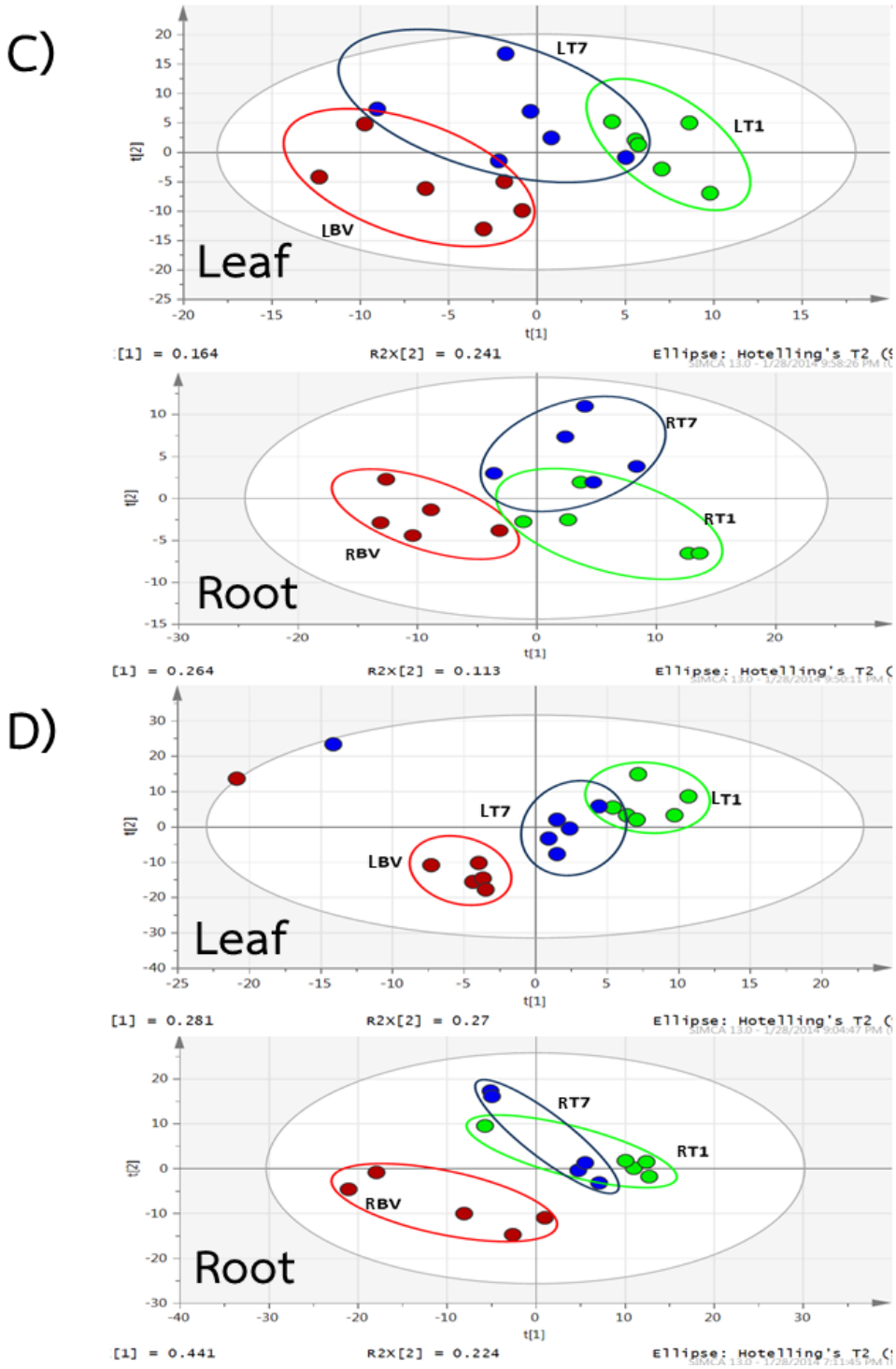

Figure 11. PLS-DA score plots of GC-TOF/MS and LC-MS/MS data. A) PLS-DA score plots of GC-TOF/MS data, **B)** reconstructed PLS-DA score plots of GC-TOF/MS data, **C)** PLS-DA score plots of positive ion mode LC-MS/MS data, and **D)** PLS-DA score plots of negative ion mode LC-MS/MS data. WT: wild type, T1: transgenic line1, T7: transgenic line7, and BV: control transgenic.

Table 6. List of differentially accumulated metabolites in transgenic rice leaves detected by GC-TOF/MS

	Metabolite	Fold change (Transgenic/BV)	
		T1	T7
Glycolysis	Glucose-6-phosohate	3.08***	2.23***
	Fructose-6-phosphate	1.91***	1.52***
Sugars and polyols	D-Ribitol	2.62**	1.98*
	D-Arabinose	2.06**	1.61*
	Inositol	1.77***	1.43**
TCA cycle	Succinate	2.49***	1.76**
	Isocitrate	2.26***	1.91**
	Citrate	1.87***	1.65***
Amino acids	Beta-alanine	3.59***	2.04*
	Glutamate	2.32***	1.73***
	Serine	2.12***	1.71***
	Homoserine	2.03***	1.91*
	Tyrosine	2.02***	1.7***
	Alanine	2.02***	1.44**
	Aspartate	1.97***	1.59***
	Threonine	1.83***	1.58**
	Cysteine	1.51***	1.42*
Etc.	Nicotinamide	2.91*	2.52*
	Threonic acid	2.87***	1.97***
	Threonic acid-1,4-lactone	2.51***	1.83***
	Galactinol	2.48***	2.01**
	Oxalate	2.34**	1.42**
	Glycerate	2.33***	1.58**
	Gluconate	2.31**	1.57*
	Glycolic acid	2.14***	1.41***
	Spermidine	2.08***	1.81***
	Pyroglutamate	1.92***	1.52***
	Phosphoric acid monomethyl ester	1.55***	1.43**
	Putrescine	1.41**	1.33*
	Nicotinate	1.38**	1.35**
	Beta-sitosterol	1.38***	1.34**

*P<0.05, **P<0.01, ***P<0.001

Table 7. List of differentially accumulated metabolites in transgenic rice roots detected by GC-TOF/MS

	Metabolite	Fold change (Transgenic/BV)	
		T1	T7
Glycolysis	Fructose-6-phosphate	1.44*	1.69*
Sugars and polyols	Mannose	3.19**	3.32**
	Fructose	2.28*	2.45*
	Trehalose	-3.42**	-2.19*
TCA cycle	Succinate	1.26*	1.34*
Amino acids	Aspartate	1.80**	1.96**
	Glutamate	1.33*	1.53**
	Tyrosine	1.32*	1.58**
	Lysine	-2.86**	-1.70*
	Histidine	-2.96**	-2.17*
Etc.	Threonic acid-1,4-lactone	3.44*	3.10**
	Threonic acid	2.74**	2.73**
	Glycerate	2.03***	1.77**
	Glycolic acid	1.82**	1.37*
	Pyroglutamate	1.45**	1.71***
	n-Hexadecanoic acid	1.26***	1.41***

*P<0.05, **P<0.01, ***P<0.001

Table 8. List of differentially accumulated metabolites detected by LC-MS/MS

Tissue	operation	m/z	Annotation	Fold change (Transgenic/BV)	
				T1	T7
Leaf	negative ion mode	491.1189	Tricin 7-*O*-glucopyranoside	4.27**	4.17**
	positive ion mode	217.0973	-	-2.79***	-2.59***
	positive ion mode	144.0810	-	-2.31***	-2.15***
Root	negative ion mode	476.2784	-	3.41**	4.34**
	negative ion mode	476.2784	-	2.62**	3.64*
	negative ion mode	564.3306	-	2.23*	2.74*
	positive ion mode	318.3006	-	2.12*	2.58*
	positive ion mode	207.0660	-	2.00***	1.79***
	negative ion mode	96.9673	-	-2.02**	-1.60*
	negative ion mode	216.9269	-	-2.41**	-1.96**
	positive ion mode	374.1089	-	-2.42***	-1.48*
	positive ion mode	183.0933	-	-2.79***	-2.81***
	negative ion mode	194.9450	-	-5.33*	-3.67*

*P<0.05, **P<0.01, ***P<0.001

- : un-annotated mass

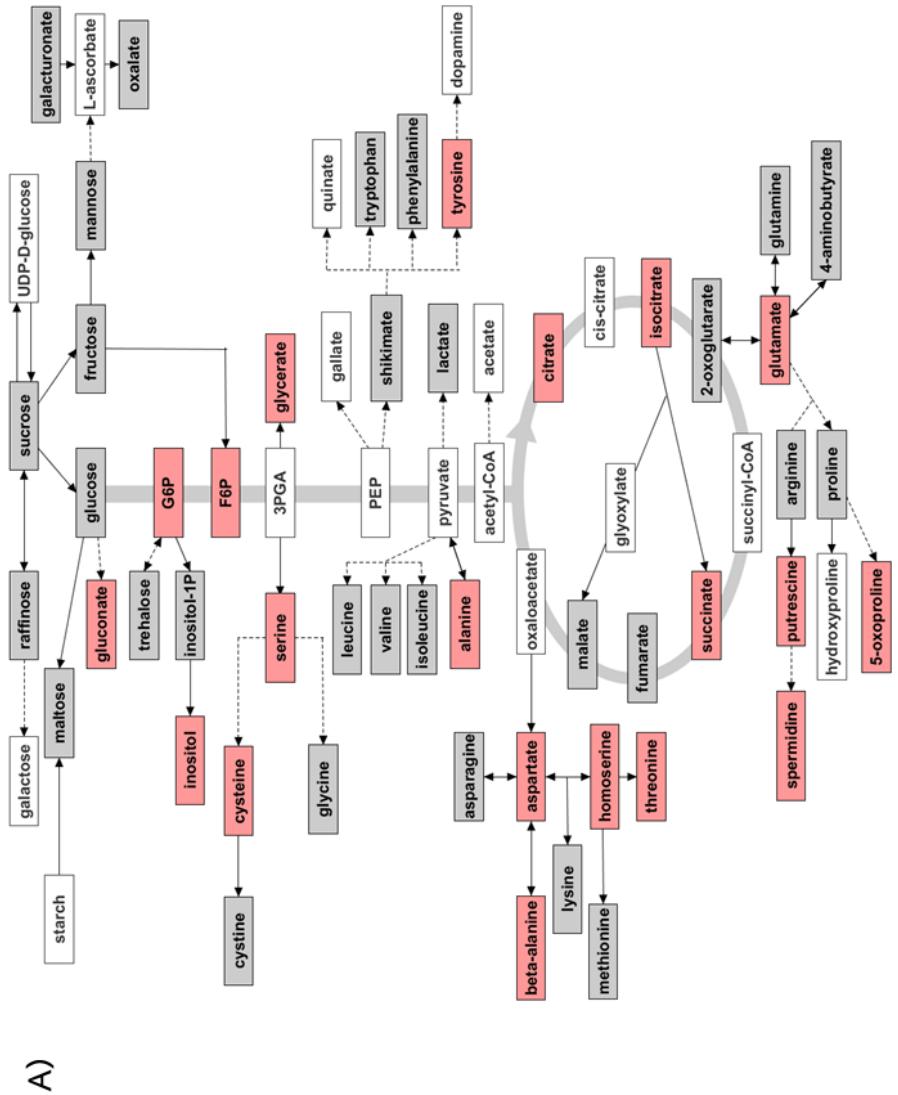
A)
galacturonate
L-ascorbate
oxalate
UDP-D-glucose
mannose
fructose
sucrose
glucose
G6P
F6P
glycerate
3PGA
PEP
pyruvate
acetyl-CoA
quinate
tryptophan
phenylalanine
dopamine
tyrosine
gallate
shikimate
lactate
acetate
citrate
cis-citrate
isocitrate
2-oxoglutarate
glutamine
4-aminobutyrate
glutamate
raffinose
gluconate
trehalose
inositol-1P
serine
leucine
valine
isoleucine
alanine
oxaloacetate
glyoxylate
succinyl-CoA
arginine
proline
galactose
maltose
inositol
cysteine
glycine
malate
fumarate
succinate
putrescine
hydroxyproline
5-oxoproline
starch
cystine
asparagine
aspartate
homoserine
threonine
spermidine
beta-alanine
lysine
methionine

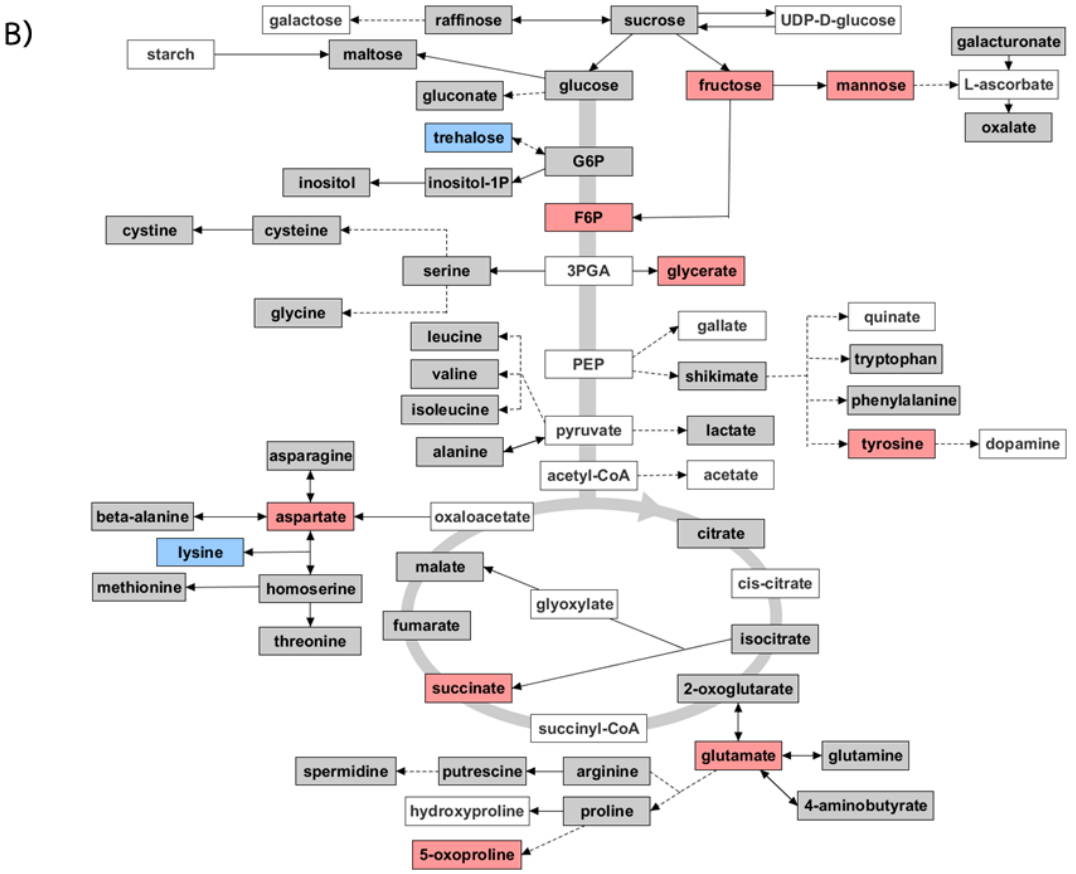

Figure 12. Metabolic maps of transgenic rice overexpressing *OsCaM1-1* leaves (A) and roots (B). The accumulation profiles were shown in relative to BV control rice. Up-accumulated metabolites were labeled in red, Down-accumulated metabolites were labeled in blue, non-significant change metabolites were labeled in grey, and undetectable metabolites were labeled in white.

3.3.3 Cluster heat maps of differential metabolite accumulations by hierarchical clustering analysis (HCA)

3.3.3.1 Cluster heat map of metabolic changes detected by GC-TOF/MS

Two-way clustering was performed on the GC-TOF/MS metabolite data and a cluster heat map was generated (Figure 13). The cluster heat map can efficiently visualize the relative content of each metabolite, ranging from relatively low to relatively high (green to black to red, respectively), across all biological samples.

For sample clustering (Figure 13), HCA could apparently separate the leaf (L) and root (R) sample clusters. However, one biological replicate of blank vector control root (RBV-2) was being separated from other RBVs. This might be caused by the fact that *OsCaM1-1* overexpression has relatively smaller effect to the roots compared to the leaves. This could make roots metabolite profiles more similar to one another since there are many leaf-specific metabolites accounted for this HCA. HCA was also not able to separate transgenic line 1 and transgenic line 7 sample groups (T1 and T7, respectively) from each other. Therefore, this HCA could substantially support that, generally, the metabolic changes observed by metabolomics were contributed by *OsCaM1-1* overexpression.

The metabolite clustering showed that metabolites were clustered based on the similarity of their accumulation profiles in six sample groups, namely RBV, RT1, RT7, LBV, LT1, and LT7 (Figure 13). All significant metabolites were classified into five clusters. Cluster I composed of glycolic acid, aspartate, and 5-oxoproline which up-accumulated in both leaves and roots of the transgenic rice. Also, cluster II consisted of many metabolites up-accumulated in leaves, namely alanine, myo-inositol, oxalate, ribitol, gluconate, and nicotinate. Some of metabolites which up-accumulated in both leaves and roots of transgenic rice plants, such as glycerate, threonic acid, threonic acid-1,4-lactone, threonic acid, glutamate, and succinate, were also clustered in this group. However these changes in the roots were barely visible on the heat map since metabolites in cluster II have relatively high content in leaves compared to roots. Cluster III comprised of leaf-specific up-accumulated metabolites. TCA cycle intermediates such as isocitrate and citrate were sorted into this cluster. Some other metabolites

were amino acids: serine, threonine, and homoserine, galactinol, and nicotinamide. Metabolites in cluster III also have higher content in the rice leaves. In cluster IV, many metabolites, namely mannose, fructose, hexadecanoic acid, lysine, histidine, and trehalose were differentially accumulated in the root-specific manner. Nevertheless, some leaves up-accumulated metabolites, such as phosphoric acid monomethyl ester, arabinose, and putrescine were grouped into this cluster due to their relatively high content in the roots. Cluster V composed of many leaf-specific up-accumulated metabolites, such as beta-alanine, cysteine, beta-sitosterol, spermidine, and glucose 6-phosphate. Tyrosine and fructose 6-phosphate are cluster V metabolites which up-accumulated in both leaves and roots of the transgenic rice. These metabolites in cluster V have comparable accumulation level across organs, leaf and root.

3.3.3.2 Cluster heat map of metabolic changes detected by LC-MS/MS

The major problem of plant metabolomic studies using LC-MS/MS is that plant secondary compounds are highly diverse. At present, publicly available mass spectral databases are still developing for efficient MS data annotation. As a result, most of the mass signals differentially detected were un-annotated, thus, they were being reported as mass/charge ratio – retention time (*m/z* - RT) in the cluster heat maps. All of the mass signatures having more than 20% difference in signal intensity were subjected to two-way clustering and heat map construction. The total of four cluster heat maps from differentially presented masses in leaves and roots metabolome of transgenic rice detected in both positive and negative mode were then generated (Figure 14-17). As for the nature of MS, fragmentation of one metabolite could result in more than one *m/z* signal, for example, mass signal from intact molecule ions or fragmentation products. Since HCA is a method which clusters masses with similar accumulation patterns together, it is possible that HCA has a power to reunite daughter ion signals fragmented from the same parent ion.

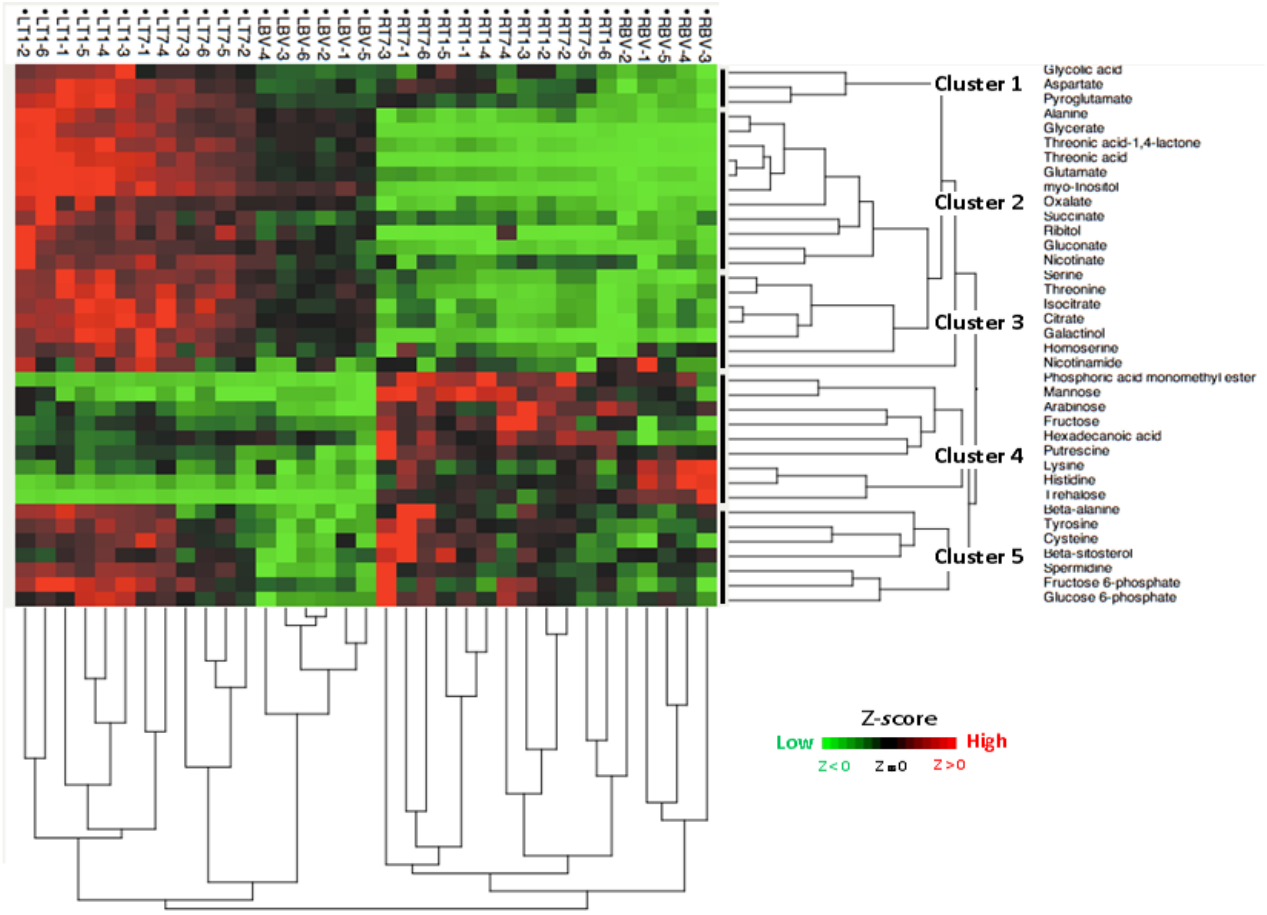

Figure 13. Cluster heat map generated from metabolite data detected by GC-TOF/MS. LT1: leaves of transgenic line1, LT7: leaves of transgenic line7, LBV: leaves of control transgenic line, RT1: roots of transgenic line1, RT7: roots of transgenic line7, and RBV: roots of control transgenic line.

Sample clustering of all four heat maps showed that HCA could separate samples into two main clusters, control transgenic samples and transgenic samples (Figure 14-17). Like GC-TOF/MS data, these HCAs further ensure that differentially presented mass signals were the effects of *OsCaM1-1* overexpression. They also showed that higher number of differentially detected masses was found in the roots. However, it cannot be confirmed whether the number of differentially accumulated metabolites would be represented proportionally by the number of mass signals. Interestingly, considering RT differences of clustered mass signals, they suggested that many mass signals might possibly be the fragmentation products of the same metabolite. These masses included one cluster in Figure 14 (**(1)** 217.0973 and 144.0810) detected in the leaves by positive ion mode, four clusters in Figure 15 (**(2)** 183.0933 and 217.0973, **(3)** 510.7847 and 426.8227, **(4)** 98.9850 and 192.9995, **(5)** 458.7713; 542.7315; and 290.8483) detected in the roots by positive ion mode, six clusters in Figure 17 (**(6)** 216.9269 and 96.9673, **(7)** 348.8966; 264.9342; 112.9853; and 180.9727, **(8)** 194.9450 and 78.9587, **(9)** 96.9617 and 96.9621, **(10)** 380.8433; 212.9208; 296.8820; 128.9592; 242.9398; and 548.7651, and **(11)** 476.2784 and 564.3306) detected in the roots by negative ion mode. They have almost the same RT compared to one another and being classified in the same sub-clusters with highly similar intensity patterns, thus, it is possible that each mass signal cluster belongs to the same LC chromatographic peak in the chromatogram. Cluster **(9)** and **(11)** each contained signals with close or identical *m/z* and very close RT which suggested that they were derived from the same peak caused by the same ion specie. Overall, HCAs of LC-MS/MS data support that biological samples used in metabolomic studies were eligible and suggest some mass lists for further study in *Os*CaM1-1 function and its biological significance.

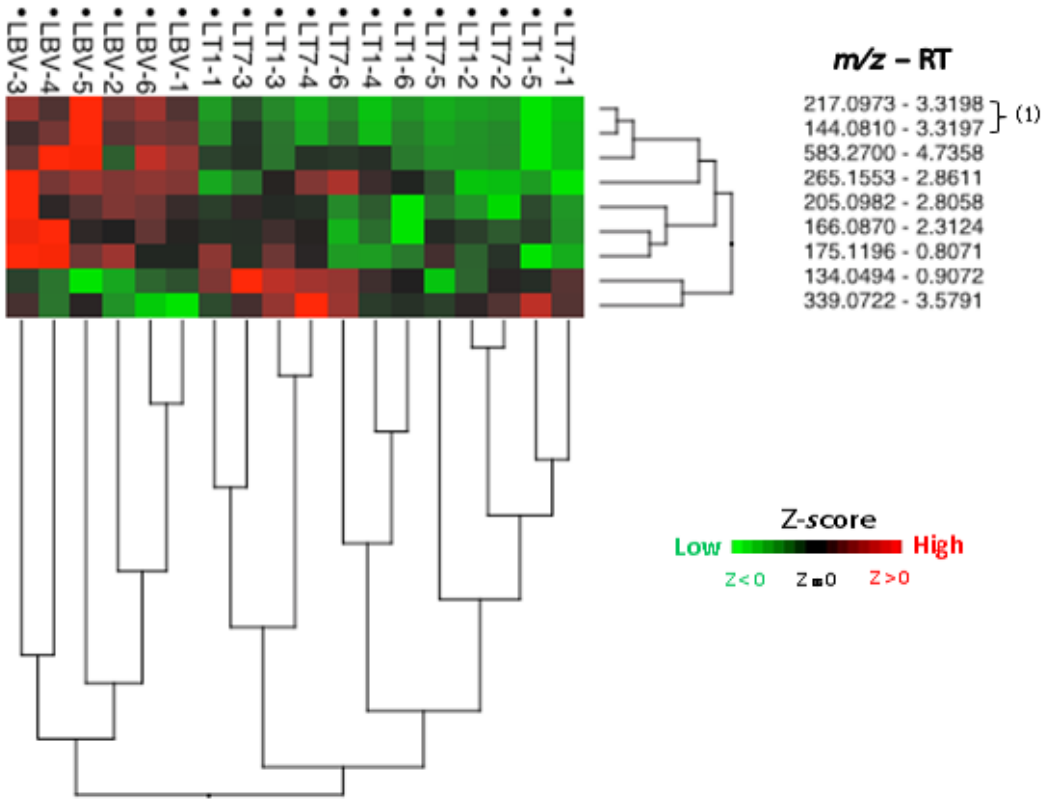

Figure 14. Cluster heat map generated from leaves metabolite data detected by positive mode LC-MS/MS. LT1: leaves of transgenic line1, LT7: leaves of transgenic line7, and LBV: leaves of control transgenic line. (1) is a mass signal cluster which might be the fragmentation products of the same metabolite.

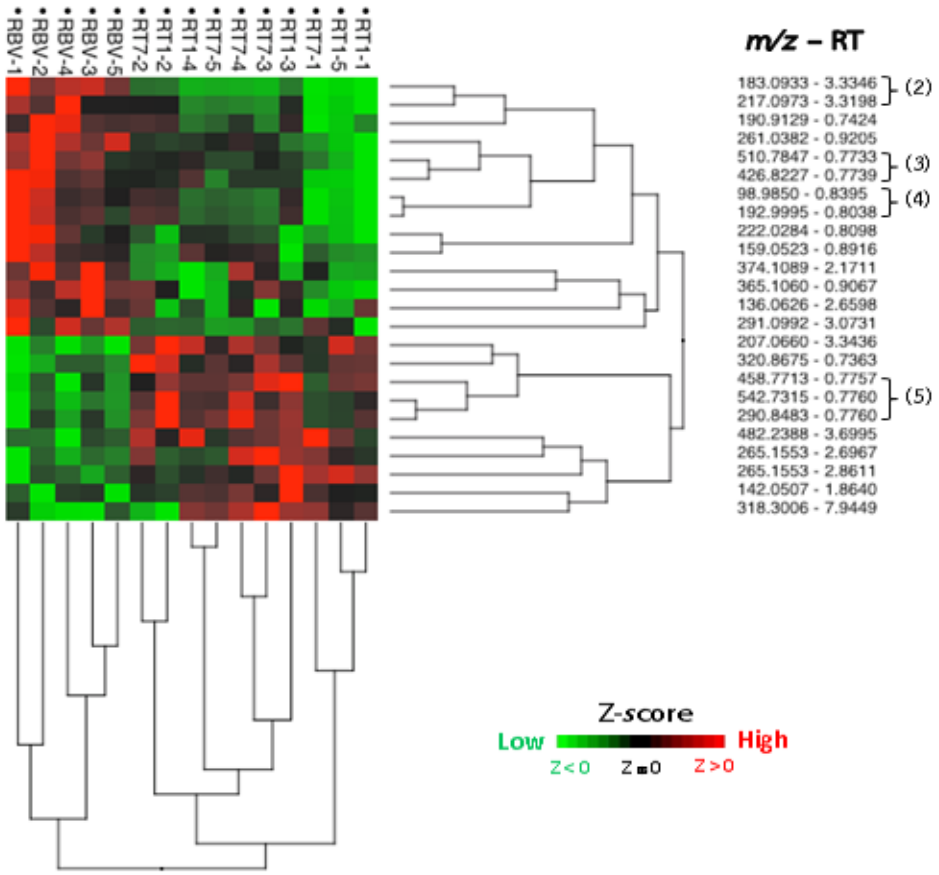

Figure 15. Cluster heat map generated from roots metabolite data detected by positive mode LC-MS/MS. RT1: roots of transgenic line1, RT7: roots of transgenic line7, and RBV: roots of control transgenic line. (2)-(5) are mass signal clusters which might be the fragmentation products of the same metabolite.

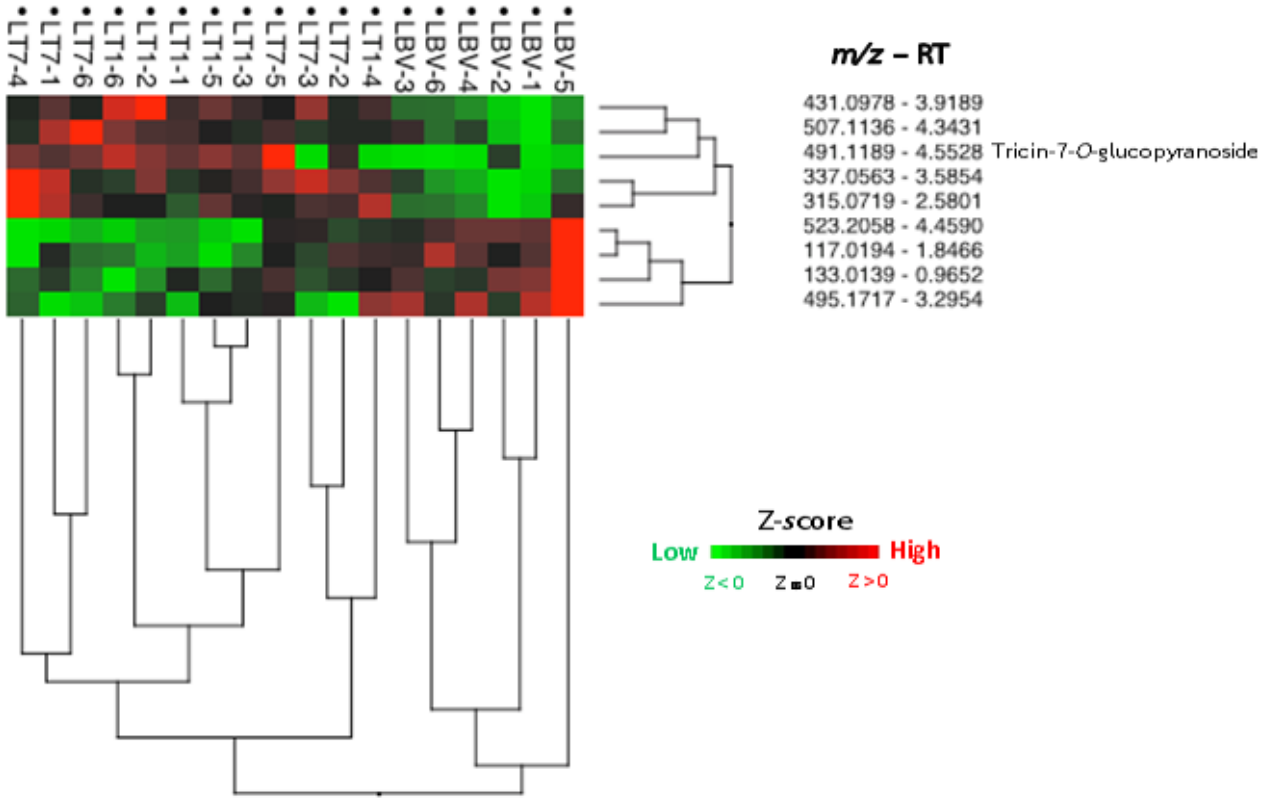

Figure 16. Cluster heat map generated from leaves metabolite data detected by negative mode LC-MS/MS. LT1: leaves of transgenic line1, LT7: leaves of transgenic line7, and LBV: leaves of control transgenic line.

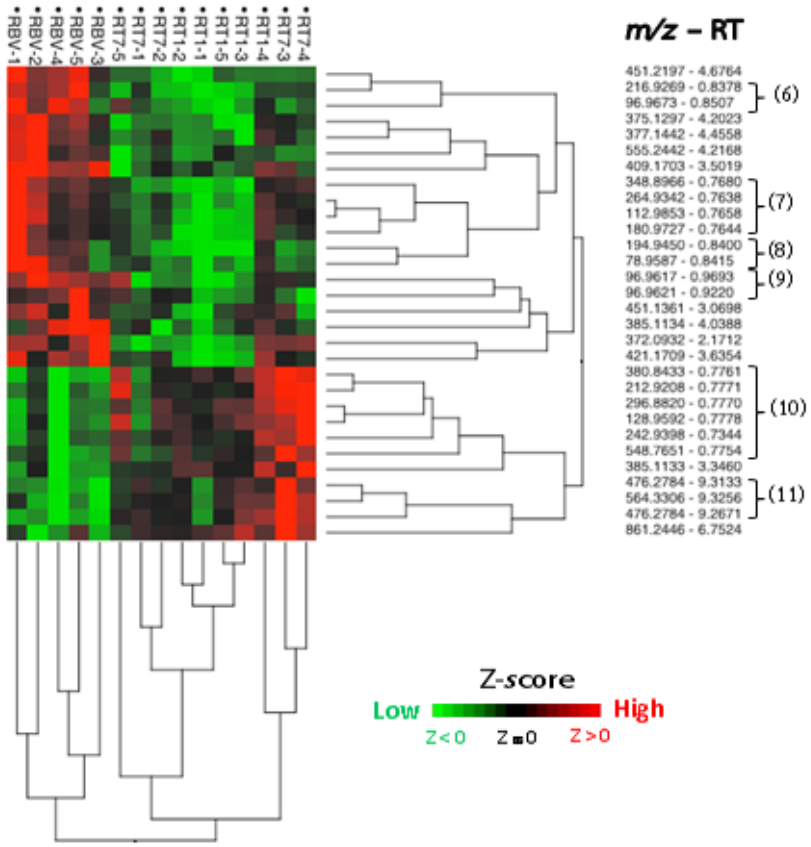

Figure 17. Cluster heat map generated from roots metabolite data detected by negative mode LC-MS/MS. RT1: roots of transgenic line1, RT7: roots of transgenic line7, and RBV: roots of control transgenic line. (6)-(11) are mass signal clusters which might be the fragmentation products of the same metabolite.

3.3.4 Selection of candidate differentially expressed genes based on metabolite data

Metabolites of interest which were differentially accumulated in transgenic rice lines were used to search corresponding genes in metabolic pathways using the KEGG database. This database is linked to the *O. sativa* japonica genome which enables the identification of genes involved in each step of the pathway. I selected six candidate genes representing three enzymes, namely arginase (Os04g0106300), glutathione synthetase (Os11g0642800, Os12g0263000, and Os12g0528400), and inositol-1-monophosphatase (Os02g0169900 and Os03g0587000), for gene expression analysis. Arginase is an enzyme catalyzing the conversion of arginine to ornithine, an intermediate in putrescine biosynthesis. Glutathione synthetase involves in glutathione biosynthesis from L-γ-glutamylcysteine. Lastly, inositol-1-monophosphatase catalyzes the conversion of inositol phosphates into inositol. These genes were chosen in response to the up-accumulations of polyamine, glutamate, cysteine, and inositol in the transgenic leaves, respectively. Reaction schemes of metabolite conversions catalyzed by these genes were represented in Figure 18. Even though, glutathione could not be detected by either GC-TOF/MS or LC-MS/MS. The up-accumulation of glutamate and cysteine suggested that glutathione biosynthesis might be increased, thus glutathione synthetases were included in the analysis. The reasons that some genes directly involve in the synthesis of up-accumulated metabolites could not be selected were because some enzymes did not present in the KEGG database or there were many enzyme isoforms with highly conserved nucleotide sequences making it difficult to design isoform-specific primers.

3.3.5 Validation of differentially expressed genes by real-time qRT-PCR

Figure 19 represents the relative expression level of each transgenic rice lines compared to the control transgenic line. The results showed that six candidate genes chosen from metabolomics data showed no significant differences in gene expression level between the transgenic and control rice plants.

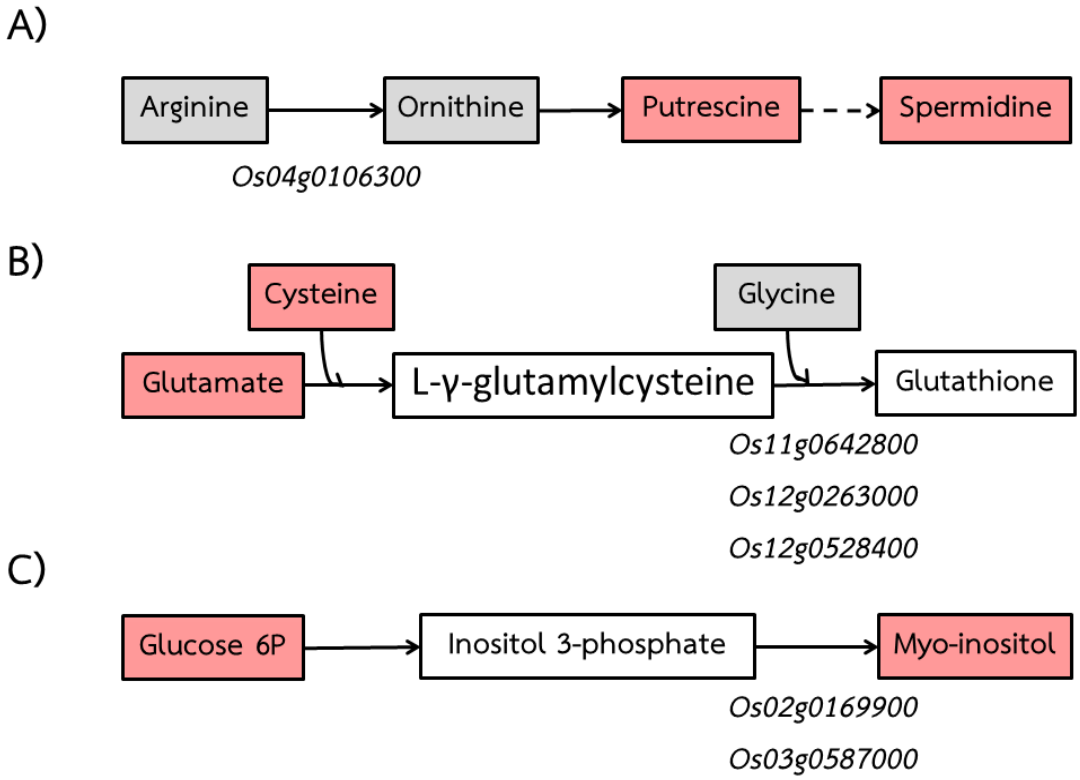

Figure 18. Bioconversion processes of metabolites catalyzed by chosen candidate proteins in accordance with metabolite levels in transgenic rice plants. Locus number(s) of the candidate genes, A) arginase; B) glutathione synthetases; and C) inositol-1-monophosphatases, were listed under the catalysis steps indicated by black arrows. Up-accumulated metabolites were labeled in red, non-significant change metabolites were labeled in grey, and undetectable metabolites were labeled in white.

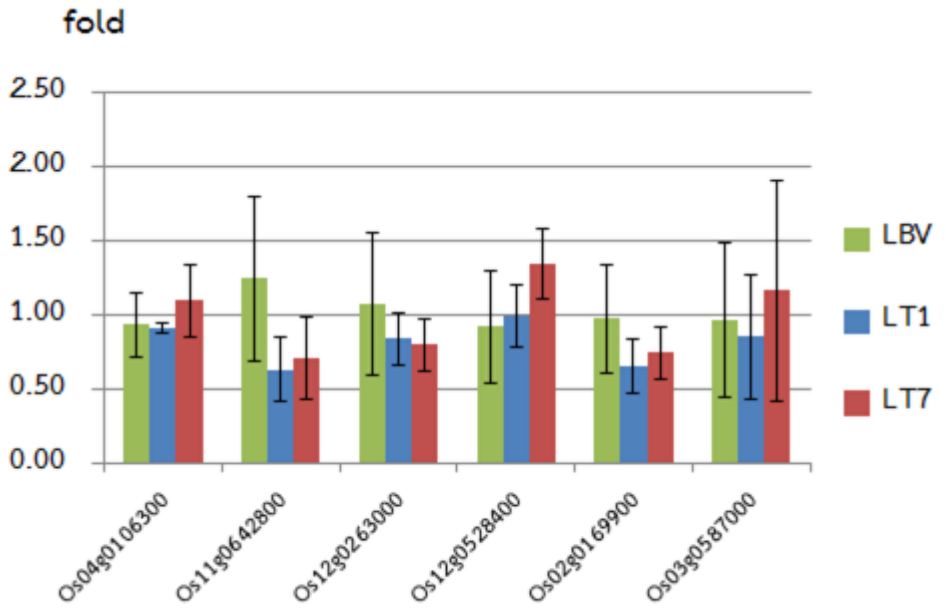

Figure 19. Relative expression levels of candidate genes in transgenic rice lines compared to blank vector control rice. LT1: leaves of transgenic line 1, LT7: leaves of transgenic line 7, and LBV: leaves of control transgenic line.

3.4 Gene expression analysis of previously identified candidate genes under salt stress condition

Although six candidate genes did not show significant changes in expression levels under normal condition, their expressions under salt-stress condition were still of interest. Since transgenic rice plants over-accumulated *OsCaM1-1* under normal condition, their responses in gene expression under stress might be different from the control transgenic line.

To perform this task, I checked if the expressions of these genes were affected under salt stress in the GENEVESTIGATOR online platform. The result showed that Os04g0106300, Os11g0642800, and Os12g0263000 have salt-affected expressions (Appendix D). In addition, I selected one more candidate genes from the cDNA-AFLP experiment, Os05g0105000 (TDF34), which was also confirmed to

be salt-affected gene. Therefore, these genes were chosen for further gene expression analysis of transgenic rice under salt stress condition.

Figure 20 represents relative expression level of each three-week-old transgenic rice line compared to the control transgenic line. The result showed that most gene expressions in three hours salt-stressed rice have no significant difference comparing between both transgenic and control rice. However, the expression of Os11g0642800 and Os05g0105000 showed numerically differences in relative expression level. The lower expressions of Os11g0642800 in T1 and Os05g0105000 in T7 were significantly different to the control group. Time course experiments under salt stress condition might be needed to elaborate these changes.

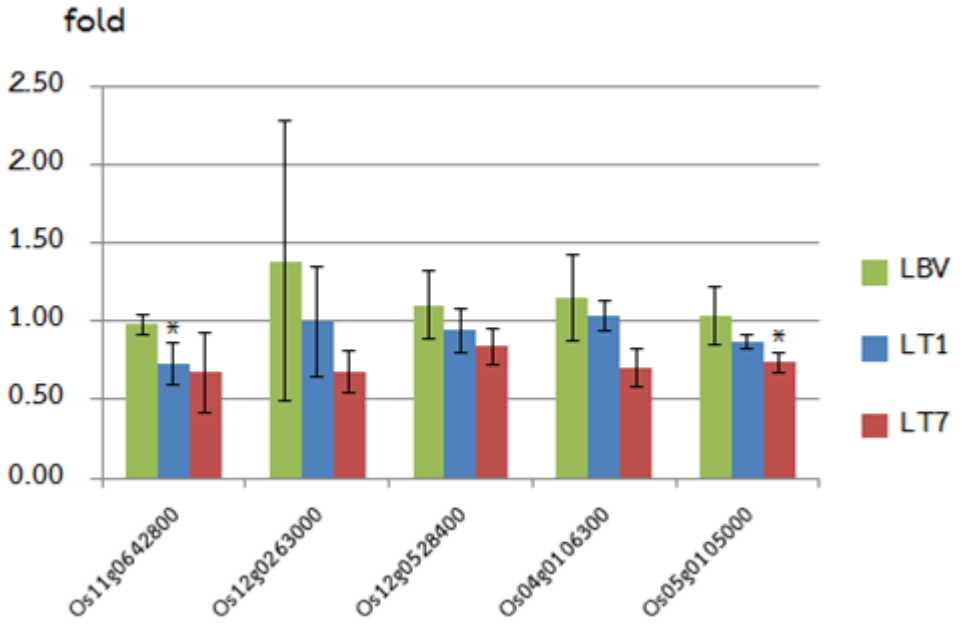

Figure 20. Relative expression levels of candidate genes in transgenic rice lines compared to control tramsgenic line at A) control (3 hr non-stress) and B) stress (3 hr salt stress) conditions. LT1: leaves of transgenic line 1, LT7: leaves of transgenic line 7, and LBV: leaves of control transgenic line. * indicates significant different in expression level at 95% confidence interval when compared to the control transgenic line.

3.5 CaM binding site prediction of candidate proteins

3.5.1 Web-based CaM binding site prediction by Calmodulin Target Database

Since the result showed that the changes in metabolite accumulations are not reflected by the change in gene expression, it is possible that these genes are regulated at protein level. It is well-known that CaM can bind to a wide range of proteins and affect target protein activities. Hence, amino acid sequences of six candidate genes chosen from metabolite data (see 3.3.4) were analyzed for putative CaM binding site using web-based Calmodulin Target Database. The result from web-based prediction was shown as a string of amino acid sequence (Figure 21-27). An individual amino acid will be given a score ranging from 0-9, the lowest to the highest probability, calculated from a "20-residue sequence walk" (Yap et al. 2000).

Regarding canonical motifs, the shortest CaM binding motif is ten amino acids in length (Mruk et al. 2014). Here, I only considered each particular sequence to be putative CaM binding site when it is composed of a string of 9s for longer than ten amino acids. The prediction results show that calcium/calmodulin-dependent protein kinase type II subunit alpha matched CaM binding motif in the database at the position 296-311 (Figure 21), arginase (Os04g0106300) contains 1 putative CaM binding site at the position 217-227 (Figure 22), glutathione synthetases; Os11g0642800 has 2 putative CaM binding sites at the position 229-239 and 388-405 (Figure 23); Os12g0263000 matches 1 unclassified database CaM-binding motif at 55-62 (labeled in red) and contains another putative binding site at 328-344 (Figure 24); Os12g0528400 has 1 putative CaM binding site at the position 269-282 (Figure 25), and inositol-1-monophosphatases; Os02g0169900 has 1 putative CaM binding site at the position 251-263 (Figure 26), while Os03g0587000 do not contains any putative binding site (Figure 27).

UniProt accession: P11275 (Calcium/calmodulin-dependent protein kinase type II subunit alpha)

```
Minimum score for sequence: 0 Maximum score: 9

....1 MATITCTRFT EEYQLFEELG KGAFSVVRRC VKVLAGQEYA AKIINTKKLS
..... 0000000000 0000000000 0000000000 0000000000 0000000000

...51 ARDHQKLERE ARICRLLKHP NIVRLHDSIS EEGHHYLIFD LVTGGELFED
..... 0000000000 0000000000 0000000000 0000000000 0000000000

..101 IVAREYYSEA DASHCIQQIL EAVLHCHQMG VVHRDLKPEN LLLASKLKGA
..... 0000000000 0000000000 0000000000 0000000000 0000000000

..151 AVKLADFGLA IEVEGEQQAW FGFAGTPGYL SPEVLRKDPY GKPVDLWACG
..... 0000000000 0000000000 0000000000 0000000000 0000000000

..201 VILYILLVGY PPFWDEDQHR LYQQIKAGAY DFPSPEWDTV TPEAKDLINK
..... 0000000000 0000000000 0000000000 0000000000 0000000000

..251 MLTINPSKRI TAAEALKHPW ISHRSTVASC MHRQETVDCL KKFNARRKLK
..... 0000000000 0000000000 0000000000 0000000000 0000099999

..301 GAILTTMLAT RNFSGGKSGG NKKNDGVKES SESTNTTIED EDTKVRKQEI
..... 9999999999 9000000000 0000000000 0000000000 0000000000

..351 IKVTEQLIEA ISNGDFESYT KMCDPGMTAF EPEALGNLVE GLDFHRFYFE
..... 0000000000 0000000000 0000000000 0000000000 0000000000

..401 NLWSRNSKPV HTTILNPHIH LMGDESACIA YIRITQYLDA GGIPRTAQSE
..... 0000000000 0000000000 0000000000 0000000000 0000000000

..451 ETRVWHRRDG KWQIVHFHRS GAPSVLPH
..... 0000000000 0000000000 00000000
```

Figure 21. Binding site search result of P11275. A number under each amino acid sequence represents a score from low (0) to high (9) probabilities which individual amino acid sequence might be involved in putative CaM binding site. Red characters represent amino acid sequence which matched CaM-binding motif in the database.

Os04g0106300 (Arginase)

```
Minimum score for sequence: 0 Maximum score: 11

....1 MGGVAAGTRW IHHVRRLSAA KVSADALERG QSRVIDASLT LIRERAKLKA
..... 0111111111 1112344444 4322222234 5554323456 7899999998

...51 ELLRALGGVK ASACLLGVPL GHNSSFLQGP AFAPPRIREA IWCGSTNSST
..... 7777776543 2110000000 0000000000 0000000000 0000000000

..101 EEGKELNDPR VLTDVGDVPI QEIRDCGVED DRLMNVVSES VKTVMEEDPL
..... 0000000000 0000000000 0000000000 0000000000 0000000000

..151 RPLVLGGDHS ISYPVVRAVS EKLGGPVDIL HLDAHPDIYD AFEGNIYSHA
..... 0000000000 0000000000 0000000000 0000000000 0000000000

..201 SSFARIMEGG YARRLLQVGI RSITKEGREQ GKRFGVEQYE MRTFSKDREK
..... 0000000112 3456789999 9999999876 5432110000 0000000000

..251 LESLKLGEGV KGVYISVDVD CLDPAFAPGV SHIEPGGLSF RDVLNILHNL
..... 0000000000 0000000000 0000000000 0000000000 0000000000

..301 QGDVVAGDVV EFNPQRDTVD GMTAMVAAKL VRELTAKISK
..... 0000000000 0000000000 1111111111 1111111111
```

Figure 22. Binding site search result of Os04g0106300. A number under each amino acid sequence represents a score from low (0) to high (9) probabilities which individual amino acid sequence might be involved in putative CaM binding site.

Os11g0642800 (Glutathione synthetase)

```
Minimum score for sequence: 0 Maximum score: 3

....1 MSSYVTTPHH HHHHGCCSGS RRLQAPAPPA RPRLVVAAAA RHVALPPRRA
..... 0000000000 0000000000 0000000036 6666666666 6666666630

...51 VASRAMSAEA PLGVAPAAAE EEMAAVVDEM AEEAAVWCAV HGLVVGDRAE
..... 0000000000 0000000000 0000000000 0000000000 0000000000

..101 PRSGTIPGVG LVHAPFALLP TRFPASFWKQ ARELAPIFND LVDRVSLDGE
..... 0000000000 0000000000 0000000000 0000000000 0000000000

..151 FLQDSLSRTR QVDDFTSRLL DIHAKMMEVN KEEDIRLGLH RSDYMLDSGT
..... 0000000000 0000000000 0000000000 0000000000 0000000000

..201 NSLLQIELNT ISSSFPGLSS LVSELHRTLL NRHGKVLGLD SKRIPQNWAA
..... 0000000000 0000000003 3333336699 9999999996 6666663300

..251 TQFAEALSMA WTEFNNKSAV IMMVVQPEER NMYDQYWLIN HLKESHGVKT
..... 0000000000 0000000000 0000000000 0000036666 6666666666

..301 IRKTLAQVEA EGQVLPDGTL VVDGQTVSVV YFRAGYSPND YPSEAEWRAR
..... 6666630000 0000000000 0000000000 0000000000 0000000000

..351 LLMEQSSAIK CPSISYHLVG TKKIQQELAK PNILERFLNN KEDIAKLRKC
..... 0000000000 0000000000 0000000000 0000036999 9999999999

..401 FAGLWSLDNE EIVKTAIEKP DLFVLKPQRE GGGNNIYGYD LRETLVRLQK
..... 9999963000 0000000000 0000000000 0000000000 0000336666

..451 EQGEALAAYI LMQRIFPRAS LTHLVQGGVC FEDLTISELG IFGAYLRNKD
..... 6666666666 6666330000 0000000000 0000000000 0000000000

..501 KVVLNNQCGY LMRTKVSSSN EGGVAAGFAV LDSILLTDEV ILHTN
..... 0000000000 0000000000 0000000000 0000000000 00000
```

Figure 23. Binding site search result of Os11g0642800. A number under each amino acid sequence represents a score from low (0) to high (9) probabilities which individual amino acid sequence might be involved in putative CaM binding site.

Os12g0263000 (Glutathione synthetase)

```
Minimum score for sequence: 0 Maximum score: 9

....1 MSFSKVYWDQ AVELAPLFNE LVDRVSLDGD FLQETLARTK EVDSFTGRLL
..... 0000000000 0000000000 0000000000 0000000000 0000000000

...51 DIHAKMMKLN KKEDVRLGLT RSDYMIDGAT DQLLQVELNT ISTSSNGLAC
..... 0000999999 9900000000 0000000000 0000000000 0000000000

..101 GVCELHRNLI RQHERELGLD PESVVGNTAI AQHAEALAGA WAEFNNQSSV
..... 0000000000 0000000000 0000000000 0000000000 0000000000

..151 VLVVVQPEER YMYDQYWITV ALREMYGVTT IRKTMAAIDA EGELRPDGTL
..... 0000000000 0002444444 4444444444 4442000000 0000000000

..201 TIDGLPVAVV YFRAGYTPND YPSEAEWRAR LLIECSSAIK CPSIAHHLVG
..... 0000000000 0000000000 0000000000 0000000000 0000000000

..251 TKKIQQELAK ENVLERFLDN KADIEKVRKC FAGLWSLEND SIVMSAIESP
..... 0000000000 0000000000 0000000000 0000000000 0000000000

..301 ELFVLKPQRE GGGNNIYGDN LRETLISLKK DGSNELAAYI LMQRIFPPAS
..... 0000000000 0000000000 0000247999 9999999999 9999742000

..351 LCYLVRDGTC IRENAVSEFG IFGAYLRNKD RVIINDQCGY LMRTKAASLN
..... 0000000000 0000000000 0000000000 0000000000 0000000000

..401 EGGVVAGYAF LNSVFLT
..... 0000000000 0000000
```

Figure 24. Binding site search result of Os12g0263000. A number under each amino acid sequence represents a score from low (0) to high (9) probabilities which individual amino acid sequence might be involved in putative CaM binding site. Red characters represent amino acid sequence which matched CaM-binding motif in the database.

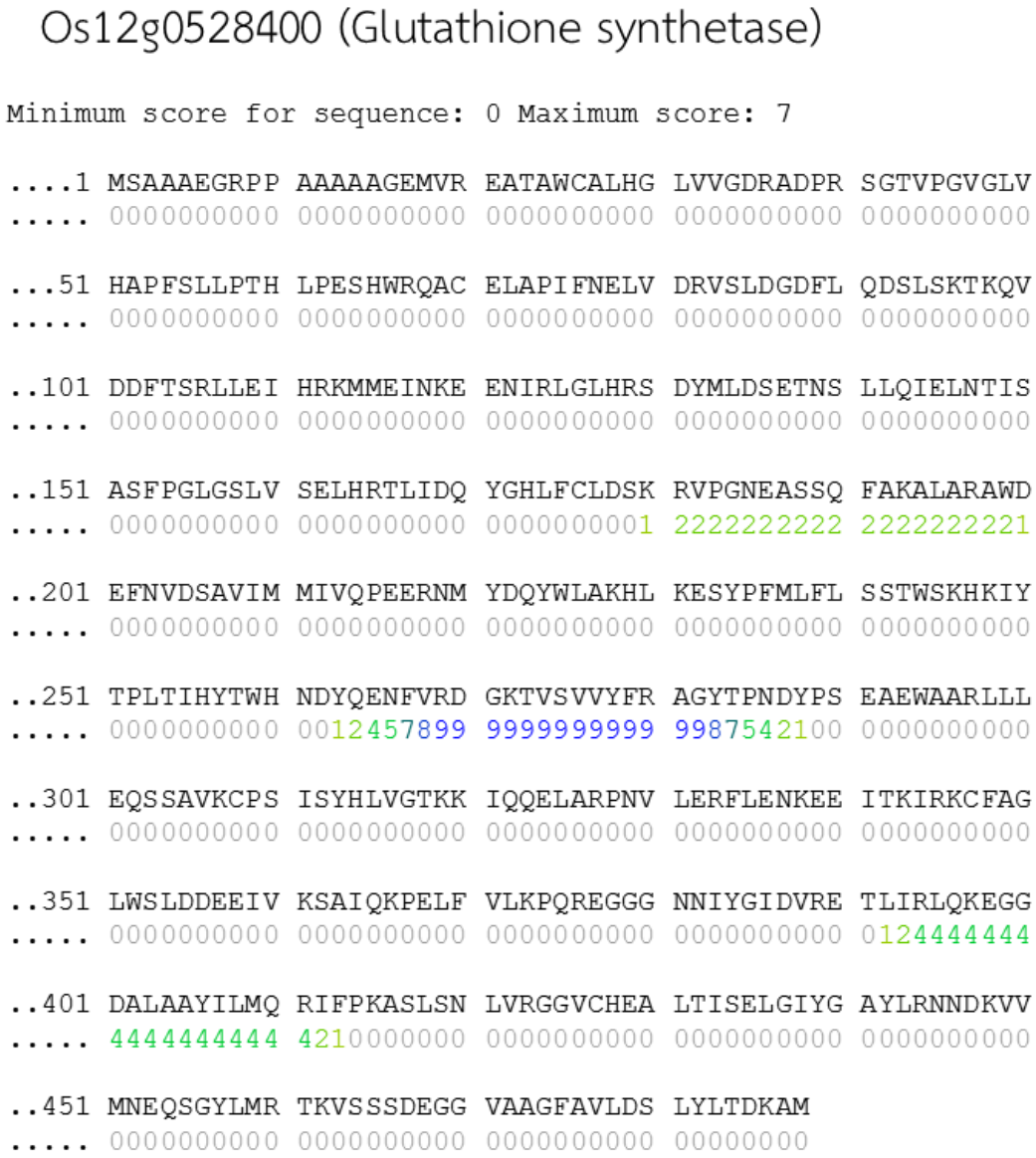

Figure 25. Binding site search result of Os12g0528400. A number under each amino acid sequence represents a score from low (0) to high (9) probabilities which individual amino acid sequence might be involved in putative CaM binding site.

Os02g0169900 (Inositol-1-monophosphatase)

```
Minimum score for sequence: 0 Maximum score: 5

....1 MARYLLRPPT AAAAAAAAAS SHRRNGTTSP RGPVLGLRAL ASRAGKARPV
..... 0000000000 0000000000 0000000000 0000000000 0000000000

...51 MAVASEQPAA RGKCPKVAAP TTGPIPAAEL LGVIQDAARA GAEVIMEAVN
..... 0000000000 0000000000 0000000000 0000000000 0000000000

..101 KPRNIHYKGV ADLVTDTDKL SESVILEVVR KTFPDHLILG EEGGLIGDAL
..... 0000000000 0000000000 0000000000 0000000000 0000000000

..151 SEYLWCIDPL DGTTNFAHGY PSFSVSIGVL FRGKPAASTV VEFCGGPMCW
..... 0000000000 0000000000 0000000000 0000000000 0000000000

..201 STRTVSASSG GGAYCNGQKI HVSKTDKVEQ SLLVTGFGYE HDDAWVTNIN
..... 0000000000 0000000000 0000000000 0000000000 0001357777

..251 LFKEYTDISR GVRRLGSAAA DMSHVALGIT EAYWEYRLKP WDMAAGVLIV
..... 9999999999 9997531111 0000000000 0000000000 0000000000

..301 EEAGGMVSRM DGGEFTVFDR SVLVSNGVVH DQLLDRIGPA TEDLKKKGID
..... 0000000000 0000000000 0000000000 0000000000 0000000000

..351 FSLWFKPDKY PTDF
..... 0000000000 0000
```

Figure 26. Binding site search result of Os02g0169900. A number under each amino acid sequence represents a score from low (0) to high (9) probabilities which individual amino acid sequence might be involved in putative CaM binding site.

Os03g0587000 (Inositol-1-monophosphatase)

```
Minimum score for sequence: 0 Maximum score: 10

....1 MAEEQFLAVA VDAAKNAGEI IRKGFYQTKN VEHKGQVSLP SSTVDLVTET
..... 0000011233 3345567889 9999987655 5543321110 0000000000

...51 DKACEDLIFN HLRKHYPDHK FIGEETSAAL GATADLTDDP TWIVDPLDGT
..... 0000000000 0000000000 0000000000 0000000000 0000000000

..101 TNFVHGFPFV CVSIGLTVGK IPTVGVVYNP IMNELFTAVR GKGAFLNGSP
..... 0000000000 0000000000 0000000000 0000000000 0000000000

..151 IKTSSQNELV KALLVTEVGT KRDKATLDDT TNRINKLLFK IRSIRMCGSL
..... 0000000000 0000000000 0000000000 1123333333 3333333333

..201 ALNMCGVACG RLDLCYEIGF GGPWDVAAGA LILREAGGFV FDPSGGEFDL
..... 2110000000 0000000000 0000000000 0000000000 0000000000

..251 MARRMAGSNS YLKDQFIKEL GDTS
..... 0111111111 1111111111 1000
```

Figure 27. Binding site search result of Os03g0587000. A number under each amino acid sequence represents a score from low (0) to high (9) probabilities which individual amino acid sequence might be involved in putative CaM binding site.

3.5.2 Visualization of putative CaM binding sites by homology modeling

According to Yap et al. (2000), 1/3 of the predicted CaM binding sites are false positives and do not bind to CaM. To preliminary screen out some of the false positive results, putative CaM binding sites were checked if they located at the surface of tertiary structure of the protein. Homology modeling of each protein was performed by Phyre[2]. All selected models were modeled from the template with the highest raw alignment score. The model outputs have 100% confidence but vary in %identity between the query and its respective template as shown in Table 9. Even though the template of arginase has %identity lower than 30% (according to Phyre[2], extremely high accuracy model should have >30% identity), the confidence as high as 100% could confidently support that the model adopts overall fold correctly. Thus, the model should have enough quality to identify whether putative CaM binding site is at the protein surface or not.

UCSF Chimera software was used to visualize putative CaM binding sites on the protein model. For the positive control, the prediction of calcium/calmodulin-dependent protein kinase type II subunit alpha showed that the predicted CaM binding site (residue 296-311) is overlapped with actual CaM binding site (290-314) (Figure 28). This example showed that Calmodulin Target Database has the potential to detect CaM binding site from protein amino acid sequence. As for candidate proteins, the modeled 3D structures showed that only the small part of putative CaM binding site of Os12g0528400 was presented at the surface (Figure 32), hence, this putative binding site is unlikely to bind to a CaM. Even though, the rest of the putative CaM binding sites of candidate proteins, namely Os04g0106300; Os11g0642800; Os12g0263000; and Os02g0169900, were presented at the protein surfaces (Figure 29-31, 33), the secondary structure of some predicted CaM binding sites show that they have low probability to bind CaM. From the search in Protein Data Bank and published literatures, all solved 3D structures showed that CaM binding motifs are mostly alpha helix. Only a few CaM binding motifs are formed as the combination of loop and helix (PDB accession: 2MGU and 1IWQ). These characteristics of CaM binding motifs indicate

that putative CaM binding sites in Os04g0106300 (Figure 29) and Os12g0263000 (Figure 31) are possibly not CaM binding sites, since their secondary structure are loops/turns and beta- sheets or helices that are smaller than known CaM binding motifs. In conclusion, CaM binding site prediction showed that the predicted CaM binding sites in Os11g0642800 (glutathione synthetase) and Os02g0169900 (inositol-1-monophosphatase) are potential CaM binding sites. These results suggest the possibility that these enzymes might be post-translationally regulated by CaM and, therefore, contribute to the changes in metabolite contents in those steps.

Table 9. Templates selected by Phyre[2] and parameters reflecting the quality of the model

locus number	query	template	PDB accession	% identity	model	
					% confidence	% coverage
UniProt: P11275	protein kinase subunit alpha	protein kinase holoenzyme	3SOA	96	100	91
Os04g0106300	arginase	3-guanidinopropionase	3NIP	28	100	83
Os11g0642800	glutathione synthetase	homoglutathione synthetase	3KAL	63	100	86
Os12g0263000	glutathione synthetase	homoglutathione synthetase	3KAL	63	100	98
Os12g0528400	glutathione synthetase	homoglutathione synthetase	3KAL	60	100	94
Os02g0169900	inositol-1-monophosphatase	inositol-1-monophosphatase	2QFL	34	100	70
Os03g0587000	inositol-1-monophosphatase	inositol-1-monophosphatase	2QFL	39	100	94

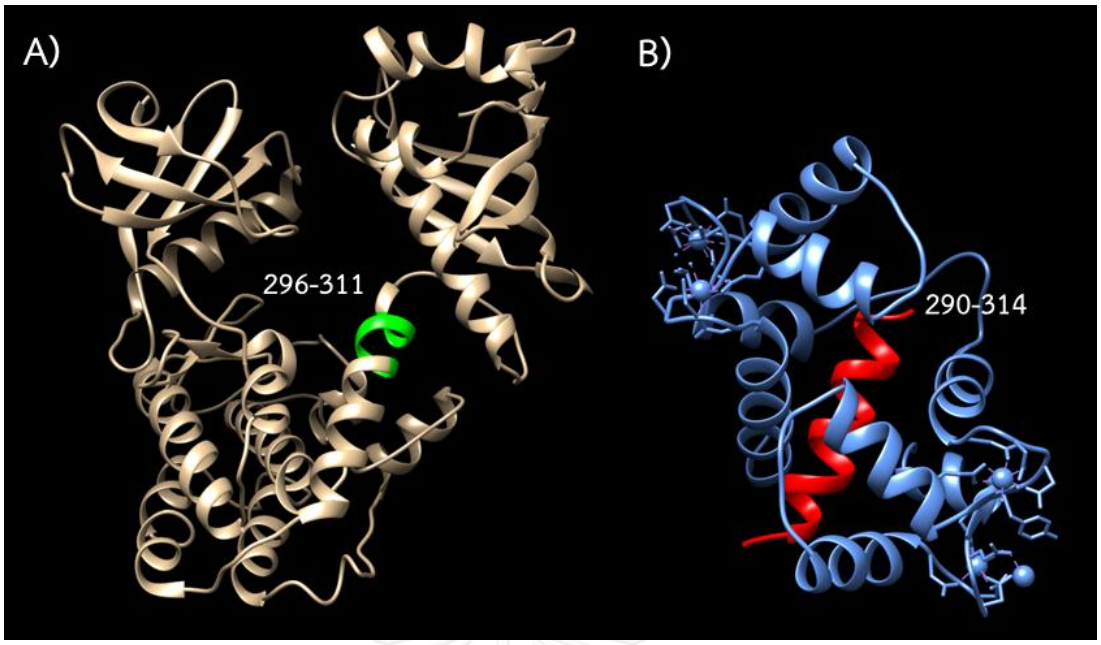

Figure 28. Positive control for CaM binding site prediction. A) The illustration of predicted CaM binding site of P11275 (calcium/calmodulin-dependent protein kinase type II subunit alpha) on the Phyre[2] model**.** The predicted CaM binding site (residue 296-311) was labeled in green. **B)** Crystal structure (PDB accession: 1CM1) of CaM binding with CaM-binding peptide derived from calcium/calmodulin-dependent protein kinase type II subunit alpha**.**

Figure 29. The position of putative CaM binding site on the Phyre[2] model of Os04g0106300 (arginase). The predicted CaM binding site (residue 217-227) was labeled in green.

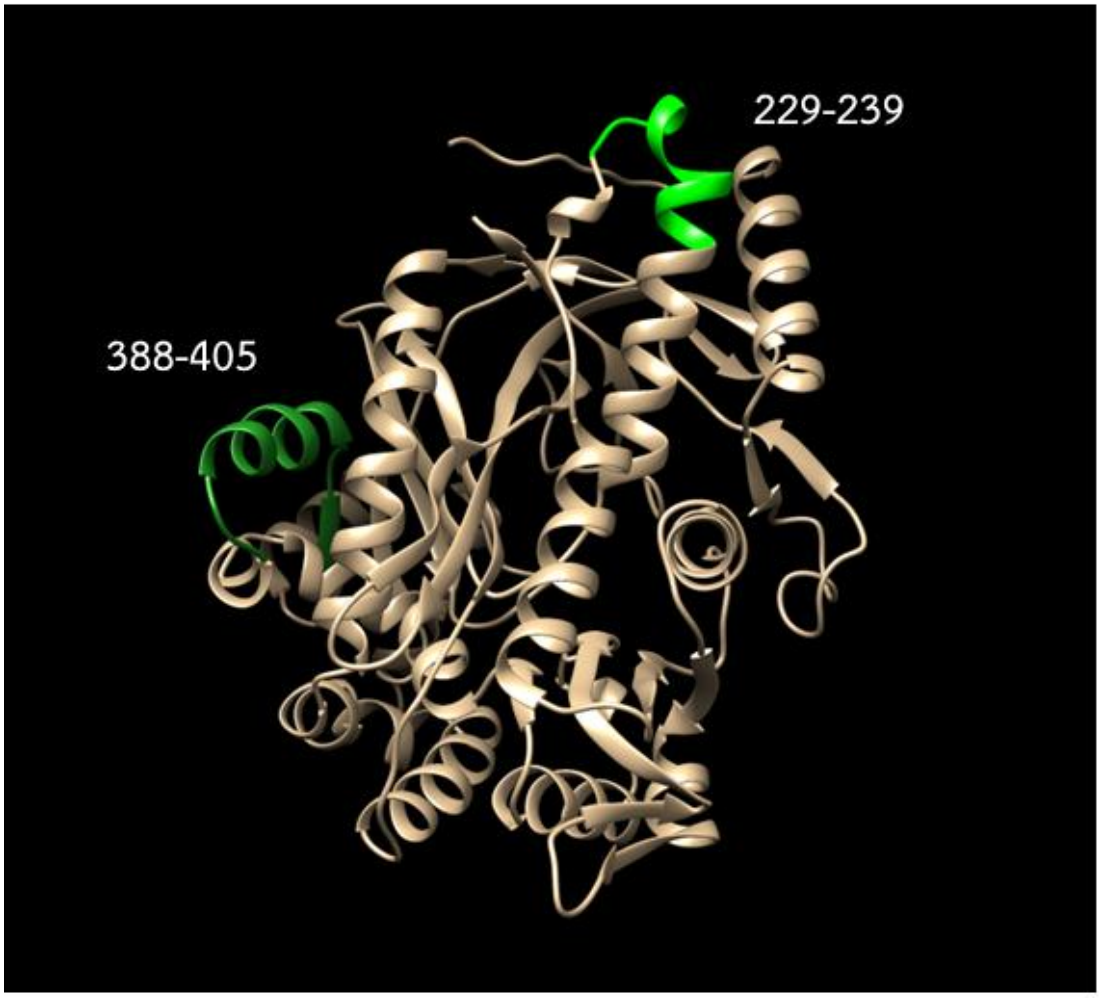

Figure 30. The position of putative CaM binding sites on the Phyre[2] model of Os11g0642800 (glutathione synthetase). The predicted CaM binding sites (residue 229-239 and 388-405) were labeled in green.

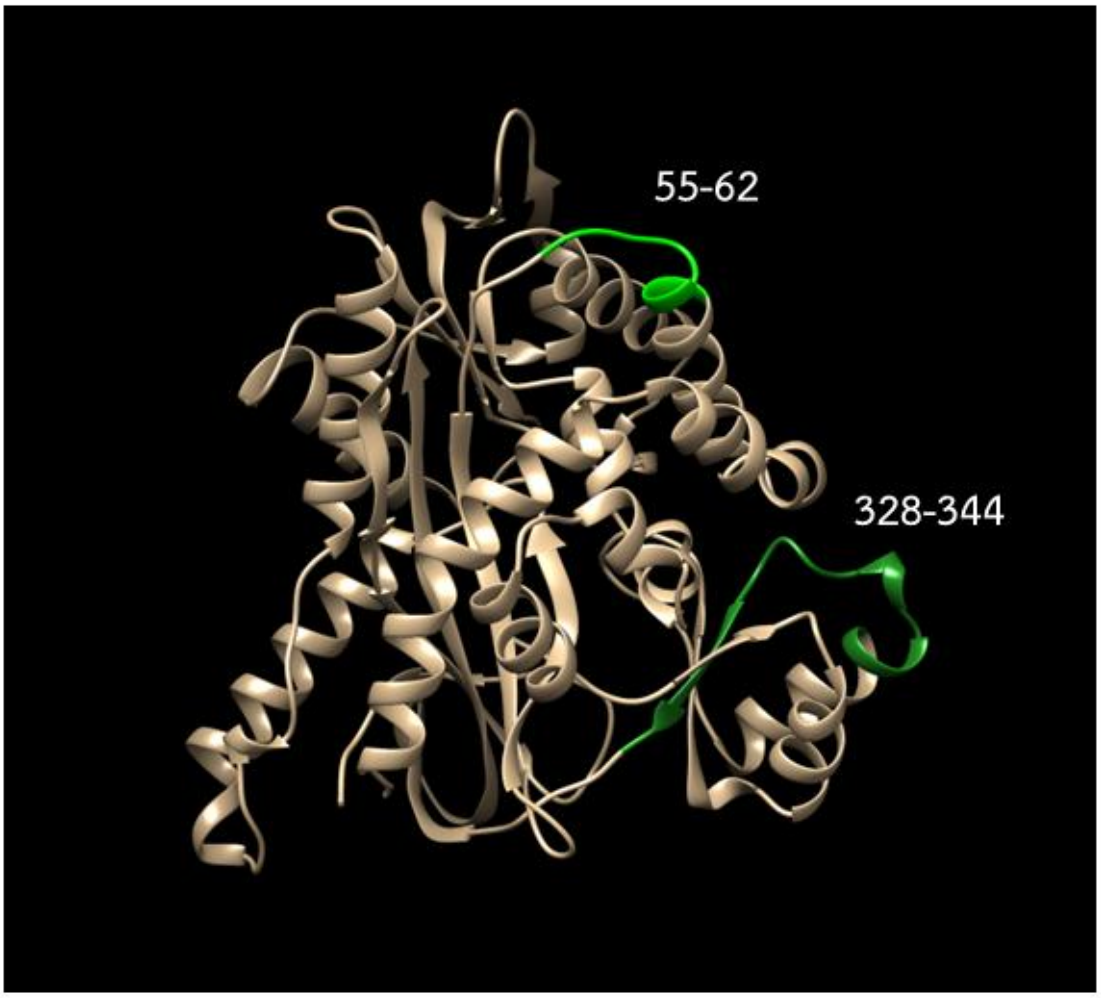

Figure 31. The position of an unclassified database CaM-binding motif and a putative CaM binding site on the Phyre[2] model of Os12g0263000 (glutathione synthetase). The unclassified database CaM-binding motif (residue 55-62) and the predicted CaM binding site (residue 328-344) were labeled in green.

Figure 32. The position of putative CaM binding site on the Phyre^2 model of Os12g0528400 (glutathione synthetase). The predicted CaM binding site (residue 269-282) was labeled in green.

Figure 33. The position of putative CaM binding site on the Phyre[2] model of Os02g0169900 (inositol-1-monophosphatase). The predicted CaM binding site (residue 252-263) was labeled in green.

CHAPTER IV
DISCUSSION

4.1 Identification of differentially expressed genes by cDNA-AFLP

At present, there are only a few studies involving *OsCaM1-1* functions in rice. It has been reported that *OsCaM1-1* could be induced by salt stress, heat stress, osmotic stress, wounding, and exogenous ABA application (Phean-o-pas et al. 2005; Saeng-ngam et al. 2012; Wu et al. 2012; Sripinyowanich et al. 2013). However, very little information is known about downstream processes occurred after *OsCaM1-1* expression. In Thai rice 'KDML 105', the overexpression of *OsCaM1-1* resulted in higher level of ABA accumulation and induced expression of ABA biosynthetic genes. Also, transgenic rice overexpressing *OsCaM1-1* was found to have higher salt tolerance by being able to maintain their dry mass during salt stress better than control plants (Saeng-ngam et al. 2012). Another study in japonica rice 'Tainung No.67' showed that *OsCaM1-1* mediated heat-shock signaling in rice. It also caused the up-regulation of heat-shock responsive genes in *OsCaM1-1*-overexpressing transgenic Arabidopsis grown under normal condition. As a result, the transgenic Arabidopsis showed increased thermotolerance. Nuclear localization of GFP-tagged *Os*CaM1-1 in transformed Arabidopsis protoplast after heat-shock treatment was also observed (Wu et al. 2012). Interestingly, many plant transcription factors were reported to be CaM targets (Szymanski et al. 1996; Bouche et al. 2002; Yang and Poovaiah 2003; Park et al. 2005), thus, it might be possible that nuclear localization of *OsCaM1-1* following stress signal involves in such phenomenon. If this hypothesis is true, a large portion of genes should be affected by *Os*CaM1-1 through its interaction with transcription factors. Since there is no study regarding *Os*CaM1-1-mediated transcriptomic response, in this study, cDNA-AFLP was used to screen for

candidate genes which might be affected by the overexpression of *OsCaM1-1* in the transgenic rice.

Pooled sample from six replicates of leaves and roots of the T1 was used to compare cDNA-AFLP transcript profiles with respective WT sample. These samples were collected from the rice grown under normal condition since it has been reported that *OsCaM1-1* expression could be highly induced by salt stress. It is possible that endogenously induced *Os*CaM1-1 could interfere with the comparison between the *OsCaM1-1*-overexpressing samples and WT samples. cDNA-AFLP analysis showed that transcript profiles from 33 PCs yield at least 100 TDFs with differential band intensities. By subsequent TDF recovery, cloning, and sequencing steps, 31 candidate genes differentially expressed in the transgenic rice were identified. However, from real-time qRT-PCR result, a total of 10 leaf candidate genes tested did not show significant different in gene expression level between transgenic and WT samples. This could be explained by many possible reasons. First of all, the rice samples used for real-time qRT-PCR were 3-week-old rice cultivated in the transgenic green house (prepared by Mr.Worawat for his gene expression analysis experiment) while cDNA-AFLP samples were two-week-old rice cultured in the growth chamber. Even though the rice was in the same developmental stage (seedling), the 1-week different might be the reason for the conflict between cDNA-AFLP and real-time qRT-PCR result. Also, there are many factors that could lead to false positive results of cDNA-AFLP. The nature of cDNA-AFLP technique involves amplification with very high cycle number, i.e., in this case, 25 cycles of pre-amplification and 41 cycles of selective amplification. High number of amplification cycle could overstate the differences of biological variations, thus, pooled sampling might be inappropriate for cDNA-AFLP. Also, the TDF band showing differential band intensity may consist of many TDF species (maximum of three genes per band were found). To solve this problem, at least three individual clones of *E. coli* transformants were chosen from

each TDF cloning reaction for subsequent sequencing. However, any false positive TDFs which have higher expression than differentially expressed gene could substantially lead to misinterpretation, relying on the gel-extracted TDF mixture. These reasons support why the identification of differentially expressed genes by cDNA-AFLP was unsuccessful.

Another attempt to identify differentially expressed genes in the transgenic rice was done by our research group. We used RNA-sequencing (RNA-seq) to compare transcriptomes of the wild type and the transgenic rice (T1) to investigate *Os*CaM1-1-affected gene expression. The result showed that only small number of genes were differentially expressed in the transgenic rice. For more than 28,000 genes detected, roughly 400 genes (<1.5%) were found to be differentially expressed (more than 2-fold up/down -regulated). Around 1,300 genes were found to be slightly affected (<2 fold change). This finding might suggest that high-cycle-number amplification could lead to false-positive in cDNA-AFLP analysis.

4.2 Metabolomics reveals that *OsCaM1-1* overexpression affects rice metabolite profiles.

Apart from cDNA-AFLP analysis, another interesting approach in identifying the function of *Os*CaM1-1 is metabolomics. The accumulation of metabolites in the cell affects plant phenotype and physiological response directly. The identification of differentially accumulated metabolite in the transgenic rice plants would then, help in explaining how the transgenic rice has increased tolerance to salinity stress. By using GC-TOF/MS and LC-MS/MS, snapshots of hundreds of metabolite levels were assessed in the relative manner among wild type rice, *OsCaM1-1* overexpressing rice, and control transgenic rice expressing *OsCaM1-1* at basal level. Since metabolomics is a very powerful technique, it generates very large amount of data. PLS-DA was applied to cluster datasets and screen for differentially accumulated metabolites.

PLS-DA score plots of metabolites detected by GC-TOF/MS from every sample group, namely wild type (WT), transgenic (T1 and T7) and control transgenic (BV) group was constructed (Figure 11A). The metabolite data of six biological replicates of each sample group were clustered together. Also, the clustering of all sample groups was clearly distinguishable on the score plot, i.e., the metabolite variations among biological replicates were smaller than the metabolite variations between sample groups. However, the clustering of WT metabolites was isolated away from both transgenic and BV group. This is the reason why I decided to use BV instead of WT rice as a control group for analyzing the metabolomics data. It is possible that the process of transgenic plant construction might have caused an unintended effect on the transgenic plant. The BV rice, transformed by the empty vector, should serve as a better control in this experiment. More score plots were then constructed from the data of three sample groups without WT (Figure 11B-11D). These results demonstrated that the overexpression of *OsCaM1-1* was responsible for the differential of metabolite profiles in the transgenic rice.

4.3 Overexpression of *OsCaM1-1* induces pre-adaptive response in the transgenic rice.

PLS-DA loading plots suggested the list of metabolites having significantly different in content comparing transgenic and BV rice. After the validation by student's t-test (95% CI), metabolites with same accumulation trend in both two transgenic lines were listed in Table 6-8. Interestingly, from GC-TOF/MS data, even though both transgenic rice lines show the same metabolite accumulation pattern, the leaves of T1 always show higher degree of up-accumulation compared to the leaves of T7 (Table 6). This suggests the possibility that *Os*CaM1-1 might exhibit dose-dependent regulatory effect. This hypothesis was supported by many studies which demonstrated that CaM could affect DNA replication of mammalian cells (*in vivo*) (Reddy et al. 1992), ATP-dependent calcium uptake of rat basolateral membrane (*in*

vitro) (Nellans and Popovitch 1981), and enzymatic activity of plant GAD (*in vitro*) (Snedden et al. 1996) in a dose-dependent manner. It is interesting to see if different kind of stresses would trigger different magnitude of *OsCaM1-1* induction in plant cells. However, this relationship was not found in the roots. These results suggest that mode of action of *Os*CaM1-1 might be different between leaves and roots.

These changes were also used to map into the primary pathway to help in understanding the effects caused by the overexpression of *OsCaM1-1* (Figure 12). Accumulation of primary metabolites, such as proteinogenic amino acids, glycolytic and TCA cycle intermediates were found in both leaves and roots of the transgenic rice plants, however, the effects in the leaves were more pronounced. Many stress-associated metabolites were also found to be up-accumulated in transgenic rice, for example, inositol, spermidine, putrescine, and tricin 7-*O*-beta-D-glucopyranoside. Taken together, the results demonstrate that the overexpression of *OsCaM1-1* has induced the transgenic rice into a proactive state.

Urano et al. (2009) reported that amino acid accumulations in response to dehydration depended on ABA production. Since the transgenic rice used in this study was reported to have increased ABA content (Saeng-ngam et al. 2012), it suggests that up-accumulations of many amino acids in the transgenic rice lines may be ABA-related. High availability of amino acids would accelerate the stress-responsive mechanisms of the transgenic rice at the protein level by readily synthesizes proteins following the expression of stress-counteracting genes. The up-accumulations of glucose 6-phosphate, fructose 6-phosphate, citrate, isocitrate, and succinate can be inferred that transgenic rice has more active energy metabolism than control transgenic rice and would be more competent at maintaining cellular homeostasis under stress condition.

Inositol was previously determined as a stress-related metabolite which has been studied in many plant species. Phosphorylated derivatives of myo-inositol were reported to be involved in stress signal transduction in plants (Zhu 2002). The oxidation pathway of myo-inositol was also found to play a role in cell wall polysaccharide biogenesis (Loewus and Murthy 2000). Inositol derivatives (methyl-inositols), namely ononitol and pinitol act as osmoregulators in some plant species.

For example, two enzymes involving in the bioconversion of myo-inositol into methylated inositols were induced during salinity stress in halophyte *Mesembryanthemum crystallinum* (Ishitani et al. 1996). In *M. crystallinum,* the transportation of inositol was found to be positively correlated with Na^+ from plant roots to the plant leaves. Ononitol and pinitol accumulated in the cytosol while Na^+ was sequestered in the vacuole (Bohnert and Sheveleva 1998; Nelson et al. 1998). In rice, the activity of inositol synthase activity was highly induced in chloroplast during salt stress in salt-tolerant varieties while the increases in salt-sensitive varieties were marginal. The result suggested the possible role of myo-inositol as an osmolyte in the chloroplast (Raychaudhuri and Majumder 1996; Loewus and Murthy 2000). Further studies are needed to answer the biological relationships between inositol and salt tolerant capability of the rice since rice cannot synthesize ononitol and pinitol.

For polyamines, they are well-known metabolites accumulating in plants under various stress conditions. Many studies have supported that polyamines have positive effects in plant stress tolerance and adaptation (for review, see Hussain et al. (2011)). Supplementation of exogenous polyamines was documented to help maintain cell membrane integrity (Zhang et al. 2009), reduce growth cessation caused by stress (Ali 2000), reduce free radicals contents (Yiu et al. 2009), and increase antioxidant enzymes activities (Afzal et al. 2009). Construction of many transgenic plants was also used to study the roles of polyamines in plant stress response. For example, Arabidopsis mutants with reduced arginine decarboxylase activity failed to accumulate polyamine under salt stress condition and showed reduced salt tolerance comparing to wild type Arabidopsis (Kasinathan and Wingler 2004). Many transgenic rice lines were constructed with an aim to improve polyamine biosynthesis and stress tolerance. Transgenic rice expressing *Datura stramonium* arginine decarboxylase accumulated higher amount of putrescine under drought condition and showed higher tolerance to drought stress (Capell et al. 2004). *Tritordeum* S-adenosylmethionine decarboxylase was also introduced into transgenic rice leading to up to four-fold higher accumulation of spermine and spermidine content than non-transgenic plant under salt stress condition. As a result, transgenic

seedings showed higher growth after NaCl treatment comparing to non-transgenic control (Roy and Wu 2002). These accumulating evidences have clearly supported that higher content of putrescine and spermidine in the transgenic rice overexpressing *OsCaM1-1* is beneficial.

In term of secondary metabolites, there are many unknown metabolites found to differentially accumulate in the transgenic rice. This is because of the highly diverse nature of the secondary compounds; the number of compound in the database used was not enough for efficient mass signal annotation. Nevertheless, a high up-accumulation of up to 4-fold of tricin 7-*O*-beta-D-glucopyranoside was found in both lines of transgenic rice leaves. Tricin was recently reported to be a lignin monomer in all monocots examined to date (Lan et al. 2015). This flavonoid was also previously reported to have protective effect for plant against fungal pathogens, *Pyricularia oryzae* and *Rhizoctonia solani*, and brown planthopper nymphae (Kong et al. 2004; Bing et al. 2007). Therefore, the up-accumulation of these metabolites in the transgenic rice grown under normal condition showing many stress-response signatures has suggested that the overexpression of *OsCaM1-1* induced transgenic rice to proactive state.

4.4 Hierarchical Clustering Analysis (HCA) of differential metabolite accumulations

Two-way HCA was applied on Z-score transformed GC-TOF/MS and LC-MS/MS metabolite data and cluster heat maps were then generated. For GC-TOF/MS, HCA was performed on the data of differentially accumulated metabolite in leaf and root altogether (Figure 13). The cluster heat map shows that metabolites were classified into five clusters according to their accumulation patterns in each sample. It suggests that biosynthesis of metabolites which were grouped in the same cluster might be controlled by *Os*CaM1-1 via similar mechanisms. Mosaic plot of the heat map also provide efficient comparison of metabolite abundance in two organs, leaf and root. It highlights the fact that the presentation of fold-change alone could be misleading. For example, the color shift of three-fold up-accumulation of threonic acid-1,4-

lactone in transgenic rice roots can barely be seen in this heat map in contrast to leaf samples (1.8-2.5 fold up-accumulation) (Figure 13). It suggests that higher fold change does not always mean higher change when considering the actual content of the metabolite, therefore, the actual amount of the metabolites in each organ should also be considered before judging the importance of each metabolite (e.g. transgenic rice leaves have 15-fold higher content of threonic acid-1,4-lactone than transgenic rice roots).

For LC-MS/MS data, secondary metabolites prefer to present in an organ-specific manner which makes it impossible to combine leaf and root data to generate a single heat map. Highly diverse plant secondary compounds also lead to difficulty in mass signal annotation. One strategy to deal with the data with many unknowns is by using statistical analysis. As demonstrated by Kuzina et al. (2009), four different statistical approaches, namely correlation analysis, principal component analysis, UPGMA cluster analysis and two-way HCA, were used to identify bioactive compounds contributing to the insect resistance in *Barbarea vulgaris*. They found that four different methods could reduce data complexity and lead to the same group of mass signals correlate with the insect resistant phenotype which successively narrow-down the mass signatures for further annotation. In this study, HCAs show that there were 11 clusters of mass signals with each cluster consisted of mass signals having similar signal patterns and almost identical retention time (Figure 14, 15, and 17). It suggests that each cluster is mass signals which might come from the same compound. This could facilitate the annotation of mass signatures for the identification of secondary metabolites which differentially accumulated in response to *OsCaM1-1* overexpression.

4.5 *Os*CaM1-1 might involve, but not as a master regulator, in proline biosynthesis in rice.

Even though there is no outstanding accumulation of osmoprotectant in the transgenic rice. The possibility that *Os*CaM1-1 might play roles in the regulation of osmolyte biosynthesis should not be excluded, since the rice used in this experiment

was grown under non-stress condition. Tightly regulated metabolism in maintaining plant water homeostasis might be responsible for the explanation. The previous study by Sripinyowanich et al. (2013) has demonstrated that *Os*CaM mediates proline accumulation in rice during salt stress. The treatment of CaM-antagonist, W-7, during salt stress resulted in more than 3-fold reduction of proline content in rice seedling. Until now, it could not rule out that *Os*CaM1-1 involves in such phenomenon. Interestingly, according to my result, glutamate was found to be up-accumulated in both leaves and roots of the transgenic rice (Table 6-7). It has been shown that glutamate is an important substrate in proline biosynthesis in stressed plant. Rice Δ^1-pyrroline-5-carboxylate synthetase, a key enzyme in proline biosynthetic pathway, was up-regulated in correlation with proline accumulation in rice following salt stress (Igarashi et al. 1997). Roosens et al. (1998) also showed that four-week-old Arabidopsis plant do not use ornithine but depend solely on glutamate as a substrate for proline biosynthesis under salt stress condition. Despite the up-accumulation of the glutamate, proline contents remain unchanged in the transgenic rice. It could only suggest whether *Os*CaM1-1 is not the specific CaM isoform mediating the signaling for proline accumulation or the cell osmotic adjustment mechanism needs other key factors than *Os*CaM signaling alone. The latter case was supported by the study conducted in Arabidopsis subjected to the combination of drought and heat stress. It was found that proline accumulated in drought-stressed plant but not in the drought & heat -stressed plant. Furthermore, heat stress was reported to promote exogenous proline toxicity by significantly reduced the root growth of Arabidopsis under combination of proline and high temperature treatment (Rizhsky et al. 2004). Taken together, due to the fact that *Os*CaM1-1 involves in a broad range of stresses including heat stress, *Os*CaM1-1 alone, is not likely act as a key regulator in proline biosynthesis.

4.6 No-change in expression of candidate genes suggested the possibility of post-translational regulation at some metabolic steps.

With the aim of trying to identify metabolite-to-gene correlation, metabolite of interest, e.g. stress-related and up-accumulated in the transgenic rice, was searched against the KEGG metabolic pathway database. Candidate genes involving in the metabolism of metabolite of interest were then chosen, nonetheless, some enzymes having too many isoforms i.e. more than three, were screened out for the ease of gene expression analysis experiment. Total of six candidate genes representing three enzymes namely, arginase, glutathione synthetase, and inositol-1-monophosphatase were chosen in response to the up-accumulation of polyamines, glutamate, and inositol, respectively. However, gene expression analysis by real-time qRT-PCR revealed no significant change of any genes comparing between transgenic and BV rice grown under normal condition. Also, some of the candidate genes that were reported to be salt-responsive were assayed in the 3-hour salt-stressed rice, yet, no significant change in gene expression levels of these genes was found. To elaborate on the detail, some data showed significant different in gene expression level (Figure 20), but these significances present only in one of the two transgenic lines. In fact, it has been demonstrated that endogenous *OsCaM1-1* could be induced up to five-fold in one hour following salt stress treatment before dramatically decrease to two-fold induction at three hour after treatment (Chinpongpanich et al. 2012). So, the result has suggested a few possibilities. Firstly, candidate genes tested were not regulated by *Os*CaM1-1. Next, cellular-response to *Os*CaM1-1 was already saturated by endogenous *Os*CaM1-1 highly induced after stress. In such case, I suggest that expression analysis of these genes at the time point of less than 1 hour after salt treatment should be performed. It would explain whether *OsCaM1-1* overexpression could induce the faster response of these genes, considering the stage which endogenous *Os*CaM1-1 is not yet maximally induced.

Apart from my experiment, our research group has also performed transcriptomic study of the transgenic rice using RNA sequencing (RNA-seq). I found that RNA-seq result was in accordance with the real-time qRT-PCR experiment in

which arginase, glutathione synthetase, and inositol-1-monophosphatase showed no significant difference in gene expression comparing transgenic and wild type rice. In addition, I also manually screened RNA-seq data of enzymes in many metabolic pathways for any possible metabolite to gene correlations (Appendix E). However, no correlation was found between the changes in metabolite accumulation and gene expression in all pathway examined. Overall, these results suggested that some differentially accumulated metabolite might be caused by *Os*CaM1-1-mediated post-translational regulation.

4.7 CaM binding site prediction reveals that some candidate genes might be CaM targets.

Since selected candidate genes showed no significant different in gene expression, their corresponding proteins were predicted for putative CaM binding site using Calmodulin Target Database. This database has been used to successfully identify CaM binding domain in human chloride channel and plant kinase receptor (Vocke et al. 2013; Hartmann et al. 2014). CaM can act as a regulatory protein by binding to its target. If the candidate proteins happen to be CaM target, it would explain why transgenic rice overexpressing *OsCaM1-1* did not show regulated gene-expression but have affected metabolite levels. Web-based prediction showed that most of the candidate genes except one isoform of an inositol-1-monophosphatase (Os03g0587000) possessed at least one putative CaM binding site (Figure 22-27). However, Yap et al. (2000) mentioned that 1/3 of putative CaM binding sites predicted by Calmodulin Target Database are generally false positives which do not bind to CaM. To further screen out possible false positive binding site, homology modeling was used to reveal if the predicted CaM binding sites were located at the surface of protein tertiary structure or not. As a result, Phyre^2 model of the proteins showed that putative CaM binding site in Os12g0528400 sequence is likely to be false positive since only a small portion of the string was exposed at the protein model surface (Figure 32). An arginase (Figure 29, Os04g0106300) and a glutathione synthetase (Figure 31, Os12g0263000) were also disregarded since the secondary

structure of predicted CaM binding sites are different from reported CaM binding motifs. As a result, only one glutathione synthetase (Figure 30, Os11g0642800) and an inositol-1-monophosphatase (Figure 33, Os02g0169900) could be regarded as potential CaM interacting partners. Further experiment is needed to confirm the interaction between *Os*CaM1-1 and these candidate proteins since these proteins might undergo conformational change under physiological conditions or allosteric binding.

Other enzymes reported to be CaM targets, such as GAD, is also interesting (Yap et al. 2003). GAD catalyzes the decarboxylation of glutamate to gamma-aminobutyric acid (GABA) and CO_2. Akama et al. (2001) reported that there are two GAD isoforms in rice, *Os*GAD1 and *Os*GAD2, with contrasting ability to bind CaM. *In vitro* CaM-binding assay between bovine CaM and the C-terminal peptides of either *Os*GAD1 or *Os*GAD2 produced in *E. coli* showed that *Os*GAD1 could be able to bind CaM while *Os*GAD2 could not. Their expression levels in many organs and developmental stages were also analyzed. Comparing between *Os*GAD1 and *Os*GAD2, their expressions were found to be similar in cotyledons, green leaves, and yellow leaves, while *Os*GAD2 expressed at higher level in roots and *Os*GAD1 expressed at much higher level in maturing seeds. From this study, I found that GABA was not up-accumulated in the 2-week-old *OsCaM1-1*-overexpressing transgenic rice lines. It suggests that GABA biosynthesis in 2-week-old rice is mainly catalyzed by CaM-independent GAD. It is well known that germinating brown rice accumulate high content of GABA (Saikusa et al. 1994), so, perhaps germinating transgenic rice grains might accumulate higher GABA content than the wild type rice.

CHAPTER V
CONCLUSIONS

*Os*CaM1-1 is a stress signaling protein which could increase rice salt-tolerance in the transgenic rice lines overexpressing *OsCaM1-1*. In this study, cDNA-AFLP analysis and metabolomics were used to identify the effect of *OsCaM1-1* overexpression in rice. The results suggested many possible roles of *Os*CaM1-1 which might support rice acclimation to stresses. Conclusions are as follows:

1. cDNA-AFLP analysis yielded many false-positive results, possibly due to high-cycle-number amplification and low transcriptomic change in the transgenic rice.
2. Metabolomics is a powerful technique to provide an overview of the metabolic changes in both primary and secondary pathways in the *OsCaM1-1* overexpressing rice lines.
3. Overexpression of *OsCaM1-1* induced the transgenic rice plants to a proactive state by the up-accumulations of certain metabolites, such as glycolytic and TCA cycle intermediates, amino acids, and tricin glucoside, under normal condition.
4. Targeted gene expression analysis and RNA-seq result suggested that *Os*CaM1-1 post-translationally regulates some metabolic pathways.
5. *In silico* analyses demonstrated that a glutathione synthetase and an inositol-1-monophosphatase are potential CaM targets. Thus, they could possibly be regulated by CaM at protein level.

I suggest that metabolomes of transgenic rice lines and control transgenic rice under stress condition, which leads to contrasting phenotypes, should be compared. It would substantially support that up-accumulation of many metabolites under optimal growth condition are beneficial for rice acclimation to stress. However, the

duration under stress condition should be carefully selected to eliminate the effect of early up-regulation of endogenous CaM.

REFERENCES

Afzal I, Murnir F, Ayub CM, Basra SMA, Hameed A, Nawaz A (2009) Changes in antioxidant enzymes, germination capacity and vigour of tomato seeds in response of priming with polyamines. Seed Sci Technol 37:765-770

Akama K, Akihiro T, Kitagawa M, Takaiwa F (2001) Rice (Oryza sativa) contains a novel isoform of glutamate decarboxylase that lacks an authentic calmodulin-binding domain at the C-terminus. Biochim Biophys Acta 1522:143-150

Ali RM (2000) Role of putrescine in salt tolerance of *Atropa belladonna* plant. Plant Sci 152:173-179

Allwood JW, Clarke A, Goodacre R, Mur LA (2010) Dual metabolomics: a novel approach to understanding plant-pathogen interactions. Phytochemistry 71:590-597

Arazi T, Kaplan B, Fromm H (2000) A high-affinity calmodulin-binding site in a tobacco plasma-membrane channel protein coincides with a characteristic element of cyclic nucleotide-binding domains. Plant Mol Biol 42:591-601

Babu YS, Bugg CE, Cook WJ (1988) Structure of calmodulin refined at 2.2 Å resolution. J Mol Biol 204:191-204

Bachem CWB, Oomen RJFJ, Visser RGF (1998) Transcript imaging with cDNA-AFLP: a step-by-step protocol. Plant Mol Biol Rep 16:157-173

Bassam BJ, Caetano-Anolles GC, Gresshoff PM (1991) Fast and sensitive silver staining of DNA in polyacrylamide gels. Anal Biochem 196:80-83

Baum G, Lev-Yadun S, Fridmann Y, Arazi T, Katsnelson H, Zik M, Fromm H (1996) Calmodulin binding to glutamate decarboxylase is required for regulation of glutamate and GABA metabolism and normal development in plants. EMBO J 15:2988-2996

Baxter CJ, Redestig H, Schauer N, Repsilber D, Patil KR, Nielsen J, Selbig J, Liu J, Fernie AR, Sweetlove LJ (2007) The metabolic response of heterotrophic Arabidopsis cells to oxidative stress. Plant Physiol 143:312-325

Bender KW, Snedden WA (2013) Calmodulin-related proteins step out from the shadow of their namesake. Plant Physiol 163:486-495

Bing L, Hongxia D, Maoxin Z, Di X, Jingshu W (2007) Potential resistance of tricin in rice against brown planthopper *Nilaparvata lugens* (Stål). Acta Ecol Sin 27:1300-1306

Bohnert HJ, Sheveleva E (1998) Plant stress adaptations — making metabolism move. Curr Opin Plant Biol 1:267-274

Boonburapong B, Buaboocha T (2007) Genome-wide identification and analyses of the rice calmodulin and related potential calcium sensor proteins. BMC Plant Biol 7:4

Bouche N, Scharlat A, Snedden W, Bouchez D, Fromm H (2002) A novel family of calmodulin-binding transcription activators in multicellular organisms. J Biol Chem 277:21851-21861

Bouche N, Yellin A, Snedden WA, Fromm H (2005) Plant-specific calmodulin-binding proteins. Annu Rev Plant Biol 56:435-466

Bown AW, Shelp BJ (1997) The metabolism and function of **γ**-aminobutyric acid. Plant Physiol 115:1-5

Breyne P, Dreesen R, Cannoot B, Rombaut D, Vandepoele K, Rombauts S, Vanderhaeghen R, Inze D, Zabeau M (2003) Quantitative cDNA-AFLP analysis for genome-wide expression studies. Mol Genet Genomics 269:173-179

Capell T, Bassie L, Christou P (2004) Modulation of the polyamine biosynthetic pathway in transgenic rice confers tolerance to drought stress. Proc Natl Acad Sci USA 101:9909-9914

Chial H (2008) DNA fingerprinting using amplified fragment length polymorphisms (AFLP): No genome sequence required. Nat Educ 1:176

Chinpongpanich A, Limruengroj K, Phean-o-pas S, Limpaseni T, Buaboocha T (2012) Expression analysis of calmodulin and calmodulin-like genes from rice, *Oryza sativa* L. BMC Res Notes 5:625

Das R, Pandey A, Pandey GK (2014) Role of calcium/calmodulin in plant stress response and signaling. In: Gaur RK, Sharma P (eds) Approaches to plant stress and their management. Springer, India, pp 53-84

Drum CL, Yan S-Z, Bard J, Shen Y-Q, Lu D, Soelaiman S, Grabarek Z, Bohm A, Tang W-J (2002) Structural basis for the activation of anthrax adenylyl cyclase exotoxin by calmodulin. Nature 415:396-402

Durso NA, Cyr RJ (1994) A calmodulin-sensitive interaction between microtubules and a higher plant homolog of elongation factor-Iα. Plant cell 6:893-905

Eisenreich W, Bacher A (2007) Advances of high-resolution NMR techniques in the structural and metabolic analysis of plant biochemistry. Phytochemistry 68:2799-2815

Gnanamanickam SS (2009) Rice and its importance to human life. In: Gnanamanickam SS (ed) Biological Control of Rice Diseases, vol 8. Springer, Texas, pp 1-10

Gong Q, Li P, Ma S, Indu Rupassara S, Bohnert HJ (2005) Salinity stress adaptation competence in the extremophile *Thellungiella halophila* in comparison with its relative *Arabidopsis thaliana*. Plant J 44:826-839

Harding SA, Oh S-H, Roberts DM (1997) Transgenic tobacco expressing a foreign calmodulin gene shows an enhanced production of active oxygen species. EMBO J 16:1137-1144

Harper JF, Hong B, Hwang I, Guo HQ, Stoddard R, Huang JF, Palmgren MG, Sze H (1998) A novel calmodulin-regulated Ca2+-ATPase (ACA2) from Arabidopsis with an N-terminal autoinhibitory domain. J Biol Chem 273:1099-1106

Hartmann J, Fischer C, Dietrich P, Sauter M (2014) Kinase activity and calmodulin binding are essential for growth signaling by the phytosulfokine receptor PSKR1. Plant J 78:192-202

Hasegawa PM, Bressan RA (2000) Plant cellular and molecular responses to high salinity. Annu Rev Plant Physiol Plant Mol Biol 51:463-499

Hernandez JA, Olmos E, Corpas FJ, Sevilla F, del Rio LA (1995) Salt-induced oxidative stress in chloroplasts of pea plants. Plant Sci 105:151-167

Hoshida H, Tanaka Y, Hibino T, Hayashi Y, Tanaka A, Takabe T, Takabe T (2000) Enhanced tolerance to salt stress in transgenic rice that overexpresses chloroplast glutamine synthetase. Plant Mol Biol 43:103-111

Hsieh H-L, Tong C-G, Thomas C, Roux SJ (1996) Light-modulated abundance of an mRNA encoding a calmodulin-regulated, chromatin-associated NTPase in pea. Plant Mol Biol 30:135-147

Hussain SS, Ali M, Ahmad M, Siddique KH (2011) Polyamines: natural and engineered abiotic and biotic stress tolerance in plants. Biotechnol Adv 29:300-311

Igarashi Y, Yoshiba Y, Sanada Y, Yamaguchi-Shinozaki K, Wada K, Shinozaki K (1997) Characterization of the gene for pyrroline-5-carboxylate synthetase and correlation between the expression of the gene and salt tolerance in *Oryza sativa* L. Plant Mol Biol 33:857-865

Ikura M (1996) Calcium binding and conformational response in EF-hand proteins. Trends Biochem Sci 21:14-17

Ikura M, Clore GM, Gronenborn AM, Zhu G, Klee CB, Bax A (1992) Solution structure of a calmodulin-target peptide complex by multidimensional NMR. Science 256:632-638

Ishitani M, Majumder AL, Bornhouser A, Michalowski CB, Jensen RG, Bohnert HJ (1996) Coordinate transcriptional induction of myo-inositol metabolism during environmental stress. Plant J 9:537-548

Jayaraman A, Puranik S, Rai NK, Vidapu S, Sahu PP, Lata C, Prasad M (2008) cDNA-AFLP analysis reveals differential gene expression in response to salt stress in foxtail millet (*Setaria italica* L.). Mol Biotechnol 40:241-251

Ji H, Pardo JM, Batelli G, Van Oosten MJ, Bressan RA, Li X (2013) The Salt Overly Sensitive (SOS) pathway: established and emerging roles. Mol Plant 6:275-286

Jonsson P, Gullberg J, Nordstrom A, Kusano M, Kpwalczyk M, Sjostrom M, Moritz T (2004) A strategy for identifying differences in large series of metabolomic samples analyzed by GC/MS. Anal Chem 76:1738-1745

Jonsson P, Johansson AI, Gullberg J, Trygg J, A J, Grung B, Marklund S, Sjostrom M, Antti H, Moritz T (2005) High-throughput data analysis for detecting and identifying differences between samples in GC/MS-based metabolomic analyses. Anal Chem 77:5635-5642

Jonsson P, Johansson ES, Wuolikainen A, Lindberg J, Schuppe-Koistinen I, Kusano M, Sjostrom M, Trygg J, Moritz T, Antti H (2006) Predictive metabolite profiling

applying hierarchical multivariate curve resolution to GC-MS data-a potential tool for multi-parametric diagnosis. J Proteome Res 5:1407-1414

Kant MR, Ament K, Sabelis MW, Haring MA, Schuurink RC (2004) Differential timing of spider mite-induced direct and indirect defenses in tomato plants. Plant Physiol 135:483-495

Kaplan F, Kopka J, Haskell DW, Zhao W, Schiller KC, Gatzke N, Sung DY, Guy CL (2004) Exploring the temperature-stress metabolome of Arabidopsis. Plant Physiol 136:4159-4168

Kasinathan V, Wingler A (2004) Effect of reduced arginine decarboxylase activity on salt tolerance and on polyamine formation during salt stress in *Arabidopsis thaliana*. Physiol Plantarum 121:101-107

Kelley LA, Sternberg MJ (2009) Protein structure prediction on the web: a case study using the Phyre server. Nat Protoc 4:363-371

Kim JK, Bamba T, Harada K, Fukusaki E, Kobayashi A (2007) Time-course metabolic profiling in *Arabidopsis thaliana* cell cultures after salt stress treatment. J Exp Bot 58:415-424

Kinkema M, Schiefelbein J (1994) A myosin from a higher plant has structural similarities to class V myosins. J Mol Biol 239:591-597

Kogel KH, Voll LM, Schafer P, Jansen C, Wu Y, Langen G, Imani J, Hofmann J, Schmiedl A, Sonnewald S, von Wettstein D, Cook RJ, Sonnewald U (2010) Transcriptome and metabolome profiling of field-grown transgenic barley lack induced differences but show cultivar-specific variances. Proc Natl Acad Sci USA 107:6198-6203

Kong-nrern K, Buaphan T, Tulaphitak D, Phuvongpha N, Wongpakonkul S, Threerakulpisut P (2011) Yield, yield components, soil minerals and aroma of KDML 105 rice in Tungkularonghai, Roi-Et, Thailand. World Acad Sci Eng Technol 5:297-302

Kong C, Xu X, Zhou B, Hu F, Zhang C, Zhang M (2004) Two compounds from allelopathic rice accession and their inhibitory activity on weeds and fungal pathogens. Phytochemistry 65:1123-1128

Kopka J, Schauer N, Krueger S, Birkemeyer C, Usadel B, Bergmuller E, Dormann P, Weckwerth W, Gibon Y, Stitt M, Willmitzer L, Fernie AR, Steinhauser D (2005) GMD@CSB.DB: the Golm Metabolome Database. Bioinformatics 21:1635-1638

Kusano M, Fukushima A, Kobayashi M, Hayashi N, Jonsson P, Moritz T, Ebana K, Saito K (2007) Application of a metabolomic method combining one-dimensional and two-dimensional gas chromatography-time-of-flight/mass spectrometry to metabolic phenotyping of natural variants in rice. J Chromatogr B Analyt Technol Biomed Life Sci 855:71-79

Kusano M, Tohge T, Fukushima A, Kobayashi M, Hayashi N, Otsuki H, Kondou Y, Goto H, Kawashima M, Matsuda F, Niida R, Matsui M, Saito K, Fernie AR (2011) Metabolomics reveals comprehensive reprogramming involving two independent metabolic responses of Arabidopsis to UV-B light. Plant J 67:354-369

Kuzina V, Ekstrom CT, Andersen SB, Nielsen JK, Olsen CE, Bak S (2009) Identification of defense compounds in Barbarea vulgaris against the herbivore *Phyllotreta nemorum* by an ecometabolomic approach. Plant Physiol 151:1977-1990

Lan W, Lu F, Regner M, Zhu Y, Rencoret J, Ralph SA, Zakai UI, Morreel K, Boerjan W, Ralph J (2015) Tricin, a flavonoid monomer in monocot lignification. Plant Physiol:114

Lee DH, Kim YS, Lee CB (2001) The inductive responses of the antioxidant enzymes by salt stress in the rice (*Oryza sativa* L.). J Plant Physiol 158:737-745

Lehmann M, Laxa M, Sweetlove LJ, Fernie AR, Obata T (2012) Metabolic recovery of Arabidopsis thaliana roots following cessation of oxidative stress. Metabolomics : Official journal of the Metabolomic Society 8:143-153

Lehmann M, Schwarzlander M, Obata T, Sirikantaramas S, Burow M, Olsen CE, Tohge T, Fricker MD, Moller BL, Fernie AR, Sweetlove LJ, Laxa M (2009) The metabolic response of Arabidopsis roots to oxidative stress is distinct from that of heterotrophic cells in culture and highlights a complex relationship between the levels of transcripts, metabolites, and flux. Mol Plant 2:390-406

Liu X, Zhang L, You L, Wu H, Zhao J, Cong M, Li F, Wang Q, Li L, Li C, Han G, Wang G, Xia C, Yu J (2011) Metabolomic study on the halophyte *Suaeda salsa* in the Yellow River Delta. CLEAN - Soil, Air, Water 39:720-727

Loewus FA, Murthy PPN (2000) myo-Inositol metabolism in plants. Plant Sci 150:1-19

Lopez-Gresa MP, Maltese F, Belles JM, Conejero V, Kim HK, Choi YH, Verpoorte R (2010) Metabolic response of tomato leaves upon different plant-pathogen interactions. Phytochem Anal 21:89-94

Lu Y-T, Hidaka H, Feldman LJ (1996) Characterization of a calcium/calmodulin-dependent protein kinase homolog from maize roots showing light-regulated gravitropism. Planta 199:18-24

Mahajan S, Pandey GK, Tuteja N (2008) Calcium- and salt-stress signaling in plants: shedding light on SOS pathway. Arch Biochem Biophys 471:146-158

Malmstrom S, Askerlund P, Palmgren MG (1997) A calmodulin-stimulated Ca^{2+}-ATPase from plant vacuolar membranes with a putative regulatory domain at its N-terminus. FEBS letters 400:324-328

Maniatis T, Fritsch EF (1982) Molecular cloning: a laboratory manual. Cold Spring Harbor Laboratory, New York

Matsuda F, Okazaki Y, Oikawa A, Kusano M, Nakabayashi R, Kikuchi J, Yonemaru J, Ebana K, Yano M, Saito K (2012) Dissection of genotype-phenotype associations in rice grains using metabolome quantitative trait loci analysis. Plant J 70:624-636

Moldenhauer K, Wilson CE, Counce P, Hardke J (2013) Rice growth and development. In: Hardke JT (ed) Arkansas rice production handbook. University of Arkansas Division of Agriculture, Arkansas, pp 9-20

Monton MR, Soga T (2007) Metabolome analysis by capillary electrophoresis-mass spectrometry. J Chromatogr A 1168:237-246

Mruk K, Farley BM, Ritacco AW, Kobertz WR (2014) Calmodulation meta-analysis: predicting calmodulin binding via canonical motif clustering. J Gen Physiol 144:105-114

Narasimhulu SB, Kao Y-L, Reddy ASN (1997) Interaction of Arabidopsis kinesin-like calmodulin-binding protein with tubulin subunits: modulation by Ca^{2+}-calmodulin. Plant J 12:1139-1149

Nelson DE, Rammesmayer G, Bohnert HJ (1998) Regulation of cell-specific inositol metabolism and transport in plant salinity tolerance. Plant Cell 10:753-764

Obata T, Fernie AR (2012) The use of metabolomics to dissect plant responses to abiotic stresses. Cell Mol Life Sci 69:3225-3243

Oppenheimer DG, Pollock MA, Vacik J, Szymanski DB, Ericson B, Feldmann K, Marks MD (1997) Essential role of a kinesin-like protein in Arabidopsis trichome morphogenesis. Proc Natl Acad Sci USA 94:6261-6266

Park CY, Lee JH, Yoo JH, Moon BC, Choi MS, Kang YH, Lee SM, Kim HS, Kang KY, Chung WS, Lim CO, Cho MJ (2005) WRKY group IId transcription factors interact with calmodulin. FEBS Lett 579:1545-1550

Perochon A, Aldon D, Galaud JP, Ranty B (2011) Calmodulin and calmodulin-like proteins in plant calcium signaling. Biochimie 93:2048-2053

Pettersen EF, Goddard TD, Huang CC, Couch GS, Greenblatt DM, Meng EC, Ferrin TE (2004) UCSF Chimera--a visualization system for exploratory research and analysis. J Comput Chem 25:1605-1612

Phean-o-pas S, Limpaseni T, Buaboocha T (2008) Structure and expression analysis of the *OsCam1-1* calmodulin gene from *Oryza sativa* L. BMB Rep 41:771-777

Phean-o-pas S, Punteeranurak P, Buaboocha T (2005) Calcium signaling-mediated and differential induction of calmodulin gene expression by stress in *Oryza sativa* L. J Biochem Mol Biol 38:432-439

Pitman MG, Lauchli A (2002) Global impact of salinity and agricultural ecosystems. In: Lauchli A, Luttge U (eds) Salinity: environment-plants-molecules. Kluwer Academic Publishers, Dordrecht, pp 3-20

Ramachandiran S, Takezawa D, Wang W, Poovaiah BW (1997) Functional domains of plant chimeric calcium/calmodulin-dependent protein kinase: regulation by autoinhibitory and visinin-like domains. J Biochem 121:984-990

Ratcliffe RG, Shachar-Hill Y (2005) Revealing metabolic phenotypes in plants: inputs from NMR analysis. Biol Rev 80:27-43

Rathinasabapathi B, Gage DA, Mackill DJ, Hanson AD (1993) Cultivated and wild rices do not accumulate glycinebetaine due to deficiencies in two biosynthetic steps. Crop Sci 33:534-538

Raychaudhuri A, Majumder AL (1996) Salinity-induced enhancement of L-myo-inositol 1-phosphate synthase in rice (*Oryza sativa* L.). Plant Cell Environ 19:1437-1442

Reddy ASN (2001) Calcium: silver bullet in signaling. Plant Sci 160:381-404

Reijans M, Lascaris R, Groeneger AO, Wittenberg A, Wesselink E, van Oeveren J, Wit Ed, Boorsma A, Voetdijk B, van der Spek H, Grivell LA, Simons G (2003) Quantitative comparison of cDNA-AFLP, microarrays, and genechip expression data in *Saccharomyces cerevisiae*. Genomics 82:606-618

Rizhsky L, Liang H, Shuman J, Shulaev V, Davletova S, Mittler R (2004) When defense pathways collide. The response of Arabidopsis to a combination of drought and heat stress. Plant Physiol 134:1683-1696

Roosens NHCJ, Thu TT, Iskandar HM, Jacobs M (1998) Isolation of the ornithine-d-aminotransferase cDNA and effect of salt stress on its expression in *Arabidopsis thaliana*. Plant Physiol 117:263-271

Roy M, Wu R (2002) Overexpression of S-adenosylmethionine decarboxylase gene in rice increases polyamine level and enhances sodium chloride-stress tolerance. Plant Sci 163:987-992

Saeng-ngam S, Takpirom W, Buaboocha T, Chadchawan S (2012) The role of the *Os*Cam1-1 salt stress sensor in ABA accumulation and salt tolerance in rice. J Plant Biol 55:198-208

Sahi C, Singh A, Kumar K, Blumwald E, Grover A (2006) Salt stress response in rice: genetics, molecular biology, and comparative genomics. Funct Integr Genomics 6:263-284

Saika H, Oikawa A, Nakabayashi R, Matsuda F, Saito K, Toki S (2012) Changes in primary and secondary metabolite levels in response to gene targeting-mediated site-directed mutagenesis of the anthranilate synthase gene in rice. Metabolites 2:1123-1138

Saikusa T, Horino T, Mori Y (1994) Accumulation of **γ**-aminobutyric acid (Gaba) in the rice germ during water soaking. Biosci Biotech Biochem 58:2291-2292

Sanchez DH, Pieckenstain FL, Escaray F, Erban A, Kraemer U, Udvardi MK, Kopka J (2011) Comparative ionomics and metabolomics in extremophile and glycophytic Lotus species under salt stress challenge the metabolic pre-adaptation hypothesis. Plant Cell Environ 34:605-617

Sanders D (2000) Plant biology: the salty tale of Arabidopsis. Curr Biol 10:R486-R488

Schauer N, Steinhauser D, Strelkov S, Schomburg D, Allison G, Moritz T, Lundgren K, Roessner-Tunali U, Forbes MG, Willmitzer L, Fernie AR, Kopka J (2005) GC-MS libraries for the rapid identification of metabolites in complex biological samples. FEBS Lett 579:1332-1337

Schmittgen TD, Livak KJ (2008) Analyzing real-time PCR data by the comparative CT method. Nat Protoc 3:1101-1108

Schumacher MA, Rivard AF, Bachinger HP, Adelman JP (2001) Structure of the gating domain of a Ca^{2+}-activated K^{+} channel complexed with Ca^{2+}/calmodulin. Nature 410:1120-1124

Schuurink RC, Shartzer SF, Fath A, Jones RL (1998) Characterization of a calmodulin-binding transporter from the plasma membrane of barley aleurone. Proc Natl Acad Sci USA 95:1944-1949

Shulaev V, Cortes D, Miller G, Mittler R (2008) Metabolomics for plant stress response. Physiol Plant 132:199-208

Snedden WA, Fromm H (1998) Calmodulin, calmodulin-related proteins and plant responses to the environment. Trends Plant Sci 3:299-304

Snedden WA, Koutsia N, Baum G, Fromm H (1996) Activation of a recombinant Petunia glutamate decarboxylase by calcium/calmodulin or by a monoclonal antibody which recognizes the calmodulin binding domain. J Biol Chem 271:4148-4153

Sojikul P, Kongsawadworakul P, Viboonjun U, Thaiprasit J, Intawong B, Narangajavana J, Svasti MR (2010) AFLP-based transcript profiling for cassava genome-wide expression analysis in the onset of storage root formation. Physiol Plant 140:189-198

Sripinyowanich S, Klomsakul P, Boonburapong B, Bangyeekhun T, Asami T, Gu H, Buaboocha T, Chadchawan S (2013) Exogenous ABA induces salt tolerance in indica rice (*Oryza sativa* L.): The role of *OsP5CS1* and *OsP5CR* gene expression during salt stress. Environ Exp Bot 86:94-105

Steinhauser D, Usadel B, Luedemann A, Thimm O, Kopka J (2004) CSB.DB: a comprehensive systems-biology database. Bioinformatics 20:3647-3651

Szymanski DB, Liao B, Zielinski RE (1996) Calmodulin isoforms differentially enhance the binding of cauliflower nuclear proteins and recombinant TGA3 to a region derived from the Arabidopsis *Cam-3* promoter. Plant Cell 8:1069-1077

Terskikh VV, Feurtado JA, Borchardt S, Giblin M, Abrams SR, Kermode AR (2005) In vivo 13C NMR metabolite profiling: potential for understanding and assessing conifer seed quality. J Exp Bot 56:2253-2265

Tuteja N, Mahajan S (2007) Calcium signaling network in plants. Plant Signal Behav 2:79-85

Urano K, Maruyama K, Ogata Y, Morishita Y, Takeda M, Sakurai N, Suzuki H, Saito K, Shibata D, Kobayashi M, Yamaguchi-Shinozaki K, Shinozaki K (2009) Characterization of the ABA-regulated global responses to dehydration in Arabidopsis by metabolomics. The Plant journal : for cell and molecular biology 57:1065-1078

van Dongen JT, Frohlich A, Ramirez-Aguilar SJ, Schauer N, Fernie AR, Erban A, Kopka J, Clark J, Langer A, Geigenberger P (2009) Transcript and metabolite profiling of the adaptive response to mild decreases in oxygen concentration in the roots of Arabidopsis plants. Ann Bot 103:269-280

van Iersel MP, Kelder T, Pico AR, Hanspers K, Coort S, Conklin BR, Evelo C (2008) Presenting and exploring biological pathways with PathVisio. BMC bioinformatics 9:399

Ventelon-Debout M, Tranchant-Dubreuil C, Nguyen TT, Bangratz M, Sire C, Delseny M, Brugidou C (2008) Rice yellow mottle virus stress responsive genes from susceptible and tolerant rice genotypes. BMC Plant Biol 8:26

Vinocur B, Altman A (2005) Recent advances in engineering plant tolerance to abiotic stress: achievements and limitations. Curr Opin Biotechnol 16:123-132

Vinogradova MV, Malanina GG, Reddy VS, Reddy AS, Fletterick RJ (2008) Structural dynamics of the microtubule binding and regulatory elements in the kinesin-like calmodulin binding protein. J Struct Biol 163:76-83

Vocke K, Dauner K, Hahn A, Ulbrich A, Broecker J, Keller S, Frings S, Mohrlen F (2013) Calmodulin-dependent activation and inactivation of anoctamin calcium-gated chloride channels. J Gen Physiol 142:381-404

Vuylsteke M, Peleman JD, van Eijk MJ (2007) AFLP-based transcript profiling (cDNA-AFLP) for genome-wide expression analysis. Nat Protoc 2:1399-1413

Wagner C, Sefkow M, Kopka J (2003) Construction and application of a mass spectral and retention time index database generated from plant GC/EI-TOF-MS metabolite profiles. Phytochemistry 62:887-900

Widodo, Patterson JH, Newbigin E, Tester M, Bacic A, Roessner U (2009) Metabolic responses to salt stress of barley (*Hordeum vulgare* L.) cultivars, Sahara and Clipper, which differ in salinity tolerance. J Exp Bot 60:4089-4103

Wu HC, Luo DL, Vignols F, Jinn TL (2012) Heat shock-induced biphasic Ca($^{2+}$) signature and *Os*CaM1-1 nuclear localization mediate downstream signalling in acquisition of thermotolerance in rice (*Oryza sativa* L.). Plant Cell Environ 35:1543-1557

Wulff-Zottele C, Gatzke N, Kopka J, Orellana A, Hoefgen R, Fisahn J, Hesse H (2010) Photosynthesis and metabolism interact during acclimation of *Arabidopsis thaliana* to high irradiance and sulphur depletion. Plant Cell Environ 33:1974-1988

Xiao X, Li H, Tang C (2009) A silver-staining cDNA-AFLP protocol suitable for transcript profiling in the latex of *Hevea brasiliensis* (para rubber tree). Mol Biotechnol 42:91-99

Yang T, Poovaiah BW (2003) Calcium/calmodulin-mediated signal network in plants. Trends Plant Sci 8:505-512

Yang Z, Nakabayashi R, Okazaki Y, Mori T, Takamatsu S, Kitanaka S, Kikuchi J, Saito K (2014) Toward better annotation in plant metabolomics: isolation and structure elucidation of 36 specialized metabolites from (rice) by using MS/MS

and NMR analyses. Metabolomics : Official journal of the Metabolomic Society 10:543-555

Yap KL, Kim JK, Truong K, Sherman M, Yuan T, Ikura M (2000) Calmodulin target database. J Struct Funct Genomics 1:8-14

Yap KL, Yuan T, Mal TK, Vogel HJ, Ikura M (2003) Structural basis for simultaneous binding of two carboxy-terminal peptides of plant glutamate decarboxylase to calmodulin. J Mol Biol 328:193-204

Yiu J-C, Juang L-D, Fang DY-T, Liu C-W, Wu S-J (2009) Exogenous putrescine reduces flooding-induced oxidative damage by increasing the antioxidant properties of Welsh onion. Sci Hortic 120:306-314

Yoshida S, Forno DA, Cock JH, Gomez KA (1976) Routine procedure for growing rice plants in culture solution. In: Laboratory manual for physiological studies of rice. The international rice research institute, Philippines, pp 61-66

Yun C, Bai J, Sun D, Cui D, Chang W, Liang D (2004) Structure of potato calmodulin PCM6: the first report of the three-dimensional structure of a plant calmodulin. Acta Cryst 60:1214-1219

Zeng L, Shannon MC (2000) Salinity effects on seedling growth and yield components of rice. Crop Sci 40:996-1003

Zhang W, Jiang B, Li W, Song H, Yu Y, Chen J (2009) Polyamines enhance chilling tolerance of cucumber (*Cucumis sativus* L.) through modulating antioxidative system. Sci Hortic 122:200-208

Zhou J, Ma C, Xu H, Yuan K, Lu X, Zhu Z, Wu Y, Xu G (2009) Metabolic profiling of transgenic rice with *cryIAc* and *sck* genes: an evaluation of unintended effects at metabolic level by using GC-FID and GC-MS. J Chromatogr B Analyt Technol Biomed Life Sci 877:725-732

Zhu J-K (2001) Plant salt tolerance. Trends Palnt Sci 6:66-71

Zhu JK (2002) Salt and drought stress signal transduction in plants. Annu Rev Plant Biol 53:247-273

Zielinski RE (1998) Calmodulin and calmodulin-binding proteins in plants. Annu Rev Plant Physio Plant Mol Biol 49:697-725

APPENDIX

APPENDIX A

Vector map

pJET1.2/blunt (taken from www.lifetechnologies.com)

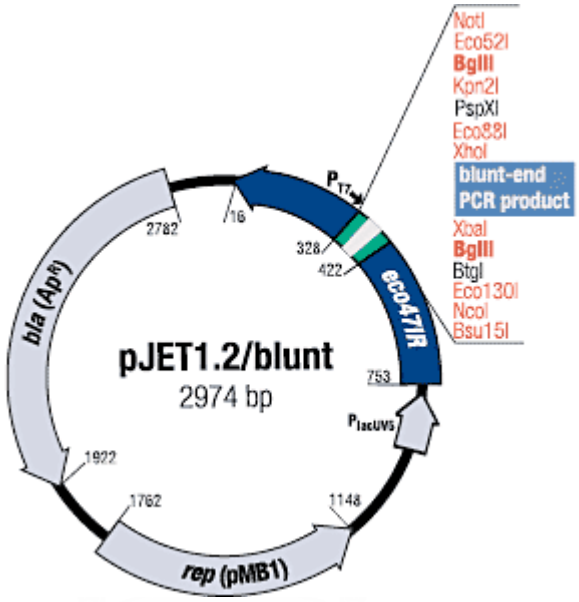

APPENDIX B

Protocols

1. mRNA extraction by Magnetic mRNA Isolation Kit (New England Biolabs)

1. Allow all kit components to come to room temperature
2. Resuspend Oligo d(T)25 beads by agitating at room temperature (RT) for 30 minutes
3. Aliquot 200 µl Oligo d(T)25 beads and add 200 µl of Lysis/Binding Buffer to beads, vortex briefly and mix with agitation for 2 minutes - Beads should remain in the lysis/binding wash solution until removal immediately before adding the sample powder
4. Add 500 µl lysis/binding buffer to the sample powder, spin at 12,000 rpm, 4°C for 1 minute
5. Place the microcentrifuge tube containing the beads and lysis/binding wash into the magnetic rack and pull the magnetic beads to the side of the tube, remove and discard the wash solution
6. Decant tissue supernatant and add to previously washed Oligo d(T)25 beads. Place sample-and-bead suspension on the agitator and incubate at RT for 10 minutes
7. Place microcentrifuge tube into the magnetic rack and pull magnetic beads to the side of the tube, remove and discard supernatant
8. Add 500 µl Wash Buffer 1 to the beads, vortex gently to suspend beads. Incubate with agitation for 1 minute
9. Place microcentrifuge tube in the magnetic rack and pull magnetic beads to the side of the tube, remove and discard wash solution
10. Repeat step 8-9 once
11. Add 500 µl Wash Buffer 2 to the beads and mix with agitation for 1 minute
12. Place microcentrifuge tube in the magnetic rack and pull magnetic beads to the side of the tube, remove and discard wash solution
13. Repeat step 11-12 once

14. Add 500 µl Low Salt Buffer to the beads and mix with agitation for 1 minute
15. Place microcentrifuge tube in the magnetic rack and pull magnetic beads to the side of the tube, remove and discard wash solution
16. Add 100 µl of Elution Buffer and vortex gently to suspend beads
17. Incubate at 50°C for 2 minutes with occasional agitation to elute poly(A)+ RNA (>90% of the poly(A)+ RNA bound to the beads is recovered in this step)
18. Place microcentrifuge tube in the magnetic rack and pull magnetic beads to the side of the tube, transfer eluent to a clean, sterile RNase-free tube. Store on ice and immediately quantitate or place at –80°C for long-term storage

2. cDNA synthesis by iScript™ Reverse Transcription Supermix for RT-qPCR (Bio-Rad)

1. Prepare the following reaction mixture in 0.2 ml tube, *** do not add iScript RT supermix until step 3**

Reagent		
iScript RT supermix	4	µl
nuclease-free water	x	µl
RNA template (up to 1 µg total RNA)	x	µl
Total volume	20	µl

2. Incubate the reaction mixture without iScript RT supermix at 65 °C for 5 minutes, chill on ice immediately for 1 minute

3. Add iScript RT supermix and incubate at the following temperature program in thermal cycler:

priming	25 °C 5 minutes
Reverse transcription	42 °C 30 minutes
RT inactivation	85 °C 5 minutes
Hold 4 °C	

4. Place cDNA at –20 °C for long-term storage

3. Preparation of competent cells *E. coli* strain DH5α

1. Inoculate a single colony of *E. coli* strain DH5**α** into 5 ml of LB medium, culture by shaking at 250 rpm at 37°C overnight

2. Inoculate 1 ml of overnight culture into 100 ml LB medium with, continue shaking at 37 °C

3. Shake until OD_{600} reaches 0.4-0.6, transfer the cell culture into a pre-chilled 50 ml falcon tube

4. Centrifuge at 3000 rpm for 10 min at 4 °C, discard the supernatant, suspended the cell pellet with 2 ml ice-cold 100 mM $CaCl_2$ by pipetting

5. Repeat step 4.

6. Incubate on ice for 20 min.

7. Add 0.5 ml ice-cold 80% glycerol and mix by pipetting

8. Aliquot 100 µl competent cell in 1.5 ml tube and store at -80 °C

4. TDF cloning using CloneJET PCR Cloning Kit (Thermo scientific)

1. Prepare the following blunting reaction mixture in 0.2 ml tube

Reagent		
2x reaction buffer	5	µl
PCR product	0.5	µl
Nuclease-free water	3	µl
DNA blunting enzyme	0.5	µl
Total volume	9	µl

2. Vortex briefly and spin-down
3. Incubate at 70 °C for 5 minutes and chill on ice
4. On ice, add 0.5 µl pJET1.2/blunt vector and 0.5 µl T4 DNA ligase to the blunting reaction mixture
5. Vortex briefly and spin-down
6. Incubate at 22 °C for 5-30 minutes
7. Reaction mixture can be used directly for transformation

5. Heat-shock transformation

1. Stand *E.coli* competent cell on ice for 10 minutes
2. Add plasmid (should not exceed 5% of competent cell volume), tap, and incubate on ice for 30 minutes
3. Heat-shock at 42 °C for 90 seconds
4. Incubate on ice for 5 minutes
5. Add 900 µl LB medium and shaking at 37 °C, 250 rpm for 1 hour
6. Spread transformant on selective agar plate

APPENDIX C

Buffers and solutions

1. Solutions for E.coli competent cell preparation

100 mM $CaCl_2$

- $CaCl_2$ 6H2O 295 mg
- Dissolve in DI water 20 ml

80% Glycerol

- Glycerol 80 ml
- H_2O 20 ml

2. Buffer used in agarose gel electrophoresis

5X Loading buffer

- Bromophenol blue 10 mg
- Sucrose 1 g
- 10000x Gel Red 15 µl
- Dissolve in DI water 5 ml

10X TBE buffer

- Tris-base 108 g
- Boric acid 55 g
- 0.5 M EDTA (pH 8.0) 40 ml
- Dissolve in DI water 1 L

3. ATP for adaptor ligation

20 mM ATP

- Adenosine-5'-triphosphate disodium salt 11mg
- Dissolve in DI water 1 ml

4. Solutions for DNA denaturing PAGE

4.5% acrylamide solution 7.5 M urea 0.5x TBE

- 40% Acrylamide (19 acrylamide : 1 bis-acrylamide) 11.36 ml
- 20x TBE 2.5 ml
- Urea 45 g
- DI water - make the final volume to 100 ml

10% ammonium persulfate

- Ammonium persulfate 1 g
- DI water – make the final volume to 10 ml

10 mg/ml Sodium thiosulfate

- Sodium thiosulfate 0.1 g
- DI water – make the final volume to 10 ml

Formamide loading dye

- Formamide 9.8 ml
- Bromophenol blue 20 mg
- Xylene cyanol 20 mg
- DI water 200 µl

5. Silver staining solutions

Developer

- DI water 1 L
- Na_2CO_3 30 g
- 37% Formaldehyde 1.5 ml
- 10mg/ml Sodium thiosulfate 200 µl

Keep cold at 4 °C until use

Silver staining solution

- DI water 1 L
- Silver nitrate 1 g
- 37% Formaldehyde 1.5 ml

Keep in the dark at RT until use

10% acetic acid (fix solution and stop solution)

- DI water 900 ml
- Glacial acetic acid 100 ml

APPENDIX D

Genevestigator microarray database

Data from five experiments involving salt stress in rice were used.

GEO accession:

GSE3053

http://www.ncbi.nlm.nih.gov/geo/query/acc.cgi?acc=GSE3053

GSE6901

http://www.ncbi.nlm.nih.gov/geo/query/acc.cgi?acc=GSE6901

GSE13735

http://www.ncbi.nlm.nih.gov/geo/query/acc.cgi?acc=GSE13735

GSE14403

http://www.ncbi.nlm.nih.gov/geo/query/acc.cgi?acc=GSE14403

GSE16108

http://www.ncbi.nlm.nih.gov/geo/query/acc.cgi?acc=GSE16108

Os04g0106300 (Arginase, LOC_Os04g01590)

- Significant in 2 experiments: GSE6901 and GSE14403

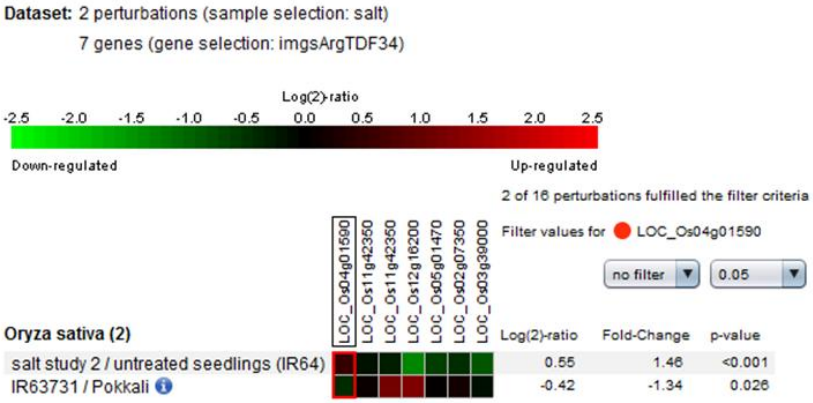

Os11g0642800 (Glutathione synthetase, LOC_Os11g42350)

- Significant in 3 experiments: GSE13735, GSE14403 and GSE16108

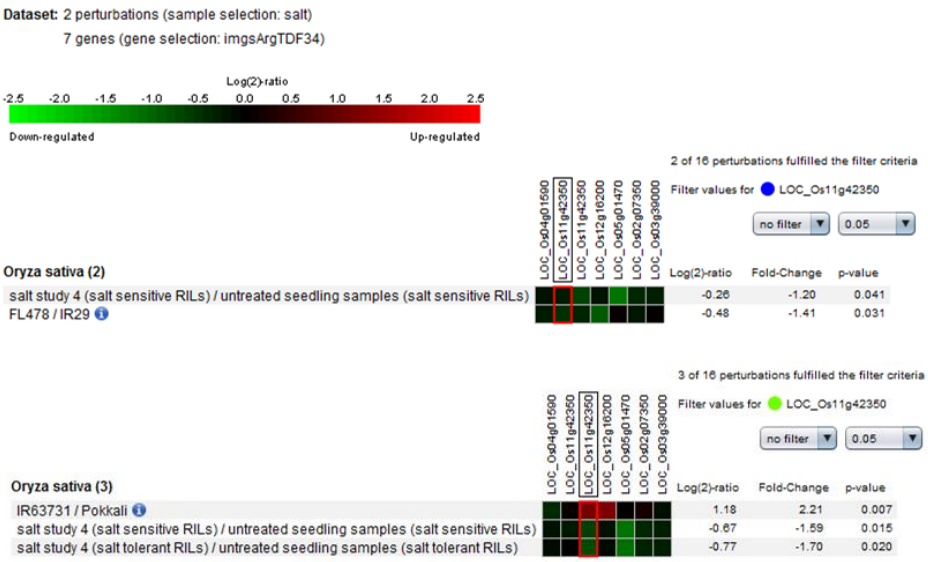

Os12g0263000 (Glutathione synthetase, LOC_Os12g16200)

- Significant in 4 experiments: GSE3053, GSE6901, GSE14403, and GSE16108

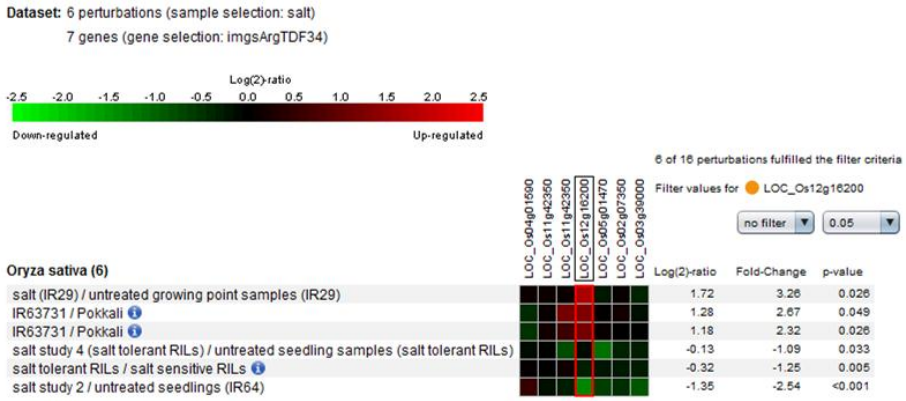

Os02g0169900 (Inositol-1-monophosphatase, LOC_Os02g07350)

- Significant in 3 experiments: GSE6901, GSE14403, and GSE16108

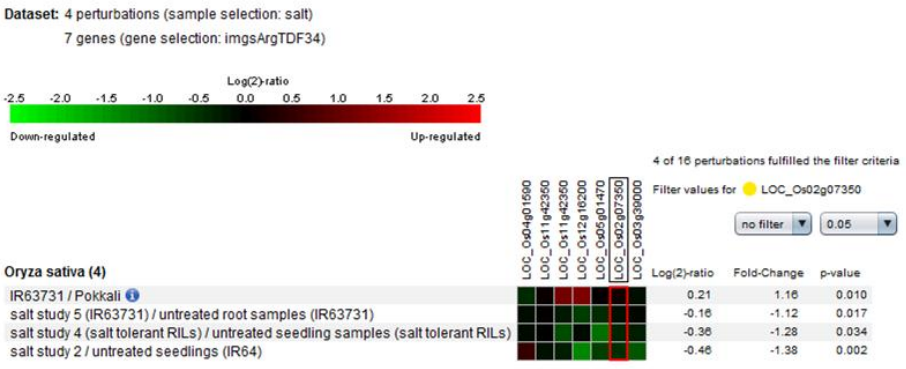

Os03g0587000 (Inositol-1-monophosphatase, LOC_Os03g39000)

- Significant in 3 experiments: GSE3053, GSE6901, and GSE14403

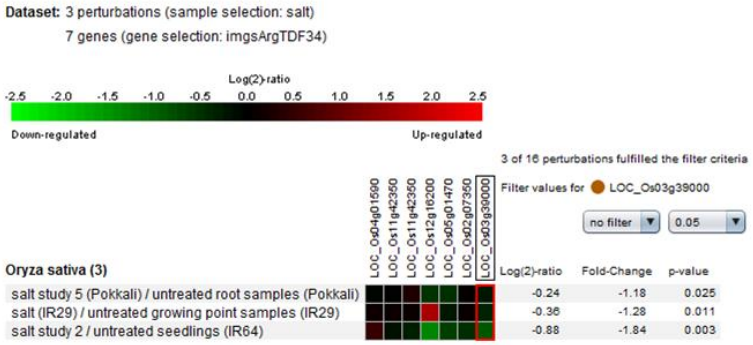

Os05g0105000 (TDF 34, LOC_Os05g01470)

Significant in 4 experiments: GSE6901, GSE13735, GSE14403, and GSE16108

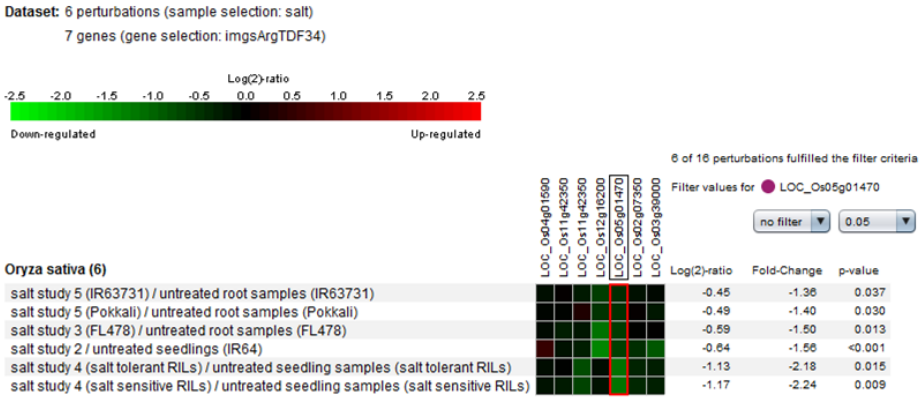

APPENDIX E

Differentially expressed gene from RNA-seq data

Using KEGG pathway database, some metabolic pathways of interest were manually checked for metabolite to gene correlations in leaves. RNA-seq was used to compare transcriptomes of transgenic rice overexpressing *OsCaM1-1* and wild type rice for the identification of differentially expressed genes.

Key for metabolite accumulation:

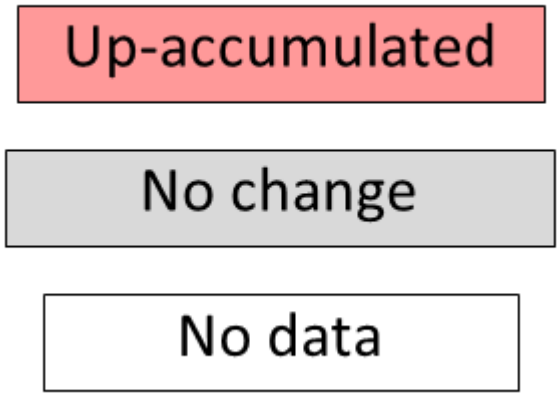

Key for gene expression:

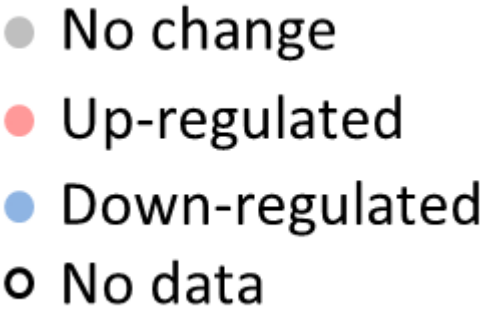

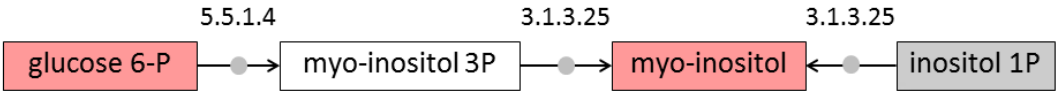

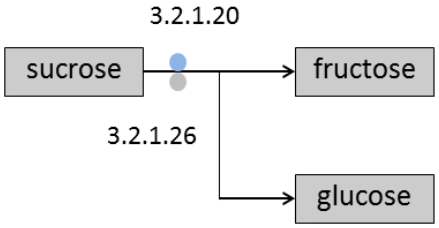

5.5.1.4

Os03g0192700

Os10g0369900

3.1.3.25

Os02g0169900

Os03g0587000

3.2.1.20

Os06g0675700

Os06g0676700

Os07g0421300

3.2.1.26

Os01g0966700

Os02g0106100

Os02g0534400

Os04g0413200

Os04g0413500

Os04g0535600

Os04g0664800

Os04g0664900

Os09g0255000

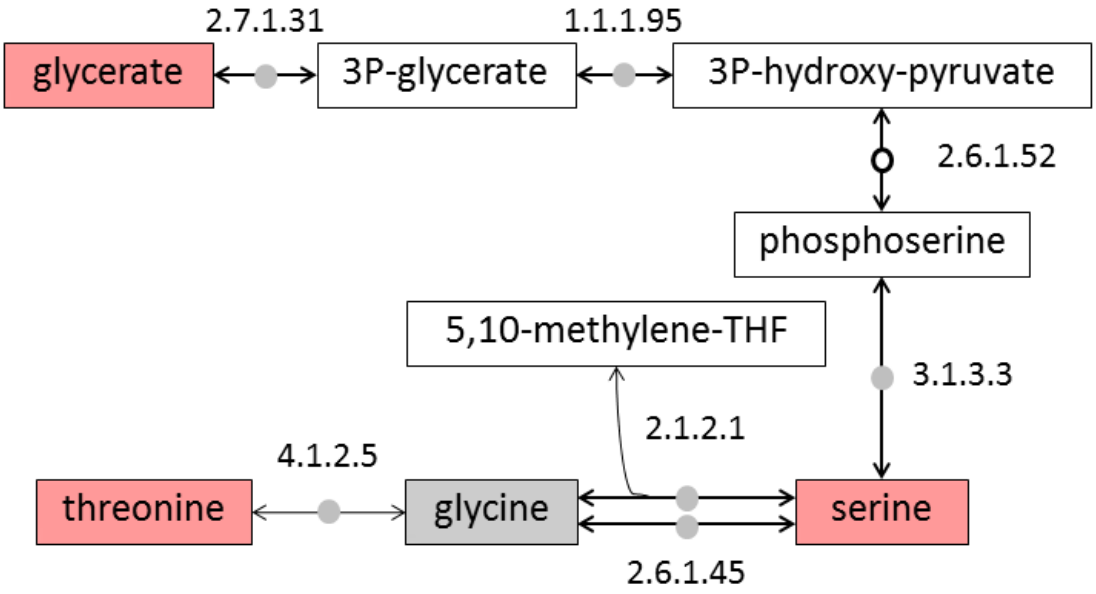

2.7.1.31
Os01g0682500

1.1.1.95
Os04g0650800
Os06g0655100

3.1.3.3
Os11g0629500
Os12g0502400

2.6.1.45
Os08g0502700

4.1.2.5
Os04g0516600

2.1.2.1
Os01g0874900
Os03g0738400
Os05g0429000
Os11g0455800
Os12g0409000

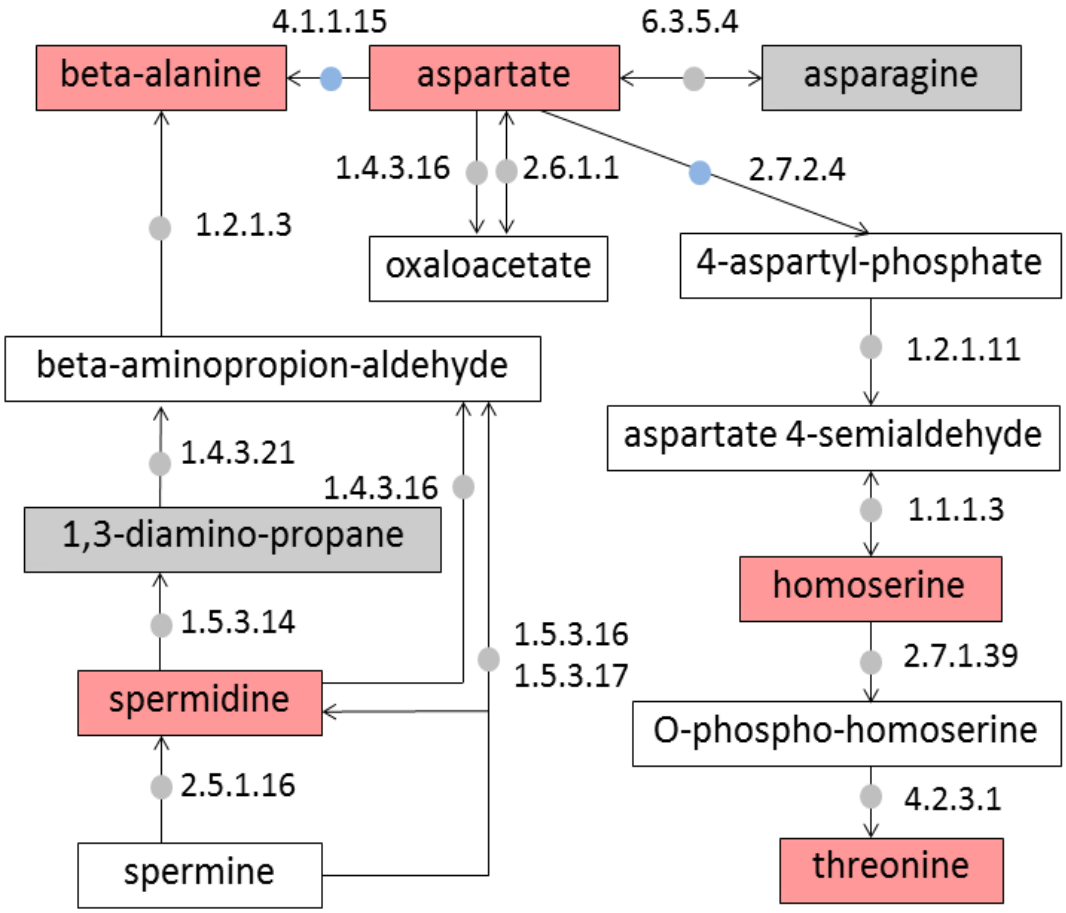
4.1.1.15
6.3.5.4
beta-alanine
aspartate
asparagine
1.4.3.16
2.6.1.1
2.7.2.4
1.2.1.3
oxaloacetate
4-aspartyl-phosphate
beta-aminopropion-aldehyde
1.2.1.11
aspartate 4-semialdehyde
1.4.3.21
1.4.3.16
1.1.1.3
1,3-diamino-propane
homoserine
1.5.3.14
1.5.3.16
1.5.3.17
2.7.1.39
spermidine
O-phospho-homoserine
2.5.1.16
4.2.3.1
spermine
threonine

4.1.1.15
Os03g0236200
Os03g0720300
Os04g0447400
Os04g0447800
Os08g0465800

6.3.5.4
Os06g0265000

1.2.1.3
Os02g0646500
Os02g0647900
Os02g0730000
Os04g0540600
Os06g0270900
Os09g0440300
Os11g0186200

1.4.3.16
Os02g0134400

2.6.1.1
Os01g0760600
Os02g0236000
Os02g0797500
Os06g0548000

2.7.2.4
Os01g0927900
Os03g0850400
Os07g0300900
Os08g0342400
Os09g0294000

1.4.3.21
Os04g0269600
Os04g0476100
Os06g0338200

1.4.3.16
Os02g0134400

1.5.3.14
Os09g0368200
Os09g0368500

2.5.1.16
Os02g0237100
Os06g0528600
Os07g0408700

1.5.3.16
Os01g0710200
Os09g0368200
Os09g0368500

1.5.3.17
Os04g0623300
Os04g0671300

1.2.1.11
Os03g0760700

1.1.1.3
Os08g0342400
Os09g0294000

2.7.1.39
Os02g0831800

4.2.3.1
Os01g0693800
Os05g0549700

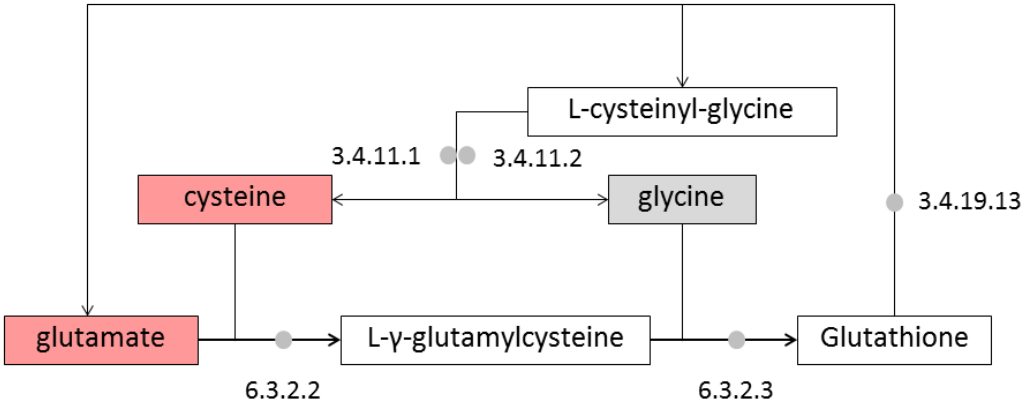

6.3.2.2

Os05g0129000

6.3.2.3

Os11g0642800

Os12g0263000

Os12g0528400

3.4.19.13

Os01g0151400

Os01g0151500

Os04g0457500

3.4.11.1

Os02g0794700

Os12g0434400

3.4.11.2

Os08g0562700

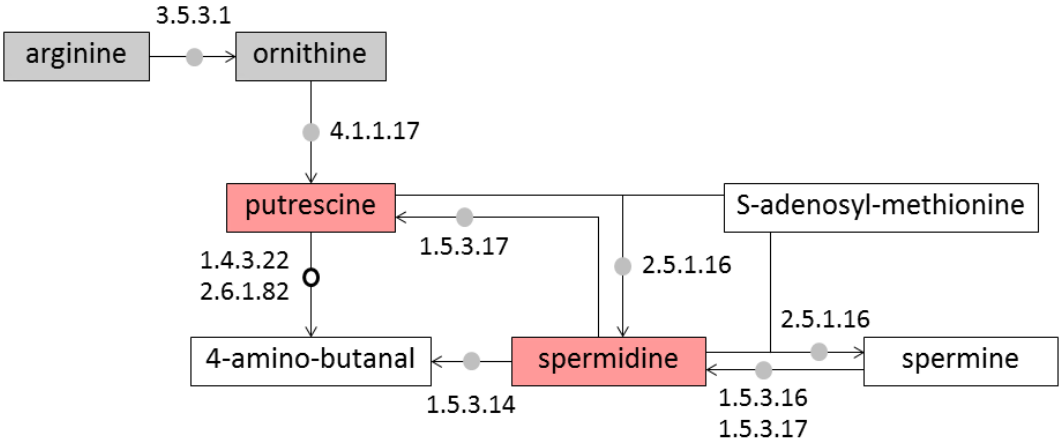

3.5.3.1

Os04g0106300

4.1.1.17

Os02g0482400

Os04g0136500

Os09g0543400

1.5.3.17

Os04g0623300

Os04g0671300

1.5.3.14

Os09g0368200

Os09g0368500

2.5.1.16

Os02g0237100

Os06g0528600

Os07g0408700

1.5.3.16

Os01g0710200

Os09g0368200

Os09g0368500

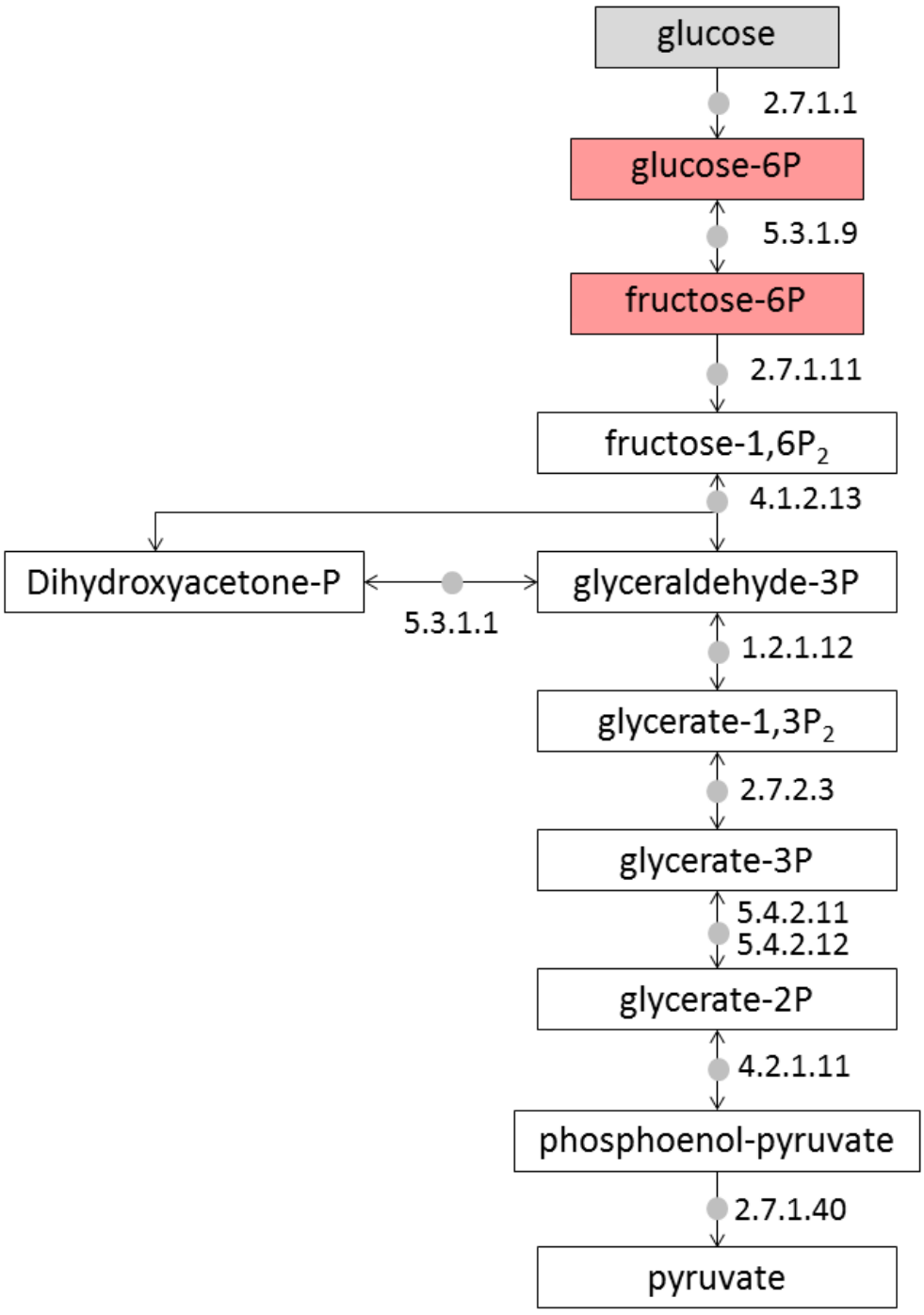
glucose
2.7.1.1
glucose-6P
5.3.1.9
fructose-6P
2.7.1.11
fructose-1,6P2
4.1.2.13
Dihydroxyacetone-P
5.3.1.1
glyceraldehyde-3P
1.2.1.12
glycerate-1,3P2
2.7.2.3
glycerate-3P
5.4.2.11
5.4.2.12
glycerate-2P
4.2.1.11
phosphoenol-pyruvate
2.7.1.40
pyruvate

2.7.1.1

Os01g0722700
Os01g0940100
Os01g0742500
Os01g0190400
Os05g0187100
Os05g0522500
Os05g0532600
Os07g0197100
Os07g0446800

5.3.1.9

Os03g0776000
Os06g0256500
Os08g0478800
Os09g0465600

2.7.1.11

Os01g0191700
Os04g0469500
Os05g0524400
Os08g0439000
Os09g0415800
Os09g0479800
Os10g0405600

4.1.2.13

Os01g0905800
Os01g0118000
Os05g0402700
Os06g0608700
Os08g0120600
Os11g0171300

1.2.1.12

Os02g0171100
Os02g0601300
Os04g0486600
Os06g0666600
Os08g0126300

2.7.2.3

Os02g0169300
Os06g0668200
Os01g0800266

5.4.2.11

Os02g0751800

5.4.2.12

Os01g0817700
Os03g0330200
Os05g0482700
Os11g0138600
Os11g0150100
Os08g0476400

4.2.1.11

Os03g0248600
Os03g0266200
Os06g0136600
Os09g0375000
Os10g0167300

5.3.1.1

Os01g0147900
Os01g0841600
Os03g0754200
Os09g0535000

2.7.1.40

Os01g0276700
Os01g0660300
Os03g0325000
Os03g0672300
Os04g0677500
Os07g0181000
Os10g0571200
Os11g0148500
Os11g0216000
Os12g0145700

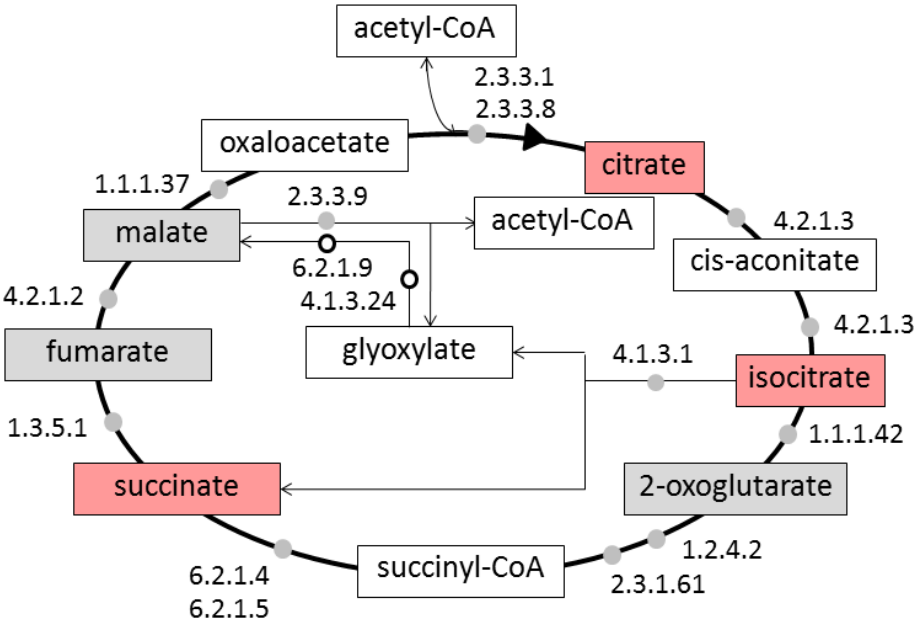

2.3.3.1
Os02g0194100
Os02g0232400
Os11g0538900

2.3.3.8
Os01g0300200
Os12g0566300

4.2.1.3
Os03g0136900
Os06g0303400

1.1.1.41
Os01g0276100
Os02g0595500
Os04g0479200

1.1.1.42
Os01g0654500
Os01g0248400
Os04g0508200
Os05g0573200

1.2.4.2
Os04g0390000
Os07g0695800

2.3.1.61
Os04g0394200

6.2.1.4
6.2.1.5
Os02g0621700
Os07g0577700

1.3.5.1
Os02g0121800
Os07g0134800
Os08g0120000
Os09g0370300

1.1.1.37
Os01g0649100
Os01g0829800
Os03g0773800
Os04g0551200
Os05g0574400
Os07g0630800
Os08g0434300
Os10g0478200
Os12g0632700

4.2.1.2
Os03g0337900

4.1.3.1
Os07g0529000

2.3.3.9
Os04g0486950

VITA

Mr. Surachat Tangpranomkorn was born on September 27th, 1990. He is a middle child and grew up in Bangkok with his family. He studies in the field of biochemistry. After graduated from Faculty of Science, Chulalongkorn University, with Second-Class Honors in 2012 for his Bachelor, he continues studying in the Program of Biochemistry and Molecular Biology at the same university for his Master's degree. He participated in many scientific conferences during those years. He got Best Poster Award in the 25th Annual Meeting of the Thai Society for Biotechnology and International Conference in 2013, Second Best Oral Presentation of the 22th Science Forum 2014 of Faculty of Science; Chulalongkorn University, and also Metabolomics Society Student Travel Award in 2014. He plans to pursue his study in Biological Science.